**USGS**
*science for a changing world*

Prepared in cooperation with the Nevada Division of Environmental Protection

# Seasonal and Long-Term Clarity Trend Assessment of Lake Tahoe, California–Nevada

Scientific Investigations Report 2022–5070

# Seasonal and Long-Term Clarity Trend Assessment of Lake Tahoe, California–Nevada

By Ramon Naranjo, Paul Work, Alan Heyvaert, Geoffrey Schladow, Alicia Cortes, Shohei Watanabe, Lidia Tanaka, and Sebnem Elci

Scientific Investigations Report 2022–5070

**U.S. Department of the Interior**
**U.S. Geological Survey**

U.S. Geological Survey, Reston, Virginia: 2022

# Acknowledgments

# Contents

## Figures

## Tables

# Conversion Factors

International System of Units to U.S. customary units

| Multiply | By | To obtain |
|---|---|---|
| Length | | |
| millimeter (mm) | 0.03937 | inch (in.) |
| meter (m) | 3.281 | foot (ft) |
| kilometer (km) | 0.6214 | mile (mi) |
| meter (m) | 1.094 | yard (yd) |
| Area | | |
| square meter ($m^2$) | 0.0002471 | acre |
| square kilometer ($km^2$) | 247.1 | acre |
| square centimeter ($cm^2$) | 0.001076 | square foot ($ft^2$) |
| square meter ($m^2$) | 10.76 | square foot ($ft^2$) |
| square kilometer ($km^2$) | 0.3861 | square mile ($mi^2$) |
| Volume | | |
| cubic meter ($m^3$) | 35.31 | cubic foot ($ft^3$) |
| cubic meter ($m^3$) | 1.308 | cubic yard ($yd^3$) |
| Speed and Flow rate | | |
| meter per second (m/s) | 3.281 | foot per second (ft/s) |
| cubic meter per second ($m^3$/s) | 35.31 | cubic foot per second ($ft^3$/s) |
| Mass to Weight | | |
| gram (g) | 0.03527 | ounce (oz) |
| kilogram (kg) | 2.205 | pound (lb) |
| metric ton (t) | 1.102 | ton, short [2,000 lb] |

Temperature in degrees Celsius (°C) may be converted to degrees Fahrenheit (°F) as follows:

°F = (1.8 × °C) + 32.

# Datum

Vertical coordinate information is referenced to North American Vertical Datum of 1988 (NAVD 88). Horizontal coordinate information is referenced to the North American Datum of 1983 (NAD 83).

Elevation, as used in this report, refers to distance above the vertical datum.

## Supplemental Information

Inflow buoyancy flux per unit width is given using cubic meters per cubic seconds ($m^3/s^3$).

Trend in buoyancy frequency is given in units of per second per year (1/s/ y).

Trend in stablity is given in units of kilograms per square meter per year ($kg/m^2/y$).

Trend in clarity is given in units of meters per year (m/y).

Urban load is given in units of kilograms per acre per inch (kg/ac/in).

*Daphnia* feeding rates are given using cells per *Daphnia* per hour (cells/*Daphnia*/hr).

*Mysis* densities are given in units of individual per square meter (ind./$m^2$).

Lake particles are given using number of particles per milliliter (mL).

Loads from urban stormwater are given in units of kilograms per acre per inch (kg/ac/in).

## Abbreviations

| | |
|---|---|
| BMP | best management practices |
| FSP | fine sediment particle |
| LCCP | Lake Clarity Crediting Program |
| LTIMP | Lake Tahoe Interagency Monitoring Program |
| LTP | Lake Tahoe profiling station |
| MLTP | mid-Lake Tahoe profiling station |
| N | buoyancy frequency |
| NWIS | National Water Information System |
| PAR | photosynthetically active radiation |
| PLRM | Pollutant Load Reduction Model |
| PSD | power spectral density |
| RSWMP | Regional Stormwater Monitoring Program |
| SI | stability index |
| SWE | snow-water equivalent |
| TCX | Tahoe City Cross |
| TERC | Tahoe Environmental Research Center |
| TMDL | total maximum daily load |
| TN | total nitrogen |
| TP | total phosphorus |
| TSS | total suspended solids |
| USGS | U.S. Geological Survey |
| WY | water year |

# Seasonal and Long-Term Clarity Trend Assessment of Lake Tahoe, California–Nevada

By Ramon Naranjo[1], Paul Work[1], Alan Heyvaert[2], Geoffrey Schladow[3], Alicia Cortes[3], Shohei Watanabe[3], Lidia Tanaka[3], and Sebnem Elci[4]

## Abstract

The clarity of Lake Tahoe, observed using a Secchi disk on a regular basis since the late 1960s, continues to be a sentinel metric of lake health. Water clarity is influenced by physical and biological processes and has declined in the five decades of monitoring, revealing differences between summer (June–September) and winter (December–March). This document summarizes key findings of a study of Lake Tahoe water clarity, including long-term variability and the relative importance of several influencing variables and processes.

This study, prepared in cooperation with the Nevada Division of Environmental Protection, focused on (1) an apparent divergence in clarity trends between summer and winter periods, (2) observed changes in in-lake physical and ecological variables that may influence or control seasonal and annual clarity trends, and (3) five research hypotheses regarding lake clarity that were developed by Lake Tahoe management agencies. Previously collected data were used to complete this study. Trend analysis confirmed that winter clarity stabilized (that is, there is no longer a statistically significant trend up or down) during the last 20 years.

[1]U.S. Geological Survey.

[2]Desert Research Institute.

[3]University of California Davis.

[4]Izmir Institute of Technology.

Evaluation of clarity for selected months in the 50-year Secchi disk clarity dataset showed that only two summer months, July and August, had statistically significant decreases in clarity from 2000–19. Different subsets of available data were analyzed to reveal the presence or absences of trends for each season, decade, and month.

Five hypotheses related to lake clarity were part of the study described by this report. Hypothesis 1 stated that clarity is controlled predominantly by the distribution and volumetric density of fine particles in suspension. This hypothesis was studied using available data describing in-lake fine (0–20 micrometers) particles from 2008–19. Water clarity was negatively correlated with in-lake particle abundance, with particles in the 1.0-4.6 μm range having the greatest effect, consistent with light-scattering theory. Estimated abundances of diatoms of the genus *Cyclotella* also were found to be negatively correlated with clarity.

Data limitations precluded a complete investigation of hypothesis 2, which stated that the observed improvements in winter water clarity are a response to decreasing fine suspended-sediment concentrations in the lake resulting from load reductions from upland sources in and near urbanized areas. Data describing fine-sediment loading from urban areas to the lake were only available since 2014, and only once or twice per month. A slight, statistically significant, negative correlation was identified between urban fine-particle loading and monthly lake clarity with a 4-month lag. Particle abundance in monitored streams is highly correlated with simultaneous particle abundance in the lake.

Hypothesis 3 stated that changing hydrodynamic conditions in the lake are increasing thermal stability and resistance to mixing. Trend analyses performed on stability index and buoyancy frequency time series computed from long-term observations of lake temperatures support the hypothesis that hydrodynamic conditions have evolved since 1969 to increase the lake's resistance to mixing. The date of maximum mixing in winter has become progressively earlier in the year. Lake density stratification, defined using the stability index, is commencing earlier in the year and extending a month longer than in the early years of the monitoring program.

Hypothesis 4 stated that the trend of decreasing summer clarity is a result of earlier, prolonged, and more intense stratification. Statistically significant correlations were found between summer clarity and (1) date of onset of stratification, (2) duration of stratification, and (3) buoyancy frequency.

Hypothesis 5 stated that ecological (food web) interactions are causing changes in the trends of seasonal or annual clarity; data supporting hypothesis 5 were limited to examples from other systems and to intermittent monitoring of Lake Tahoe and Emerald Bay. The resulting narrative assessment was motivated by a 6-year study of *Mysis* shrimp disappearance and return in Emerald Bay. The available data and a large body of published literature are consistent with the inference that *Mysis* shrimp-induced food web changes are causing changes in the trends of seasonal or annual clarity. This food-web study focused on the relations between introduced *Mysis* shrimp, the native cladocerans (*Daphnia* and *Bosmina*) that were largely eliminated following *Mysis* introduction, and the effect on fine particles within the lake. The records of *Mysis* and other zooplankton data for Lake Tahoe are episodic and have large gaps. Consequently, statistical analyses could not be conducted to compare zooplankton data with other variables. The long-term record, however, indicates that the key effect was a change to the phytoplankton assemblage, where larger diatoms disappeared, likely due to *Mysis* grazing, only to be replaced by *Cyclotella* that are an order-of-magnitude smaller and have increased the abundance and volumetric density of total fine particles in suspension (biotic and abiotic).

# A. Introduction

Lake Tahoe is designated an "Outstanding National Resource Water" and a "Waterbody of extraordinary ecological or aesthetic value" by the State of California and Nevada, respectively, for its remarkable clarity and striking blue color (California Regional Water Quality Control Board and Nevada Division of Environmental Protection, 2010). During the past half century, average annual clarity has diminished. The Lake Tahoe Total Maximum Daily Load (TMDL) Program was established in 2010 (California Regional Water Quality Control Board and Nevada Division of Environmental Protection, 2010) to guide efforts and set targets to restore historical clarity conditions. The TMDL Program was predicated on observed reductions in water clarity being primarily the result of the inorganic fine-sediment particle load entering the lake from watersheds. Extremes in hydrological variables as well as in-lake processes may contribute to interannual variations in lake clarity, however.

Trends in clarity, as measured by Secchi depth, vary between summer (June–September) and winter (December–March) seasons. The long-term summer trend is declining clarity, with a noticeable cyclic pattern. Winter clarity shows a different long-term trend. The ongoing summer clarity decline offsets improvements in winter, confounding average annual clarity restoration efforts. The cause for the diverging seasonal clarity trends has not been well documented.

In cooperation with Nevada Division of Environmental Protection, this work focused on two key water-quality management questions:

- What is driving the divergence between summer and winter clarity trends?

- How have observed changes in in-lake physical and ecological variables influenced seasonal and historical trends?

- The second question was considered through a series of five hypotheses. All work done as part of this study made use of existing data.

Quantitative observations of the clarity of Lake Tahoe date back to the late 19th century (LeConte, 1883). Goldman (1981) described in-lake water-quality and ecosystem changes based on monitoring that began in the 1960s. This monitoring program has been augmented over the years and now includes many more variables describing the physics, chemistry, and biology of the lake and watershed (Schladow, 2019).

The hypotheses in this study were clearly defined by agency representatives to improve the understanding and linkages between long-term observations and variables affecting lake clarity. Many of these variables have been influenced by climate change, and the effects on water quality and the lake ecosystem have been reported in the scientific literature. Climate change in the Lake Tahoe

basin has been reported to drive shifts in time-series trends of long-term weather and hydrological observations such as temperature, snow accumulation, snow-to-precipitation ratios, snowmelt timing, and stream runoff (Dettinger and Cayan, 1995; Hansen and others, 2006; Cayan and others, 2008, 2009; Coats, 2010; Coates and others, 2013a; Roberts and others, 2018). Predicted future climate conditions have been used to investigate degradation of lake water quality caused by thermal stratification and nutrient and sediment influx (Sahoo and others, 2013a; Riverson and others, 2013; Coats and others, 2013b). Climate-induced lake warming and strengthening of thermal stratification has also been shown to favor small-celled *Cyclotella*, which have high surface area-to-volume ratios (Winder and others, 2008). Climate change has resulted in Lake Tahoe water temperature becoming warmer and more hydrodynamically stable (Sahoo and others, 2013b), the duration of stratification is expected to increase, and the lake is expected to become more resistant to deep mixing (Sahoo and others, 2015). The body of the scientific literature—much of it reported more than a decade ago—is consistent with the overall trends in observational data collected to date. The intent of this study was to address specific questions related to seasonal clarity based on observation data already influenced by climate change.

## Purpose and Scope

The purposes of this report are to identify variables that control water clarity in Lake Tahoe and assess their relative influences on seasonal and long-term clarity conditions. Variables suspected to influence clarity include, but are not limited to, biological conditions, such as changing phytoplankton speciation and concentrations due to food web changes; thermal stratification; particle and nutrient insertion depths; and hydrological factors, such as the timing and delivery of external loads and extreme climate conditions. Watershed and in-lake monitoring data were analyzed to identify variables that control seasonal clarity conditions.

Each chapter in this report addresses a specific study objective:

(1) Assimilate available data describing water clarity, stream inflows and sediment concentrations, urban runoff, meteorology, water chemistry, and biological parameters (chapter A of this report). Some of these data were already publicly available online, but the other data have been compiled as a project deliverable for use by others (Watanabe and Schladow, 2021).

(2) Assess trends in water clarity in the lake on different timescales, including differences between summer and winter trends (chapter B of this report).

(3)  Examine five specific hypotheses:

- Hypothesis 1. Clarity is controlled predominantly by the distribution and density of fine particles in suspension (Chapter C of this report).

- Hypothesis 2. The change in trend of winter clarity is a response to decreasing fine suspended-sediment concentrations resulting from load reductions (chapter D of this report).

- Hypothesis 3. Changing hydrodynamic conditions in the lake are increasing thermal stability and resistance to mixing (chapter E of this report).

- Hypothesis 4. The trend of decreasing summer clarity is a result of earlier, prolonged, and more intense stratification (chapter F of this report).

- Hypothesis 5. Ecological (food web) interactions are causing changes in the trends of seasonal or annual clarity (chapter G of this report).

(4)  Answer the following water-quality management questions (chapter H of this report):

- What is controlling the divergence in summer and winter clarity trends?

- How have observed changes in in-lake physical and ecological variables influenced seasonal and historical trends?

New data were not collected to complete the analyses presented in this report, and the study did not include new numerical or analytical modeling. The data were assimilated and analyzed in new ways to evaluate potential trends in different parameters and processes that may be influencing water clarity on long-term timescales. This study did not include efforts to forecast future changes, but the findings may be useful for those who attempt to do so.

## Available Data

This section describes the scope of the effort to compile the data, how data are being provided to potential future users, and how data are defined by metadata.

Most of the data utilized in this project came from one of the following sources:

- The long-term lake monitoring program led by the University of California-Davis (UC Davis) since the 1960s (Watanabe and Schladow, 2021; https://tahoe.ucdavis.edu/monitoring).

- The Lake Tahoe Interagency Monitoring Program (LTIMP) managed by the U.S. Geological Survey as part of the National Water Information System (NWIS; Rowe, 2000; U.S. Geological Survey, 2021; https://waterdata.usgs.gov/nwis).

- The Tahoe Resource Conservation District Regional Stormwater Monitoring Program (RSWMP; Tahoe Regional Planning Agency, 2021; https://monitoring.laketahoeinfo.org/RSWMP).

- The data assimilated during this project are summarized in appendixes 1 and 2. Each time series is discussed briefly here. Many of the data-collection sites are shown in figure A1. Data that are readily publicly available online, such as the U.S. Geological Survey NWIS data repository noted above, were not included in the dataset published in support of this report (Watanabe and Schladow, 2021).

For the purposes of this report, definitions of seasonal periods are consistent with the commonly used "water year" that extends from October 1 to September 30. October 1 of calendar year X is part of water year X+1. "Winter" is defined as the period from December 1 through March 31. Summer is defined as June 1 through September 30. Monitoring data were organized by water year to be consistent with reported values of summer and winter clarity and to account for climatic and hydrologic drivers of water clarity. Differences may exist between reported calendar-year annual averages and water-year annual average values reported here.

## In-Lake Data

The data shown in table A1 that were collected within the lake (as opposed to within tributaries or on land) represent results of the UC Davis and National Aeronautics and Space Administration (NASA) long-term monitoring program at Lake Tahoe. Most of these "in-lake" datasets used in this report were collected at two stations, referred to as LTP and MLTP (Lake Tahoe profiling and mid-Lake Tahoe profiling stations; Watanabe and others, 2016; table A2; fig. A1). All in-lake data used in this report are available publicly from UC Davis (Watanabe and Schladow, 2021).

Secchi disk data were used to define water clarity, in meters (m) of water depth. Jassby and others (1999) discussed the data collection methods and consistency. The methodology for the collection of Secchi disk data has remained constant throughout the measurement program, with data typically collected twice per month since 1967 at the LTP station and once per month since 1970 at the MLTP station.
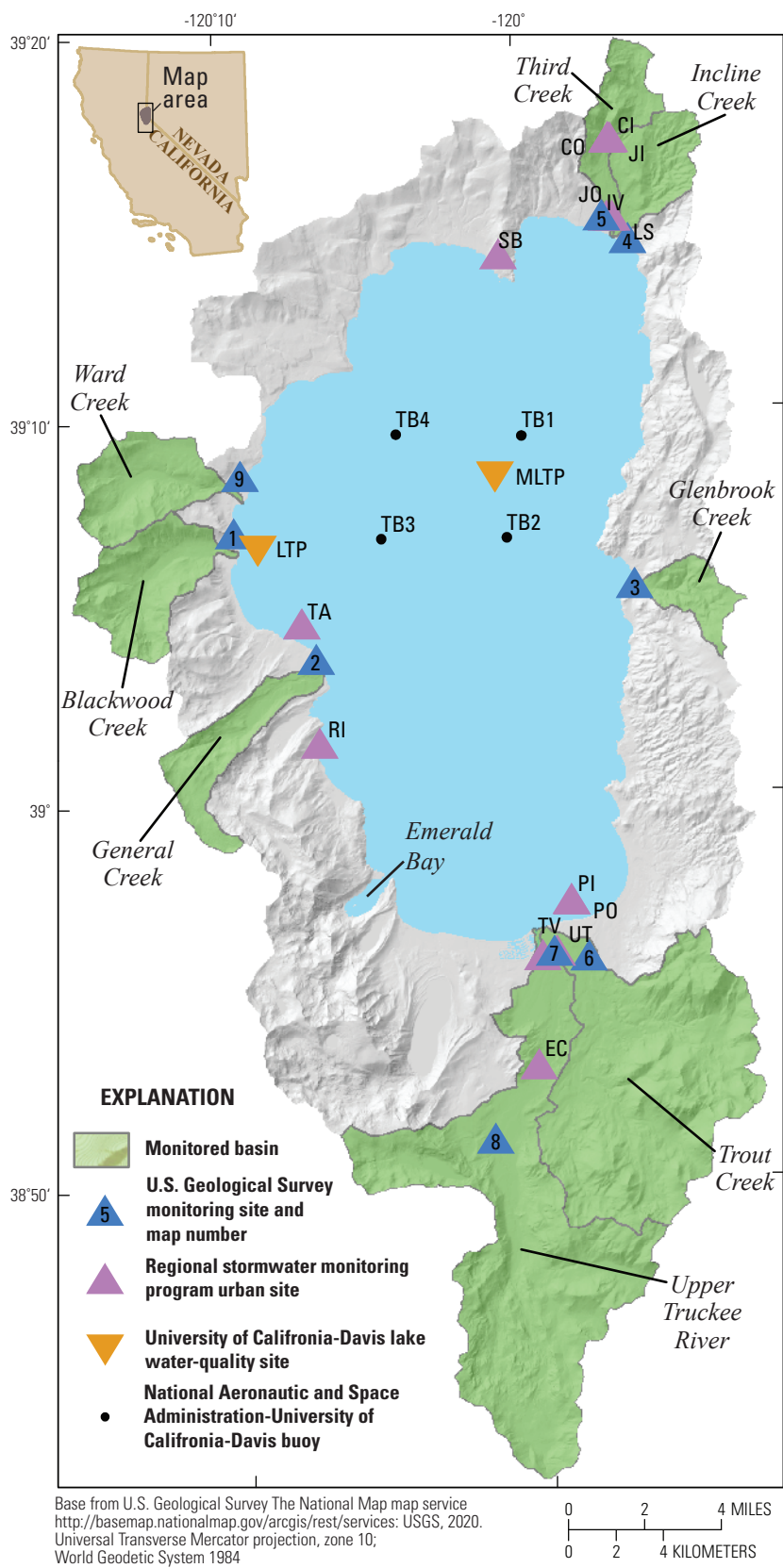
**Figure A1.** Data collection site locations in Lake Tahoe, California and Nevada (U.S. Geological Survey, 2021; Watanabe and Schladow, 2021). U.S. Geological Survey streamgages are shown in table A3 of this report.

**Table A1.**   Summary of data from 1970 to 2020 used to assess water clarity in Lake Tahoe, California and Nevada (Tahoe Regional Planning Agency, 2021; U.S. Geological Survey, 2021; Watanabe and Schladow, 2021).

[mm, month; yyyy, year; MLTP, mid-Lake Tahoe profiling station; LTP, Lake Tahoe profiling station; EB, Emerald Bay; LTMP, Lake Tahoe (interagency) monitoring program; NASA–UC-Davis, National Aeronautics and Space Administration–University of California, Davis; SNOTEL, snow telemetry; TRCD, Tahoe Resource Conservation District; N, nitrogen; P, phosphorus; SSC, suspended sediment concentration]

| Parameter | Location | Period of record (mm/yyyy) | Frequency | Data availability |
|---|---|---|---|---|
| | | | Physical | |
| Secchi depth | MLTP; LTP, EB | 04/1969–12/2019; 07/1967–12/2019; 2011–19 | Variable; 1–2 times per month | https://datadryad.org/stash/dataset/doi:10.25338/B83P8B |
| Water temperature | MLTP; LTP | 1969–96; 1967–96 | Monthly; every 10 days | https://datadryad.org/stash/dataset/doi:10.25338/B83P8B |
| Profiling temperature | MLTP; LTP | 1996–2006; 2005–present | Monthly; Every 14 days | https://datadryad.org/stash/dataset/doi:10.25338/B83P8B |
| Water temperature | NASA-UC-Davis | 2015–20 | Continuous | https://laketahoe.jpl.nasa.gov/downloads/continuous_temperature/Continuous_Temperature_TB_ReadMe.txt |
| Fine-particle size distribution | MLTP; LTP | 2008–11/2019 | Monthly; every 14 days | https://datadryad.org/stash/dataset/doi:10.25338/B83P8B |
| | | | Chemical | |
| Nitrate-nitrogen (NO3) | MLTP; LTP | 1970–present; 1968–present | Monthly; every 14 days | https://datadryad.org/stash/dataset/doi:10.25338/B83P8B |
| Total Kjeldahl nitrogen (TKN) | MLTP | 1989–present | Monthly | https://datadryad.org/stash/dataset/doi:10.25338/B83P8B |
| Toal hydrolyzable phosphorus (THP) | MLTP; LTP | 1996–present; 1996–present | Monthly; every 10 days | https://datadryad.org/stash/dataset/doi:10.25338/B83P8B |
| Total phosphorus (TP) | MLTP | 1989–92, 2000–present | Monthly | https://datadryad.org/stash/dataset/doi:10.25338/B83P8B |
| | | | Biological | |
| Chlorophyll a | LTP | 1984–present | Monthly (profile + composite) since 2007 | https://datadryad.org/stash/dataset/doi:10.25338/B83P8B |
| Chlorophyll a | MLTP | 1984–present | Monthly | https://datadryad.org/stash/dataset/doi:10.25338/B83P8B |
| *Cyclotella* and *Fragilaria* | LTP | 1969–present | Every 10 days, monthly since 2007 | https://datadryad.org/stash/dataset/doi:10.25338/B83P8B |
| Zooplankton crustaceans, rotifers | LTP, EB | 2011–19 | Monthly | https://datadryad.org/stash/dataset/doi:10.25338/B83P8B |
| *Mysis* | LTP, EB | 2011–19 | Monthly | https://datadryad.org/stash/dataset/doi:10.25338/B83P8B |
| | | | Streams | |
| Stream discharge | 10 streams | 1986–present | Continuous | Stream flow |
| Stream nutrient loads | 10 streams | 1986–present | Monthly | https://www.sciencebase.gov/catalog/item/5e4483a3e4b0ff554f642171 |
| | | | Streams—Continued | |
| Stream temperature | 10 streams | 2014–present | Continuous | Stream temperature |
| Nutrient concentrations (N&P) | 10 streams | 1986–present | Approximately 25 per year | Stream nutrient concentration |
| Stream fine sediment particles | 7 streams | 2014–present | Approximately 25 per year | Stream particles |
| Suspended sediment concentration | 10 streams | 1986–present | Approximately 25 per year | Stream suspended sediment concentration |
| | | | Climate | |
| Precipitation | Snotel Ward Creek#3 | 1981–present | Daily | https://www.nrcs.usda.gov/wps/portal/nrcs/detail/nv/snow/products/?cid=nrcseprd1685435 |
| Snow-water equivalent (SWE) | Snotel Ward Creek#3 | 1981–present | Daily | https://www.nrcs.usda.gov/wps/portal/nrcs/detail/nv/snow/products/?cid=nrcseprd1685435 |
| | | | Urban | |
| Urban precipitation | TRCD | 2014–present | Monthly | https://monitoring.laketahoeinfo.org/RSWMP |
| Fine-sediment particles | TRCD | 2014–present | Monthly | https://monitoring.laketahoeinfo.org/RSWMP |
| Total nitrogen | TRCD | 2014–present | Monthly | https://monitoring.laketahoeinfo.org/RSWMP |
| Total phosphorus | TRCD | 2014–present | Monthly | https://monitoring.laketahoeinfo.org/RSWMP |
| Pollution load credits | Basinwide | 2016–present | Yearly | Table 1.2 in *Seasonal and Long-Term Clarity Trend Assessment of Lake Tahoe, California–Nevada* |

**Table A1.** Summary of data from 1970 to 2020 used to assess water clarity in Lake Tahoe, California and Nevada (Tahoe Regional Planning Agency, 2021; U.S. Geological Survey, 2021; Watanabe and Schladow, 2021).—Continued

[mm, month; yyyy, year; MLTP, mid-Lake Tahoe profiling station; LTP, Lake Tahoe profiling station; EB, Emerald Bay; LTMP, Lake Tahoe (interagency) monitoring program; NASA–UC-Davis, National Aeronautics and Space Administration–University of California, Davis; SNOTEL, snow telemetry; TRCD, Tahoe Resource Conservation District; N, nitrogen; P, phosphorus; SSC, suspended sediment concentration]

| Parameter | Location | Period of record (mm/yyyy) | Frequency | Data availability |
|---|---|---|---|---|
| In-lake computed | | | | |
| Stratification length | LTP | 1986–present | Yearly | https://datadryad.org/stash/dataset/doi:10.25338/B83P8B |
| Peak stratification | LTP | 1986–present | Yearly | https://datadryad.org/stash/dataset/doi:10.25338/B83P8B |
| End of stratification | LTP | 1986–present | Yearly | https://datadryad.org/stash/dataset/doi:10.25338/B83P8B |
| Peak buoyancy frequency | LTP | 1986–present | Yearly | https://datadryad.org/stash/dataset/doi:10.25338/B83P8B |
| Maximum buoyancy frequency | LTP | 1986–present | Yearly | https://datadryad.org/stash/dataset/doi:10.25338/B83P8B |
| Stability index | LTP | 1986–present | Yearly | https://datadryad.org/stash/dataset/doi:10.25338/B83P8B |

**Table A2.** Locations of long-term profiling stations (Watanabe and Schladow, 2021) at Lake Tahoe, California and Nevada.

[DDD MM SS, degrees minutes seconds; m, meter; LTP, long-term monitoring station; MLTP, mid-lake long-term monitoring station; N, North; W, West]

| Station name | Location (DDD MM SS) | Water depth (m) |
|---|---|---|
| LTP | 039 07 18 N 120 04 39 W | 120 |
| MLTP | 039 07 52 N 120 00 10 W | 460 |

Water-temperature data collection methods at long-term stations LTP and MLTP have changed since the onset of measurements in 1968. A bathythermograph was utilized at the onset of the monitoring program, through 1970, with data recorded at 3 m vertical intervals. Beginning in 1970, a Martek instrument with reduced vertical resolution was utilized. From 1996 to 2006, an RBR-sourced sensor (RBR, Ltd., Ottawa, Ontario, Canada) was used, and in 2006, the switch was made to the currently utilized Sea-Bird Scientific instrumentation (Bellevue, Washington). Each sensor has different accuracy and resolution limitations, but for the purposes of this report, the data were utilized as reported. Since 2000, water-temperature data have been collected at six buoy locations around the lake.

Sea-Bird instruments were incorporated into the program in 2005 to measure water quality vertically throughout the water column. Continuous observations of water temperature, electrical conductivity, depth, dissolved oxygen, pH, turbidity, photosynthetically active radiation (PAR), and light transmission have been collected. For this study, only profile temperatures were used.

Particle-size distribution data have been collected at the two long-term lake sites since 1999 by laser diffraction using a bench-top instrument. Data collected since 2008 were used in this study because there are questions regarding the quality of some of the data prior to 2008. The post-2008 dataset includes, for multiple depths down to 50 m, the number of particles per milliliter (mL) in each of 14 size classes, spanning a range of 0.5–20 micrometers ($\mu$m).

Chemical and biological time-series datasets were also collected at long-term lake stations. Chemical parameters include nitrate as nitrogen, ammonium as nitrogen, total Kjeldahl nitrogen, total hydrolyzable phosphorus, total phosphorus, and dissolved oxygen. Biological parameters include chlorophyll-a and identification and enumeration of phytoplankton. Periods of record for these parameters vary, with many starting in the 1970s.

## Stream Data

Nine streamgages are routinely monitored by the USGS for streamflow; eight of these streamgages are also sites with water-quality data, including nitrate as nitrogen, ammonia as nitrogen, dissolved phosphorus, soluble reactive phosphorus, and suspended-sediment concentration (SSC; table A3). Streamflow is now reported every 15 minutes, whereas many of the other parameters are measured about 25 times per year. Each value is intended to represent a cross-sectional average across a stream. All USGS data are publicly available (U.S. Geological Survey, 2021).

**Table A3.**    U.S. Geological Survey streamgages on Lake Tahoe tributaries, 1968–2019, Nevada and California (U.S. Geological Survey, 2021).

[All listed stations include measurement of discharge. **Abbreviations**: USGS, U.S. Geological Survey; Calif., California; Q, discharge; T, temperature; Tu, turbidity; WQ water quality; Nev., Nevada]

| Map number | USGS station name | USGS station number | Parameters available on daily basis | Period of record (including intermittent field samples) |
|---|---|---|---|---|
| 1 | Blackwood Creek near Tahoe City, Calif. | 10336660 | Q, T, Tu | 1960–present for Q 1973–present for WQ |
| 2 | General Creek near Meeks Bay, Calif. | 10336645 | Q, T, Tu | 1980–present for Q 1980–present for WQ |
| 3 | Glenbrook Creek at Glenbrook, Nev. | 10336730 | Q, T | 1971–present for Q 1971–2011 for WQ |
| 4 | Incline Creek near Crystal Bay, Nev. | 10336700 | Q, T, Tu | 1969–present for Q 1969–present for WQ |
| 5 | Third Creek near Crystal Bay, Nev. | 10336698 | Q, T, Tu | 1969–present for Q 1969–present for WQ |
| 6 | Trout Creek near Tahoe Valley, Calif. | 10336780 | Q, T, Tu | 1973–present for Q 1973–present for WQ |
| 7 | Upper Truckee River at South Lake Tahoe, Calif. | 10336610 | Q, T, Tu | 1970–present for Q 1970–present for WQ |
| 8 | Upper Truckee River at Highway 50 above Meyers, Calif. | 103366092 | Q | 1990–present for Q 1989–2011 for WQ |
| 9 | Ward Creek at Highway 89 near Tahoe Pines, Calif. | 10336676 | Q, T, Tu | 1972–present for Q 1972–present for WQ |

The Nevada Division of Environmental Protection and the California Regional Water Quality Control Board provided estimates of annual loads of fine sediment particles, total phosphorus, and total nitrogen from urbanized regions to the lake in 2004 and estimates of reductions to these loads achieved in each of the years 2016–19, based on Pollutant Load Reduction Model (PLRM; Pollutant Load Reduction Model Development Team, 2009) results. Beginning in 2014, loads computed using field samples collected from urban monitoring sites (fig. A1 and table D3) were derived from the RSWMP (Tahoe Resource Conservation District, 2020). Urban monitoring sites only account for loading from about 0.26 percent of the terrestrial part of the lake watershed, and loads computed using field samples from urban monitoring sites only represent about 1.3 percent of total urban drainages to the lake based on loading estimates from the PLRM.

Atmospheric deposition data were obtained from UC Davis in the form of annual loads since 2000 at one location, with additional records for 1994 and 1998. Data include annual deposition of dissolved inorganic nitrogen, total nitrogen, and soluble reactive phosphorus (SRP).

Phytoplankton and zooplankton data were obtained from long-term monitoring of Lake Tahoe by UC Davis Tahoe Environmental Research Center (TERC). These data were derived from routine monitoring and individual research projects dating back to the 1960s. For routine-monitoring data, we chose to use phytoplankton monitoring data (Watanabe and Schladow, 2021) collected from 5-m depth to examine relations between phytoplankton abundance and water clarity in Lake Tahoe.

# B. Trends in Lake Tahoe Water Clarity

## Background

Lake Tahoe water clarity (Secchi depth) is a sentinel metric that is potentially influenced by physical and biological processes. Secchi depth data collected about twice per month indicate that clarity has declined throughout the decades of monitoring, with differences apparent between summer and winter patterns (fig. B1). The trendlines (dashed lines) in figure B1 were produced using a generalized additive model, or GAM (Wood, 2006), which allowed for the incorporation of nonlinearity and smoothing (Schladow, 2019).

The trend of decreasing winter water clarity was reduced during 2011–19, but summer water clarity continues to decline (Schladow, 2019). We evaluated the change in clarity and conducted trend analyses on seasonal and monthly data to compute the sign and significance of the trends. The nearly 50-year record can be evaluated over the full time or during periods that are important to evaluating restoration activities. The annual and seasonal clarity can vary widely among different climate conditions, and periodic updating of the trend analyses can inform whether improvements or declines in clarity are statistically significant. Trend analyses on different periods may yield slightly different results. Trends in reported seasonal clarity may also be dominated by only one or two months out of four. Therefore, analyzing monthly clarity data provides insight into seasonal trends and may shed light on the important processes and drivers.

## Datasets

Secchi disk data have been collected in Lake Tahoe about twice per month since 1967 at the LTP station and since 1969 at the deeper MLTP station. Earlier analysis by Jassby and others (1999) discussed the procedure and its repeatability and uncertainty. For the purposes of this report, water clarity is expressed as Secchi depth, in meters below the water surface.

## Approach

Trends in water clarity were assessed in several ways; trend analyses were focused primarily on the LTP dataset, and annual and seasonal variability were considered. In a previous evaluation of clarity trends, Jassby and others (1999) noted variations at seasonal, interannual, and decadal scales with statistically significant trends of decreasing clarity. Here, we apply a similar approach and use Sen's linear model (Helsel and others, 2020) to estimate the trend in annual and monthly data for three periods: 1967–79, 1980–99, and 2000–19. Separating the clarity data into these periods provided nearly 20-year periods to evaluate the statistical significance of long-term trends in clarity. Because the $p$-values used to determine statistical significance are affected by sample size, consideration of shorter periods (5–10 year) for clarity trend analysis resulted in $p$-values that were greater than the level of significance ($\alpha$=0.05) and thus were not statistically significant. The direction of trends is defined by the sign of the computed Z-value, where negative and positive values represent trends of decreasing and increasing water clarity, respectively. The Z-statistic associated with the level of significance ($\alpha$=0.05) is 1.96. Trends in clarity are considered significant ($p$<0.05) when the absolute value of the Z-score associated with the trend test is greater than 1.96.

## Results

### Trends in Annual, Winter, and Summer Water Clarity

Fitted linear trends through the annual, winter, and summer clarity measurements during the three periods reveal a consistent decline in annual and summer clarity, with the exception of a subtle change in the rate of decline during 1980–2000 and 2000–19 winter periods (fig. B2). Considering the period between 1967 to 2019, statistically significant negative trends in clarity were detected for annual, winter, and summer periods, with a loss in clarity of −0.17, −0.13, and −0.19 meters per year (m/yr; $p$<0.05; table B1), respectively. For summer, the negative trend in clarity was statistically significant only for the full period of record, from 1967 to 2019 ($p$<0.05). During the 1967–79 period, the clarity declines were significant at −0.36 and −0.62 m/yr for annual and winter periods only, respectively. During 1967–79, the annual and winter decline in clarity were among the highest rates of −0.36 and −0.62 m/yr, respectively. From 1980 to 1999, the change in clarity remained negative, but the rate of change for annual and winter decreased significantly from the previous analysis period to −0.19 and −0.22 m/yr ($p$<0.05), respectively. For the 2000–19 period, a statistically significant trend was not detected for annual, winter, or summer periods.
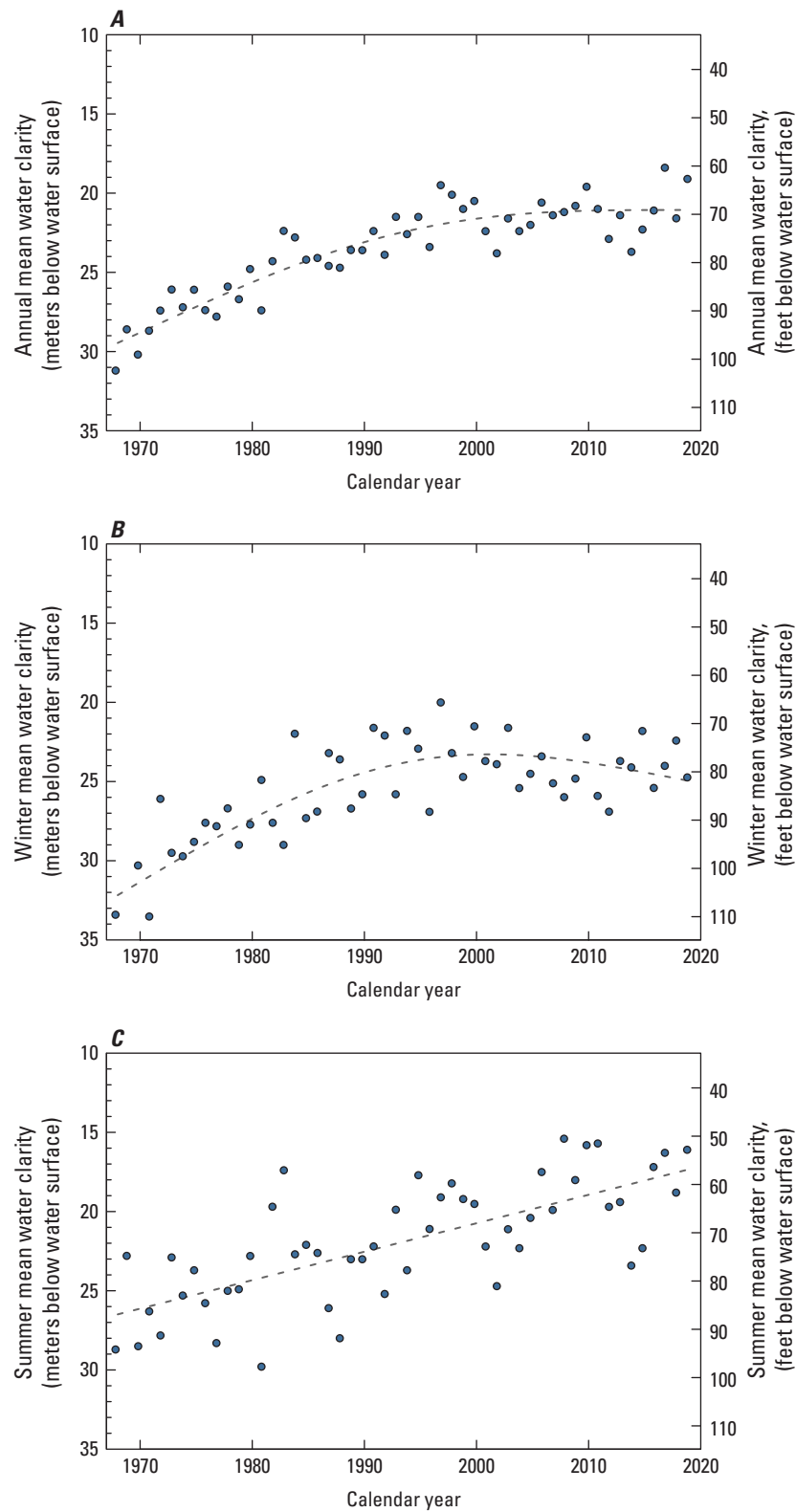
**Figure B1.** Clarity (Secchi depth) of Lake Tahoe at the Lake Tahoe profiling (LTP) station during the following periods from 1970 to 2020: *A*, annual; *B*, winter; and *C*, summer (Watanabe and Schladow, 2021). The dashed trend line is from a generalized additive model (Schladow, 2019). Calendar year was used to define annual values.
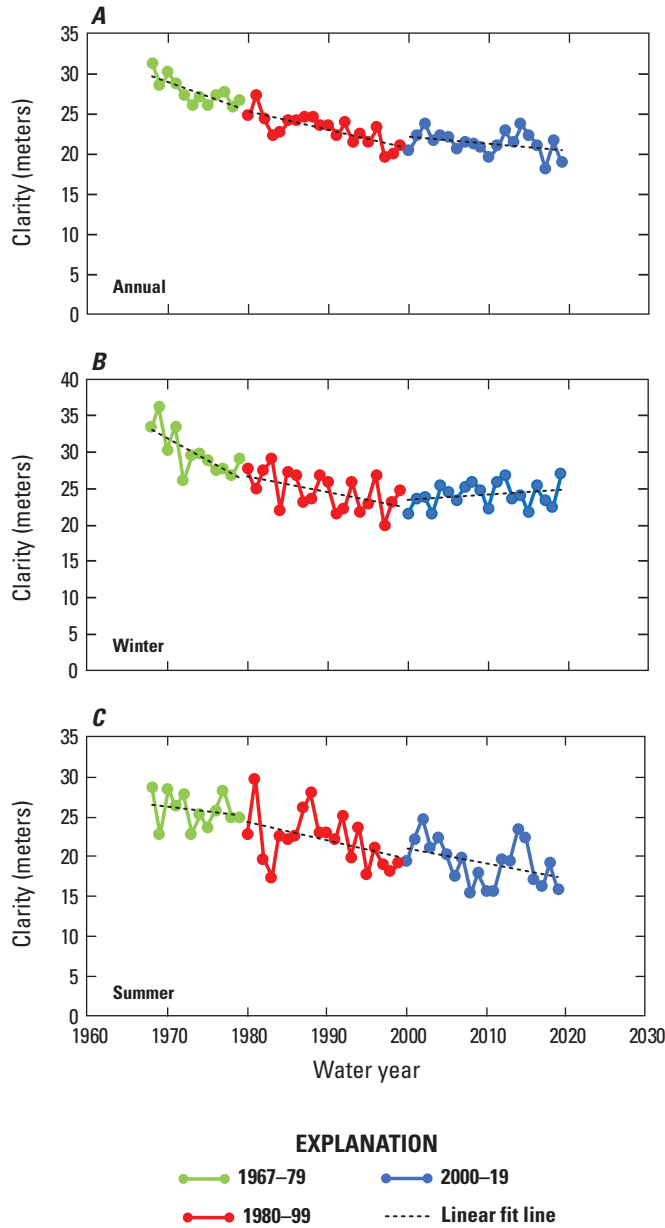
**Figure B2.**    Water clarity at Lake Tahoe profiling station, during 1967–79, 1980–99, and 2000–19, for *A*, annual; *B*, winter; and *C*, summer (Watanabe and Schladow, 2021).

**Table B1.**    Results of trend analyses of water clarity in Lake Tahoe for annual, winter, and summer seasons during 1967–2019, 1968–79, 1980–99, and 2000–19 (Watanabe and Schladow, 2021).

[Values of n represent the number of measurements, sign of test Z statistic indicates the sign of the trend (positive or negative), Sen's slope is the rate of change in clarity, in meters per year. Where p-values cell is blank, significance level is greater than 0.05. **Abbreviation**: <, less than]

| Parameter | Annual | Winter | Summer |
|---|---|---|---|
| 1967–2019 | | | |
| n | 52 | 52 | 52 |
| Test Z | −6.9 | −4.4 | −5.5 |
| p-value | <0.05 | <0.05 | <0.05 |
| Sen's Slope | −0.17 | −0.13 | −0.19 |
| 1967–79 | | | |
| n | 12.0 | 12.0 | 12.0 |
| Test Z | −2.4 | −2.3 | −0.9 |
| p-value | <0.05 | <0.05 | — |
| Sen's Slope | −0.36 | −0.62 | −0.14 |
| 1980–99 | | | |
| n | 20 | 20 | 20 |
| Test Z | −3.6 | −2.3 | −1.6 |
| p-value | <0.05 | <0.05 | — |
| Sen's Slope | −0.22 | −0.19 | −0.24 |
| 2000–19 | | | |
| n | 20 | 20 | 20 |
| Test Z | −1.1 | 1.0 | −1.8 |
| p-value | — | — | — |
| Sen's Slope | −0.08 | 0.08 | −0.22 |

## Trends in Monthly Water Clarity

Monthly clarity data were evaluated for the same analysis periods as the annual, winter, and summer data presented in the previous section (fig. B3). Trend analyses of monthly water clarity data indicated trends in fall and spring clarity in Lake Tahoe that were not observed in trend analysis of annual water clarity data. For example, trends for fall (October and November) monthly clarity were similar to those for winter (December to March; fig. B3). Declines in clarity trends in November and December for the period of 1967–2019 were −0.16 and −0.17 m/yr, respectively (table B2). The consistency in trends indicates that drivers of winter clarity are influenced by processes during the previous fall. Trend analyses revealed that significant trends in clarity were not detected during 2000–19 for all months except July and August. Comparing the 1980–99 and 2000–19 analysis periods, changes from significantly decreasing clarity to no trend were identified for November, December, and May. Several months were found to have statistically significant rates of clarity decline during 1980–99 that switched to no trend during 2000–19: November, December, May, and August. During summer

months of 2000–19, the largest statistically significant (p<0.05) negative trends were found in July (−0.33 m/yr) and August (−0.29 m/yr; table B2). For July and August, the slope of the trend in clarity slightly increased −0.13 and −0.08 m/yr since 1967.

Seasonal variations in clarity are thought to be driven by winter mixing, sediment inflows from streams and urban areas, and by biogenic particles (Jassby and others, 1999; Sahoo and others, 2010). Throughout the extent of the clarity monitoring program, winter mixing, typically in February or March, improves lake clarity by bringing up clear water from deep within the lake to the surface (fig. B4). During the 1980–99 period, however, the monthly median value of clarity was reduced in all months compared to the previous analysis period despite continuation of the same temporal pattern in water-column mixing. Since 2000, median clarity has been reduced in fall, summer, and during the month of May. Median clarity values have not changed during winter (December to March) and April since 1980. Since 1967, the largest decline in median clarity (8.5 m) was in the month of October.
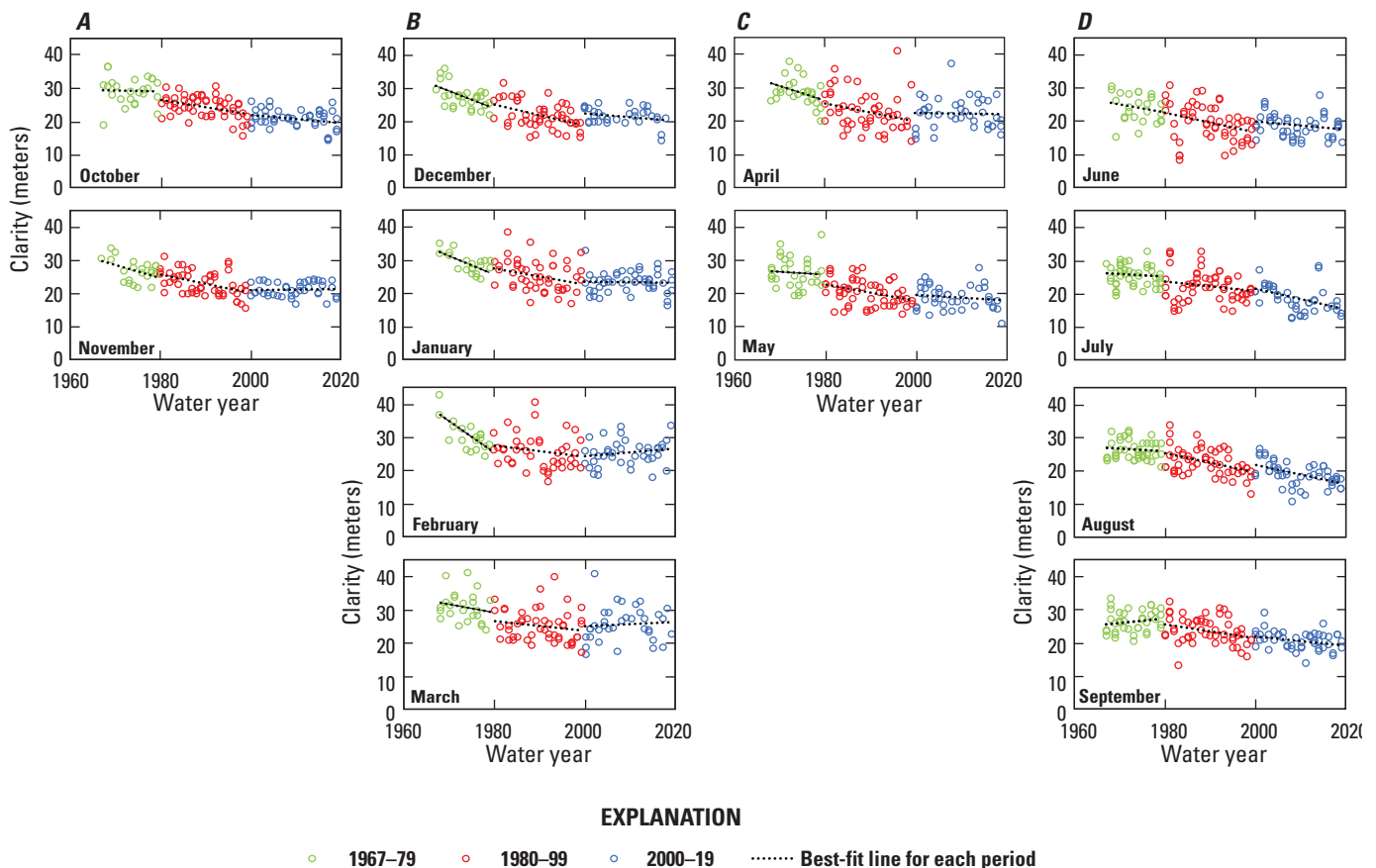


**Figure B3.** Observed water clarity (Watanabe and Schladow, 2021) in Lake Tahoe during 1967–79, 1980–99, and 2000–19 for A, fall; B, winter; C, spring; and D, summer.

**Table B2.**   Mann-Kendall trend analysis of Lake Tahoe water clarity for individual months during 1967–2019, 1967–79, 1980–99, and 2000–19 (Watanabe and Schladow, 2021).

[Values of n represent the number of measurements, sign of test statistic Z indicates the sign of the trend, Sen's slope is the rate of change in clarity, in meters per year. Where p-value cells are blank, significance level is greater than 0.05. Results indicate statistically significant declines in clarity for the entire period of record. Trends analysis over 20-year periods with monthly data resulted in no apparent trends for 10 of 12 months. **Abbreviations**: Oct, October; Nov, November; Dec, December; Jan, January; Feb, February; Mar, March; Apr, April; Jun, June; Jul, July; Aug, August; Sep, September; <, less than]

| Parameter | Fall | | Winter | | | | Spring | | Summer | | | |
|---|---|---|---|---|---|---|---|---|---|---|---|---|
| | Oct | Nov | Dec | Jan | Feb | Mar | Apr | May | Jun | Jul | Aug | Sep |
| **1967–2019** | | | | | | | | | | | | |
| n | 53 | 51 | 50 | 49 | 50 | 52 | 50 | 52 | 52 | 52 | 53 | 53 |
| Test Z | −6.2 | −5.0 | −4.9 | −4.1 | −2.4 | −2.1 | −3.7 | −4.8 | −3.9 | −5.0 | −6.3 | −4.8 |
| p-value | <0.05 | <0.05 | <0.05 | <0.05 | <0.05 | <0.05 | <0.05 | <0.05 | <0.05 | <0.05 | <0.05 | <0.05 |
| Sen's slope | −0.20 | −0.16 | −0.17 | −0.14 | −0.09 | −0.10 | −0.17 | −0.18 | −0.16 | −0.20 | −0.21 | −0.15 |
| **1967–79** | | | | | | | | | | | | |
| n | 13 | 11 | 13 | 10 | 10 | 12 | 12 | 12 | 12 | 13 | 13 | 13 |
| Test Z | 0.5 | −0.6 | −2.8 | −1.3 | −2.0 | −0.5 | −1.0 | 0.0 | −1.0 | −1.0 | −0.2 | 1.0 |
| p-value | — | — | <0.05 | — | <0.05 | — | — | — | — | — | — | — |
| Sen's slope | 0.28 | −0.42 | −0.55 | −0.50 | −0.80 | −0.28 | −0.41 | 0.00 | −0.30 | −0.34 | −0.06 | 0.18 |
| **1980–99** | | | | | | | | | | | | |
| n | 20 | 20 | 20 | 19 | 20 | 20 | 20 | 20 | 20 | 20 | 20 | 20 |
| Test Z | −1.6 | −3.5 | −2.4 | −1.6 | −0.7 | −0.8 | −1.9 | −2.0 | −1.9 | −0.3 | −2.3 | −1.4 |
| p-value | — | <0.05 | <0.05 | — | — | — | — | <0.05 | — | — | <0.05 | — |
| Sen's slope | −0.19 | −0.37 | −0.33 | −0.30 | −0.15 | −0.12 | −0.28 | −0.19 | −0.42 | −0.03 | −0.24 | −0.18 |
| **2000–19** | | | | | | | | | | | | |
| n | 20 | 20 | 17 | 20 | 20 | 20 | 18 | 20 | 20 | 19 | 20 | 20 |
| Test Z | −0.7 | 0.6 | −1.1 | 0.2 | 0.8 | 0.3 | −0.5 | −0.8 | −1.5 | −2.4 | −2.1 | −1.1 |
| p-value | — | — | — | — | — | — | — | — | — | <0.05 | <0.05 | — |
| Sen's slope | −0.07 | 0.04 | −0.06 | 0.03 | 0.12 | 0.06 | −0.05 | −0.21 | −0.19 | −0.33 | −0.29 | −0.13 |

Variations in monthly clarity can reveal whether seasonal drivers are becoming influential. For example, for the period of record (1967–2019), coefficients of variation in clarity have been lowest during the fall and highest in the spring and summer (fig. B4B). During 1967–1979, the coefficient of variation for clarity ranged from 10 percent to 17 percent with an annual average of 14 percent. During 1980 to 1999, the corresponding range of variability was 15 to 27 percent, with an average of 19 percent. Coefficient of variation values for the most recent period (2000–19) ranged from 10 to 21 percent with an annual average of 16 percent. Comparing the two periods 1980–1999 and 2000-2019, the variation in clarity readings for the six months of October, December, February, May, June, and September have been relatively stable. Since 2000, the seasonal variations in monthly clarity are lower in the fall and increase gradually during winter through mid-summer (June). From August to September, the variations gradually decrease levels consistent with October.
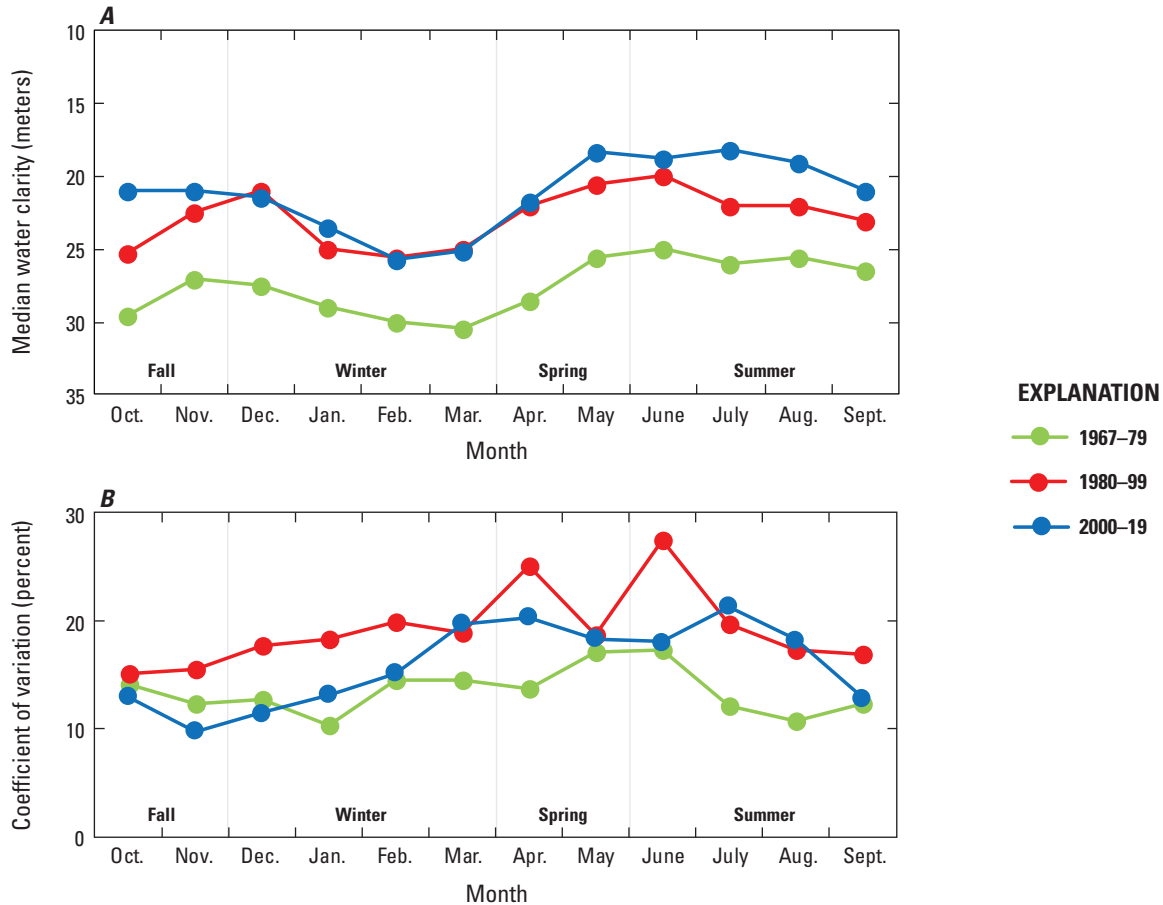
**Figure B4.**    Seasonal changes in monthly water-clarity values for Lake Tahoe during 1967–79, 1980–99, and 2000–19 (Watanabe and Schladow, 2021): *A*, median; and *B*, coefficient of variation, CV = 100*(standard deviation/mean).

## Summary of Findings for Assessment of Trends

During the period of record (1967–2019), Lake Tahoe water clarity has declined significantly based on analyses considering each month and annual data. From 2000-2019, lake clarity values did not have significant negative trends for 10 of 12 months. During this period, the slope of the clarity trend cannot be differentiated statistically from zero for 10 months of the year. This was different from the 1980–99 period, where one month in every season, or 4 out of 12 months, had statistically significant negative trends. July and August were the only months during the most recent period for which statistically significant negative trends were identified. Further, the data show more variability in fall, winter, and spring during the 1980–99 period compared to other periods. Further evaluation of climate, watershed, and lake data could provide insight into how climate change may influence future clarity conditions.

# C. Hypothesis 1: Clarity is Controlled Predominantly by the Distribution and (Volumetric) Density of Fine Particles in Suspension

## Background

Early studies of Lake Tahoe water-clarity changes focused on phytoplankton productivity and the onset of cultural eutrophication (Goldman and others, 1979). More recent work has concluded that inorganic particles play a larger role in controlling clarity (Swift and others, 2006). Jassby and others (1999) concluded that particles less than 16 μm in diameter most significantly affected clarity. Coker (2000) concluded that in-lake inorganic particles were dominated by the 1–10 μm size class. Subsequent investigations considered the spatial and temporal distribution of particles, their aggregation, abundance in streams, and effect on light attenuation (Sunman, 2004; Swift and others, 2006). In this report, a further refinement to examine the effect of particles in the 1.00–4.76-μm size range was considered because of previously published work on the effect of the size of suspended inorganic particles on light transmission. The influence of *Cyclotella* cells, which are organic in origin but contain a silica frustule, was also examined.

## Datasets

Hypothesis 1 was examined by analysis of fine-particle data obtained by UC Davis at the two long-term, in-lake profiling stations (MLTP, LTP). Characteristics of these datasets are provided in table C1. Hypothesis 1 is focused on the link between clarity and the abundance of particles per unit volume in the lake, regardless of the origin or type. Particle abundance is a more appropriate term than density because the latter term typically refers to the mass per unit volume of individual particles.

UC Davis uses a laser-diffraction instrument (LiQuilaz, Particle Measuring Systems, Inc., Boulder, Colo.) to measure particle abundance for each of 16 particle-size classes, ranging from 0.5 to 20.0 μm (table C1), from discrete samples collected at each depth. Results are reported as particle counts per milliliter (mL). This measurement technique does not provide information about particle origin, shape, or material density.

Suspended particles absorb and scatter a fraction of the light impinging on them, resulting in the attenuation of the light. The attenuation efficiency varies in a complex manner with particle size and composition. The work of Van de Hulst (1957) showed theoretically that the attenuation efficiency is maximized at a particle diameter of 1.70 μm for inorganic particles such as quartz and at about 6.50 μm for organic particles, whereas Davies-Colley and Smith (2001) reported corresponding values of 1.20 and 5.00 μm. Outside of this size range (Davies-Colley and Smith, 2001), the magnitude of light attenuation by suspended particles rapidly decreases. Diatoms, which are organic particles that possess a silica frustule, may exhibit characteristics of both organic and inorganic particles, and given the size range of diatoms commonly observed in Lake Tahoe, may be expected to scatter light at similar attenuation efficiencies. Swift and others (2006) incorporated many of these concepts in the development of the Lake Tahoe clarity model, using the data available at the time. Given the hypothesis proposed, the size resolution of the particle analyzer, and published information on light attenuation, particle analysis focused on both the total collection of particles (all sizes) and on a subset representing finer inorganic particles in the 1.00–4.76 μm range. Abundance greater than 4.76 μm is limited, so the chosen number for the upper bound of this range has little influence on the analysis or results.

**Table C1.** In-lake datasets used to examine fine-particle abundance and distribution in Lake Tahoe, 2008–19 (U.S. Geological Survey, 2021; Watanabe and Schladow, 2021).

[LTP, Lake Tahoe profiling station; MLTP, mid-Lake Tahoe profiling station; m, meter; μm, micrometer]

| Site | LTP | MLTP |
|---|---|---|
| | Fine-particle data 2008–19 | |
| Sampling depths (m) | 0, 2, 5, 10, 15, 20, 30, 40, 50 | 0, 10, 50 |
| Size classes (μm) | 0.50–0.62, 0.63–0.78, 0.79–0.99, 1.00–1.40, 1.41–1.99, 2.0–2.82, 2.83–3.99, 4.00–4.75, 4.76–5.65, 5.66–6.72, 6.73–7.99, 8.00–11.30, 11.31–15.99, 16.00–20.00 | 0.50–0.62, 0.63–0.78, 0.79–0.99, 1.00–1.40, 1.41–1.99, 2.00–2.82, 2.83–3.99, 4.00–4.75, 4.76–5.65, 5.66–6.72, 6.73–7.99, 8.00–11.30, 11.31–15.99, 16.00–20.00 |
| | *Cyclotella* 2002–19 | |
| Sampling depth (m) | 5 | — |

## Approach

Eleven years (2008–19) of particle size data were examined to determine trends in particle abundance through time, by depth, and in terms of grain size. *Cyclotella* cell abundance data, derived from labor-intensive microscopy, were available for a part of the 11-year record.

Correlation analysis (linear regression; Helsel and others, 2020) was completed to determine the influence of particle abundance on clarity. A separate correlation analysis was completed to determine the effects of *Cyclotella* cell abundance on clarity. Data collected from 5-m depth and deviations of clarity from the 20-year mean were used in both correlation analyses.

## Results

The finest particles within the measured range of 0.50–20.00 µm consistently had the greatest abundance, and abundance had little depth-dependence in the range of depths examined. Figure C1 shows abundance through time for the finest size class (0.50-0.63 m) observed at the shallower LTP station. This figure shows data from all available observations (typically twice per month) for the top 20 m of the water column (the depth range from 20 to 50 m shows similar temporal fluctuations in abundance). Other than an anomalous surface reading in water year 2011 that was thought to be erroneous, little depth dependence was observed. A marked increase in particle abundance was evident in 2017, most likely due to the high inflows to the lake following an extended drought. Some reduction is evident after 2017, but the mean value for 2017–19 is higher than the mean of the previous decade.
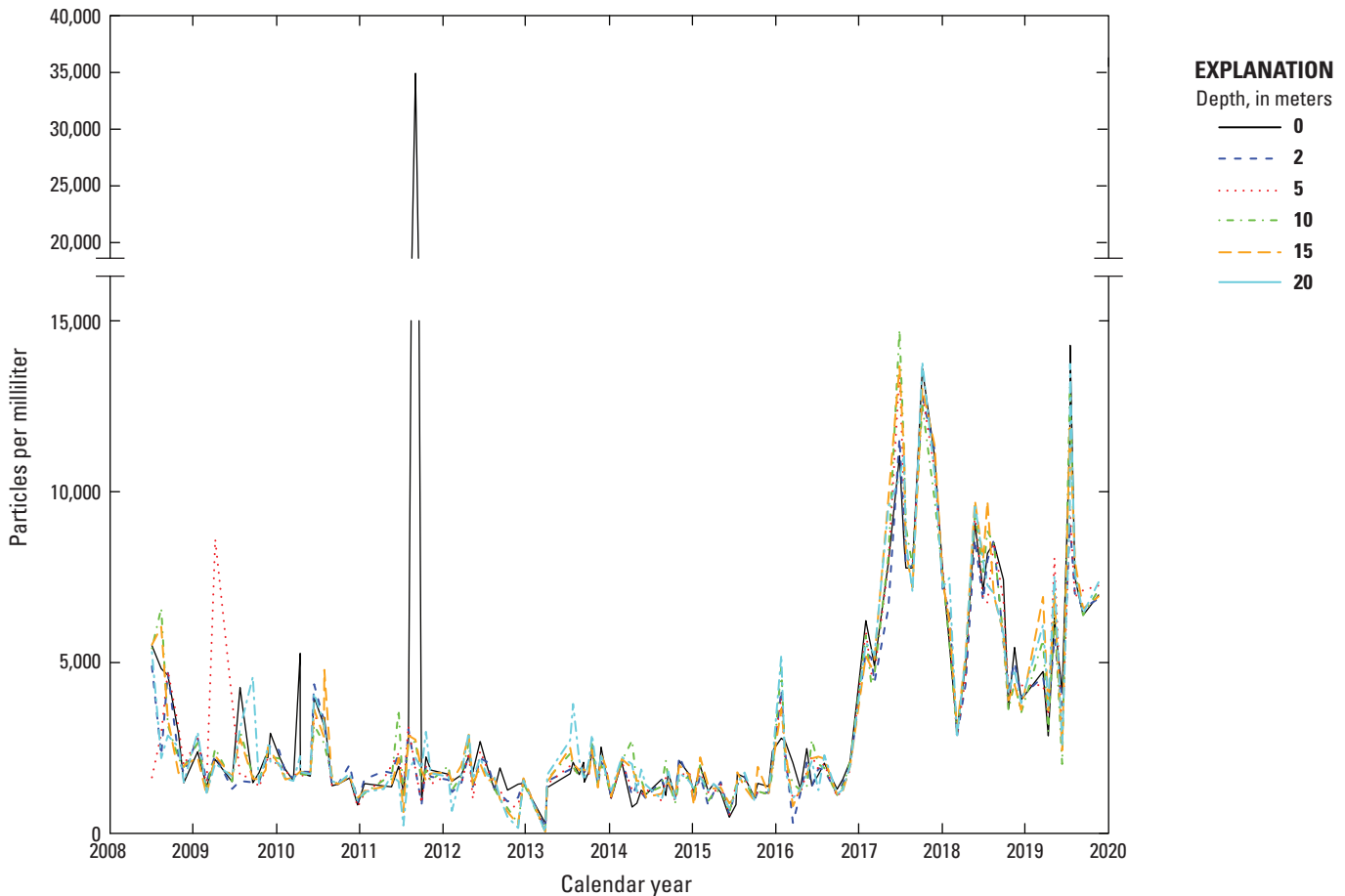


**Figure C1.** Particle count per milliliter for finest size class (0.50–0.63 micrometer) at Lake Tahoe profiling (LTP) station, 2008–19. The 2011 spike at 0-meter depth is thought to be erroneous (U.S. Geological Survey, 2021; Watanabe and Schladow, 2021). See table A1 of this report for period of record and frequency.

An annual periodicity was more evident in some of the time series for a slightly larger size class (fig. C2). The number of particles per unit volume decreased with increased particle size, as seen when comparing the scales on the y-axes in figures C1 and C2. The two smallest size classes (spanning 0.50–0.79 μm) typically represent two-thirds of the total number of particles in a sample. For size classes larger than 4.00 μm, particle counts were in the range of tens to hundreds of particles per milliliter. The periodicity apparent in figure C2 was less evident in the larger size classes, but all particle sizes increased notably in abundance beginning in 2017. The annual periodicity could be partially attributable to seasonal abundance of cells, discussed further later in this section.

Mean particle size was consistently between 0.8 and 1.2 μm, with little depth or time dependence. Analysis of the 2008–19 time series data for each depth indicated that there were no statistically significant trends in the annual mean grain diameter. The 11-year period analyzed is likely too short for interpretation of interannual trends, however.

Figure C3 shows particle abundance by season for 2008–19, focusing on data collected from a depth of 5 m and particles in the optically significant range of 1.00–4.76 μm. Each of the years during 2016–19 showed a large increase in particle abundance compared to previous years, but in different seasons. Rather than high concentrations of particles present predominantly in summer only (as was the case in 2009–15, with the exception of spring 2009), markedly high concentrations were observed during spring and fall 2017–19. This extension of the "high-particle concentration" time of year could influence the average annual clarity. The Secchi depth was greater in years 2012–15 (mean 22.6 m) and less in 2016–19 (mean depth 22.0 m).

The time series showing the distribution of particles in the water column for 2018 demonstrates the observed seasonal variability in water clarity. Figure C4 illustrates the influence of spring mixing events that result in more particles appearing at greater depths and a reduction in particle abundance near the surface. During the rest of 2018, most of the measured particles are above a depth of 50 m, where most data were collected, and a consistent relation between depth and particle abundance was not observed above this depth.

A similar analysis of particle abundance was completed with the data from the MLTP station, where data were obtained at the 0, 10, and 50 m depths. Results were similar to those for the LTP station: 70–80 percent of the suspended particles were less than or equal to 1 μm in size, little depth-dependence was evident down to 50 m, and a large increase in particle abundance in 2017 likely resulted from high inflows of sediment from streams. A statistically significant trend was not identified in particle abundance through time for any depth. Correlations of observed particle abundances in the lake and in streams are discussed in the next section.
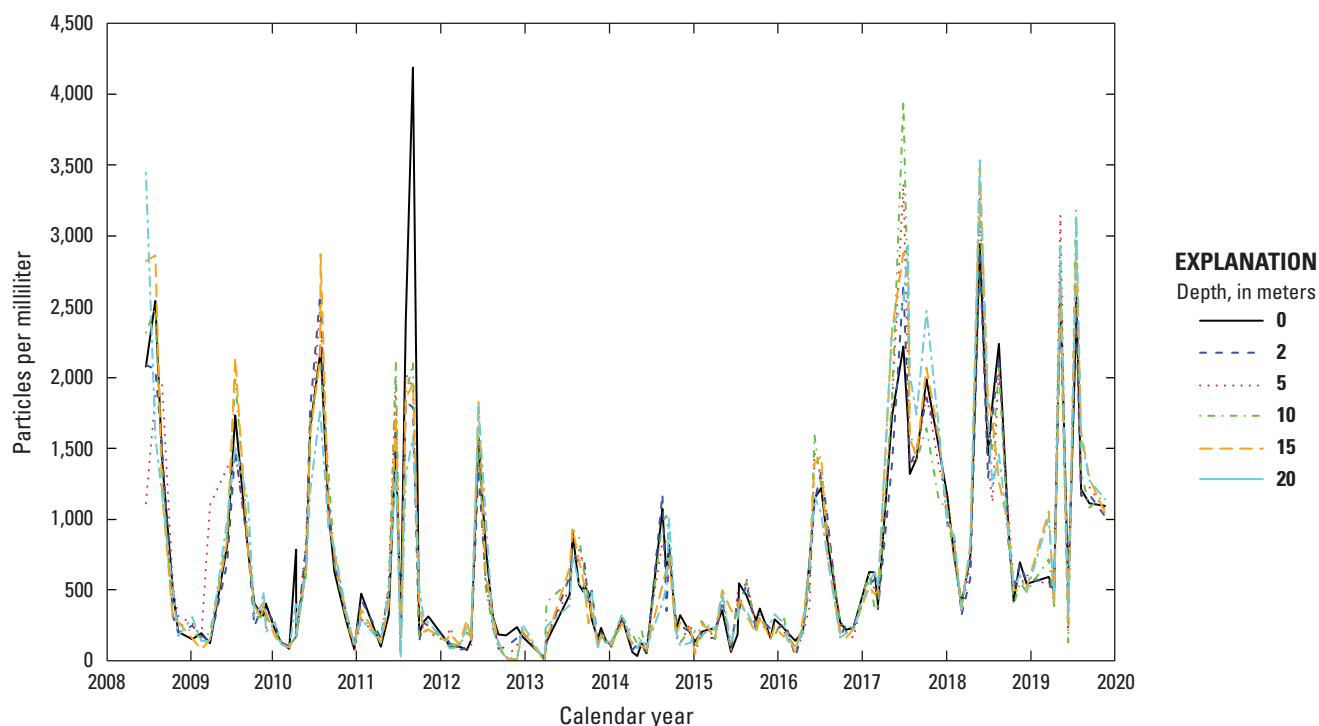


**Figure C2.**     Particle count per milliliter for 1.41–2.00-micrometer size class at the Lake Tahoe profiling (LTP) station, 2008–19 (Watanabe and Schladow, 2021). The 2011 spike at 0-meter depth is thought to be erroneous. See table A1 of this report for period of record and frequency.
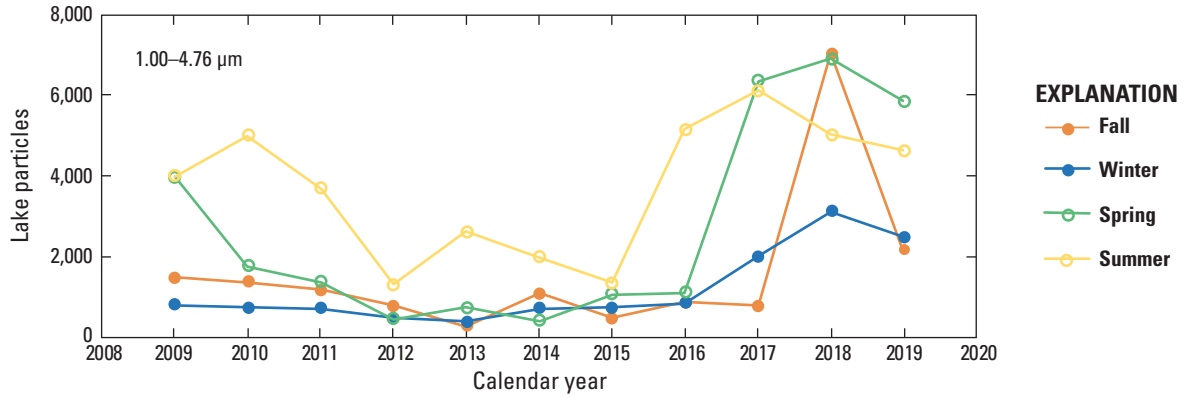
**Figure C3.** Interannual and seasonal variability in-lake particle abundance for 1.00–4.76-micrometer (µm) size class, in particles per milliliter, observed at 5-meter depth, 2009–19 (Watanabe and Schladow, 2021). Each point represents a mean value for the season and year represented.
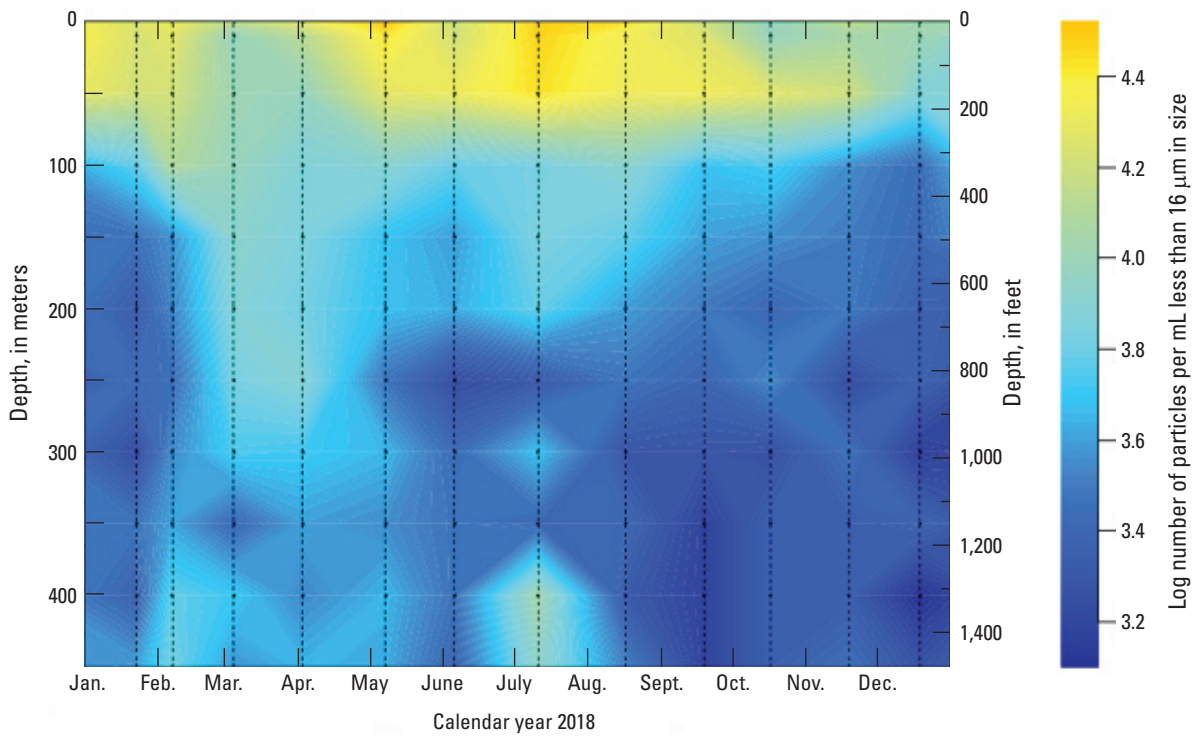


**Figure C4.** Relations between number of particles less than 16 micrometers (µm) in diameter in the lake per milliliter (mL) and depth during calendar year 2018 (Schladow, 2019). Vertical dash lines represent discrete periods of observations and the basis for interpolation.

The mean value of water clarity, based on Secchi depth observations, for the 2008–19 record was computed and subtracted from the clarity time series to yield a "clarity deviation" time series that is plotted as the gray line in figure C5B. Part C of figure C5 shows the correlation between clarity deviation and the log of the particle abundance for the 1.00–4.76 um range at 5 m depth. The coefficient of determination ($R^2$) indicates there is a negative correlation between clarity deviation and particle abundance at this depth ($R^2 = 0.397$). This correlation also indicates that during spring and summer, particle counts can exceed 1,000 counts/mL and have a negative effect on lake clarity. Particle counts less than 1,000 counts/mL do not appear to affect lake clarity.
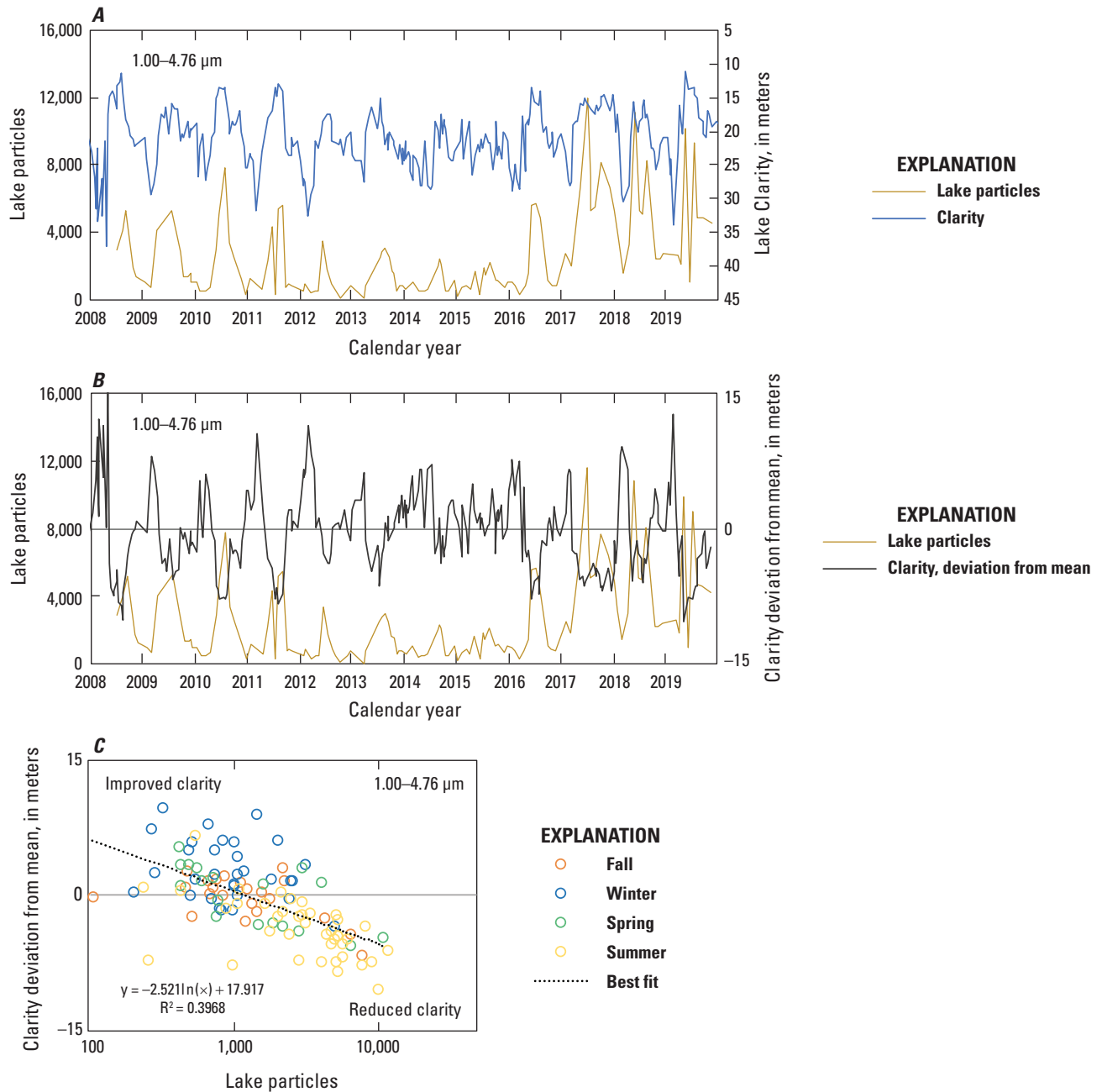


**Figure C5.**   Time-series dataset of different aspects of clarity and particle abundance at 5-meter depth in Lake Tahoe, 2008–2019 (Watanabe and Schladow, 2021). A, particle abundance per milliliter in the 1.00–4.76-micrometer (µm) size range; B, particle abundance and clarity deviation from mean (1.00–4.76 µm ); and C, clarity deviation from mean versus log of particle count per season (1.00–4.76 µm).

Figure C6 presents results comparing the deviation of clarity from its mean value to estimated abundance of *Cyclotella* cells. *Cyclotella* are small diatoms that were first reported in Lake Tahoe in 1975 (Richards and others, 1975) and more recently have been reported as displaying a decreasing size through time (Winder and others, 2008). A negative correlation between clarity deviation from the mean and *Cyclotella* was found ($R^2$=0.288). A decrease in clarity was apparent when *Cyclotella* exceeded 100 cells/mL, which typically was exceeded in summer and fall *Cyclotella*

counts less than 100 cells/mL did not appear to affect lake clarity. Seasonal variation in *Cyclotella,* lake particles, and lake clarity are shown in appendix 2.

Taken together, figures C5 and C6 indicate that the abundance of particles in the 1.00–4.76 µm range and the abundance of *Cyclotella* cells are negatively correlated with clarity deviation but do not fully explain observed trends in clarity deviation. The correlations indicate other factors or processes are also influencing clarity.
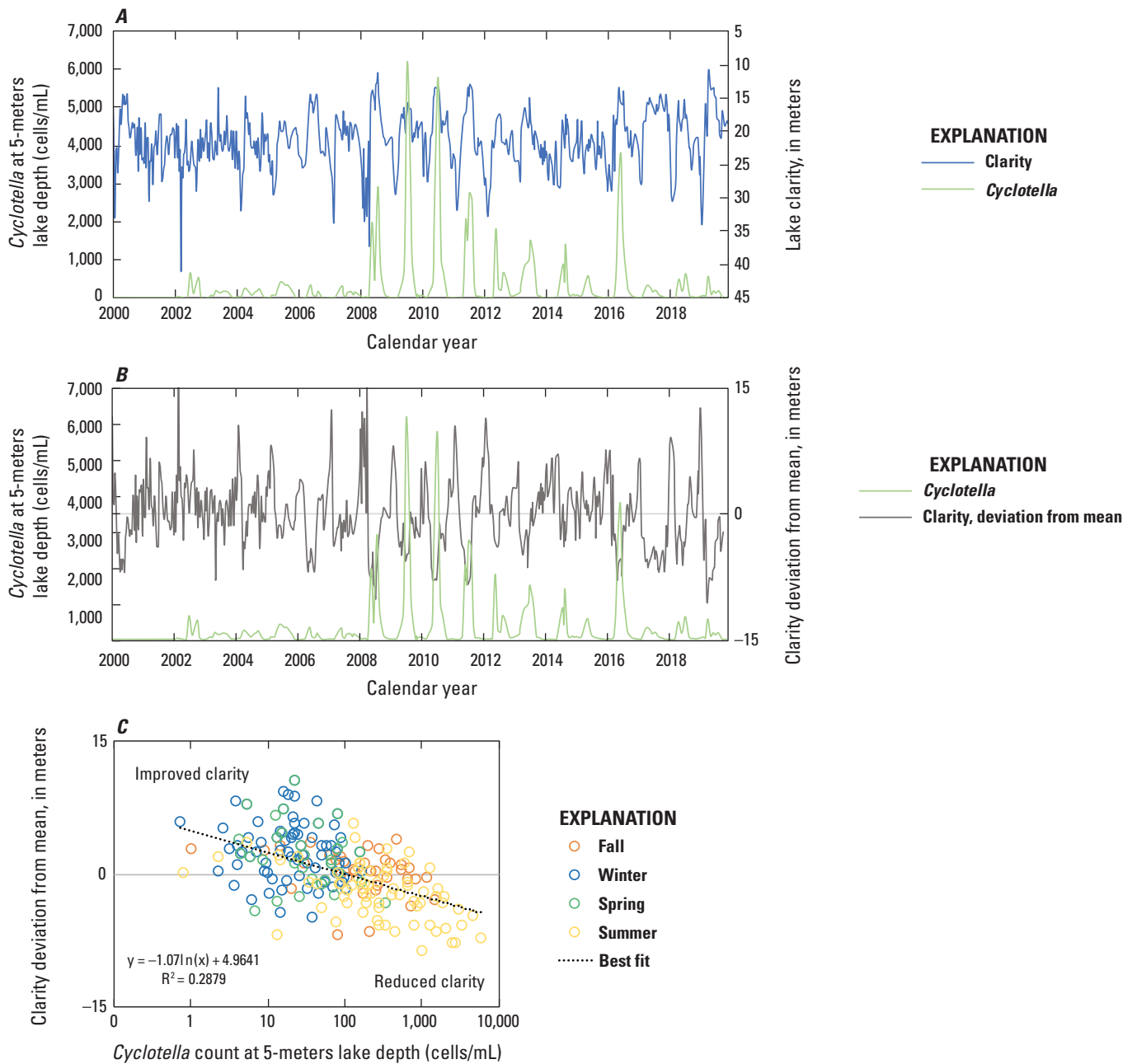


**Figure C6.**   Time-series dataset of different aspects of clarity and *Cyclotella* abundance in cells per milliliter (cells/mL) at 5-meter depth in Lake Tahoe, 2008–19 (Watanabe and Schladow, 2021), by *A*, clarity and abundance of *Cyclotella*; *B*, clarity deviation from mean and *Cyclotella* abundance; and *C*, clarity deviation from mean against log of *Cyclotella* abundance by season.

The particle abundance data include *Cyclotella* cells, live and dead. Figure C7 shows time series of the total particle abundance and estimated number of *Cyclotella* cells. In the past, the brief peaks in particle abundance have coincided with *Cyclotella* peaks and reduced clarity. The high particle abundance in 2017–19, however, does not appear to be correlated with the abundance of *Cyclotella* at the 5 m depth. The order of magnitude increase in particle abundance (0.50–20 μm) that began in 2017 did not lead to a similarly dramatic decrease in clarity, lending support to the finding that particles of different sizes have different relative influences on clarity.

In 2017, stream inflows to Lake Tahoe were exceptionally high. The 4 years of peak *Cyclotella* abundance (2008–11) coincided with the 3 lowest years of summer Secchi depth ever recorded. The next lowest Secchi depths were recorded in 2017 and 2019, when *Cyclotella* abundance was low, indicating the distinct roles of inorganic and organic fine particles.

A positive statistically significant correlation ($p<0.05$) between the inverse of the Secchi disk depth and particle abundance for different subsets of the observed size range (fig. C8). The strongest correlation is for the particle fraction larger than 1 μm, which is consistent with the earlier conclusion that organic and inorganic particles less than 1 μm in size have little effect on clarity compared to slightly larger particles.
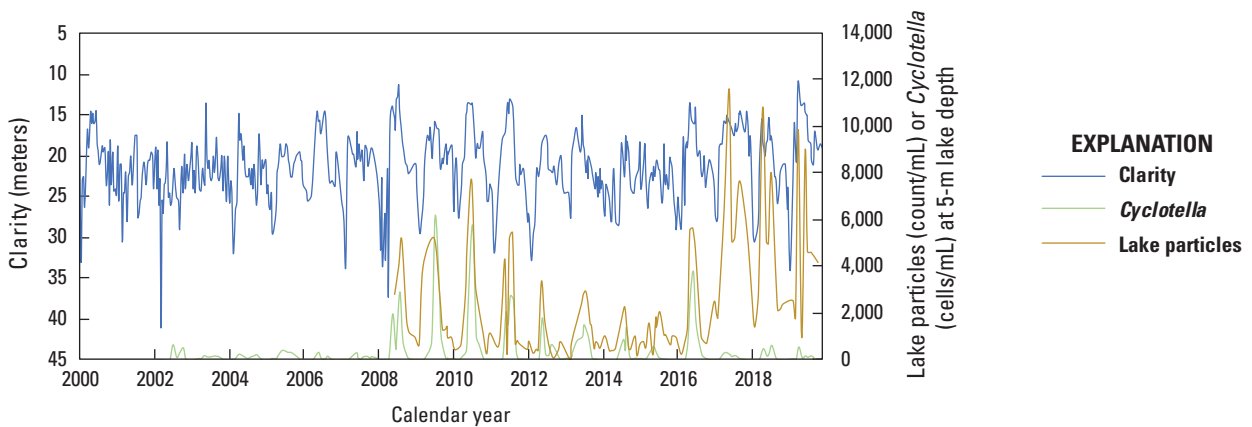


**Figure C7.**    Time series of lake clarity with counts of in-lake particles (1.00–4.76 micrometers in size) per milliliter (count/mL) and *Cyclotella* cells per milliliter (cells/mL) at 5-meter depth at the Lake Tahoe profiling (LTP) station, 2000–20 (Watanabe and Schladow, 2021).
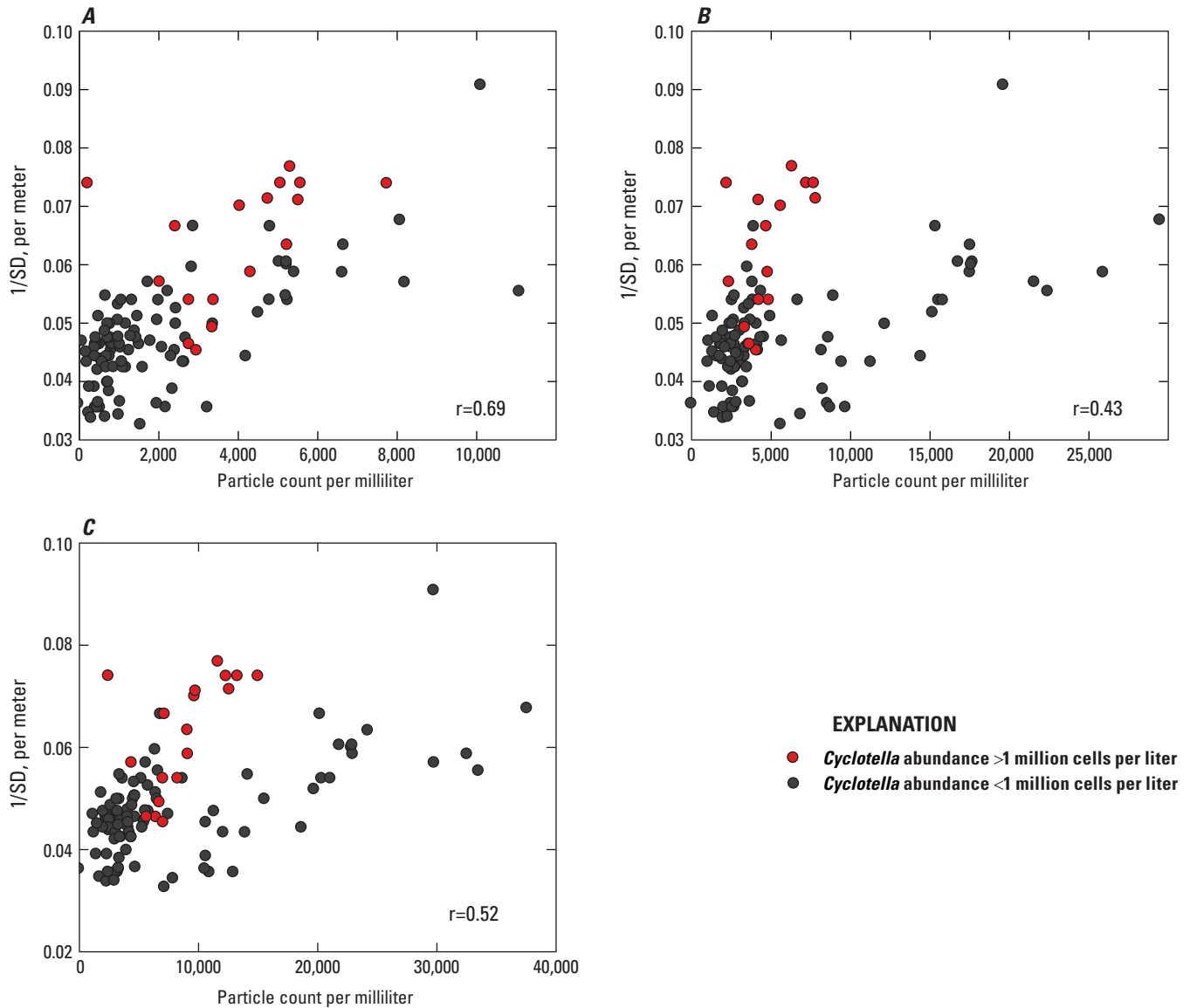
**Figure C8.** Inverse of Secchi disk depth (SD) relative to particle abundance of various size classes in Lake Tahoe at 5-meter depth, 2008–19 (Watanabe and Schladow, 2021): *A*, particles greater than 1 micrometer (μm; 1.0 to 16 μm ); *B*, less than 1 μm (0.5 to 1.0 μm); and *C*, all size classes (0.5 to 16 μm). Abbreviation: <, less than.

## Summary of Findings for Hypothesis 1

The hypothesis examined in this section is restated here:

"Clarity is controlled predominantly by the distribution and (volumetric) density of fine particles in suspension."

The evidence shown in this section, based on data from 2008–19, and for the size range of 0.50–20 μm, indicates that fine particles greater than 1 μm in diameter exert a measurable influence on clarity; however, not all particle sizes contribute equally, and other factors also likely play a role. A large observed increase in the abundance of particles less than 1 μm in size, beginning in 2017, did not result in a similarly abrupt reduction in clarity. The abundance of particles in the size range of 1.00–4.76 μm was more highly correlated with Secchi depth than was the case with other particle size classes, and high counts of *Cyclotella* tended to coincide with reduced Secchi depth; however, decreases in Secchi depth were also evident at times when *Cyclotella* were only a small fraction of the particle distribution.

Considering all observed particle sizes 0.50–20 μm, there was no statistically significant trend in annual lake-particle abundance or mean particle size. The large increase in abundance observed in 2017 was likely the result of the high flows and sediment loads in 2017.

# D. Hypothesis 2: The Change in Trend of Winter Clarity is a Response to Decreasing Fine Suspended-Sediment Concentrations Resulting from Load Reductions

## Background

Following reviews and discussions with agency representatives, examination of hypothesis 2 required consideration of three questions:

(1) Is there a statistically significant trend in the amount of fine suspended sediment in Lake Tahoe?

(2) Is there a trend in the loading of fine sediment to the lake? Potential sources include tributary streams, runoff from urbanized areas, and direct atmospheric deposition to the lake's surface.

(3) Is the fine-sediment concentration in the lake correlated with in-lake clarity time-series data?

The first and third of these questions have already been addressed to some extent in the discussion of the previous hypothesis, which was focused on all types of particles, not just those that are terrigenous in origin. Figure C7 includes a comparison of the estimated number of *Cyclotella* cells in suspension in the lake compared to the number of particles in the 1.00–4.76 μm range and shows that there were times when these numbers had similar magnitudes. This has not been true since 2016, however. The relative abundance of fine-sediment particles and *Cyclotella* varies by year and season. Also note that the data describing *Cyclotella* abundance are from the 5-m depth.

## Datasets

As with hypothesis 1, hypothesis 2 was examined by analyzing fine-particle data collected by UC Davis at the two long-term, in-lake profiling stations (MLTP, LTP; table D1) since 2008.

## Approach

Twelve years of data (2008–19) were available describing the abundance of fine particles (0.5–20 μm) in the lake and selected tributaries. Linear regressions (Helsel and others, 2020) between stream and lake particle counts were developed using summer and winter subsets of the data. Fine-sediment particle loads from the Upper Truckee River and urban loading derived from the seven RSWMP monitoring locations were inspected to reveal the seasonal variations in loads and the overall trends in data. The 6-year duration of data available for urban loads and the 4-year period for pollution-reduction credits were not long enough to demonstrate the influence of load reduction on winter clarity trends.

**Table D1.** In-lake datasets used to examine fine-particle abundance and distribution in Lake Tahoe and from urban surface runoff measured by the Tahoe Resource Conservation District Regional Stormwater Monitoring Program (RSWMP; Tahoe Regional Planning Agency, 2021), water years (WY) 2014–19, where the RSWMP provides estimates of total fine-sediment particle (FSP) loads (0.5–16.0 micrometers).

[LTP, Lake Tahoe profiling station; MLTP, mid-Lake Tahoe profiling station; m, meter; μm, micrometer]

| Site | LTP | MLTP | RSWMP |
| --- | --- | --- | --- |
| Start date | 7/2008 | 7/2008 | 10/2013 |
| End date | 11/2019 | 11/2019 | 9/2019 |
| Sampling depths (m) | 0, 2, 5, 10, 15, 20, 30, 40, 50 | 0, 10, 50 | Surface runoff |
| Size classes (μm) | 1.00–4.76 | 1.00–4.76 | FSP (0.5–16.0) |

## Results

### Lake and Stream Particles

For the full range of particle sizes in the 0.5–20-µm range (2008–19), there was no statistically significant trend of increasing or decreasing total number of particles at the two long-term lake profiling stations, considering annual values and winter values. All particle count data include both organic and inorganic particles.

Figure D1 shows summer particle counts at the monitored tributaries to Lake Tahoe that deliver water and sediment to the lake from primarily undeveloped sub-watersheds, and at profiling stations in the lake (counts represent an average of the top 50 m of the lake). Particle-count data were typically available no more than twice per month for the streams and monthly for the lake, albeit at multiple depths. For each month of the respective records, a mean value of the particle count in the 1.00–4.76 µm range was determined. This resulted in

a monthly time series of particle abundance for each site. Particle-size time series for the streams were compared to particle-size data in the lake to evaluate the correlation (linear regression) between these values.

Figure D1 demonstrates a large increase in particle abundance at the monitored tributaries in the summer of 2017 (June–September). The abundance of particles increased in 2017, and a similar increase was evident at the lake profiling stations. Figure D2 shows a similar increase in winter (December–March) particle abundances starting in 2017. Correlations between particle abundances at the tributaries and in the lake are shown for winter, summer, and annual seasons, with Upper Truckee River and Trout Creek having the greatest correlation (table D2). Similar results were obtained by Sunman (2004) and Rabidoux (2005) during the studies undertaken to establish allowable total maximum daily loads (California Regional Water Quality Control Board and Nevada Division of Environmental Protection, 2010).
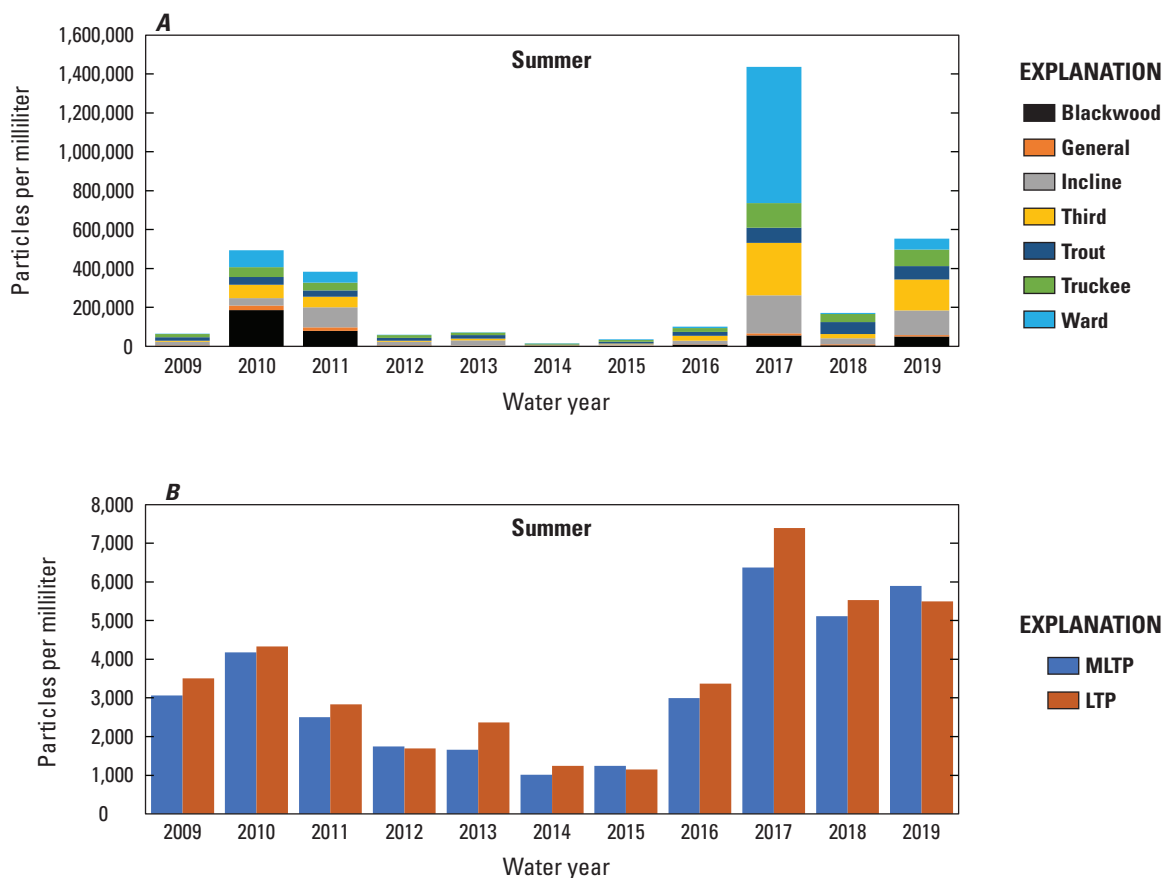


**Figure D1.**   Summer (June–September) particle counts per milliliter in the 1.00–4.76-micrometer size range, Lake Tahoe, 2008–19 (Watanabe and Schladow, 2021), at *A*, monitored tributaries (table D2; fig. A1); and *B*, at the two monitoring stations, Lake Tahoe profiling (LTP) and mid-Lake Tahoe profiling (MLTP) stations (table D3; fig. A1. Mean monthly values were averaged to determine seasonal averages. Values are vertically averaged for the top 50 meters of the lake.
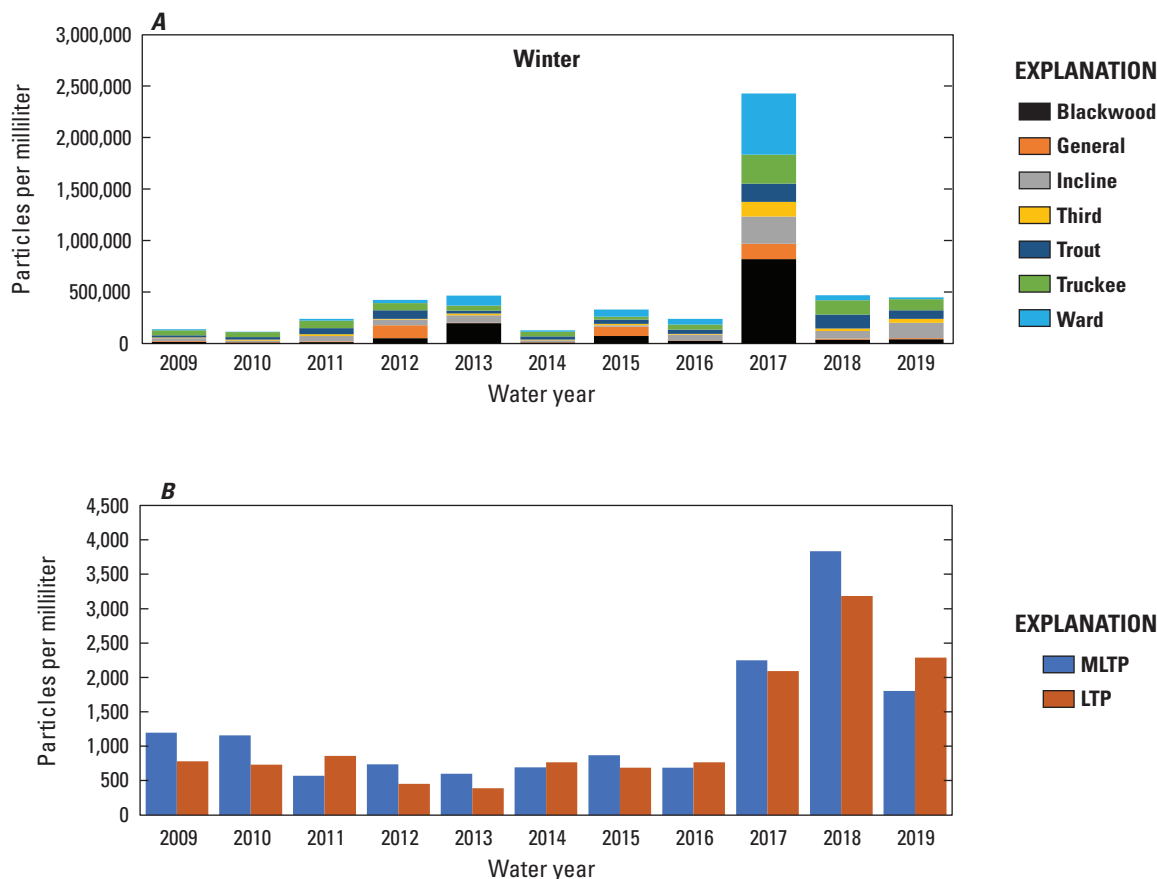
**Figure D2.** Winter (December to March) particle counts per milliliter in the 1.00–4.76-micrometer size range, Lake Tahoe, 2009–19 (Watanabe and Schladow, 2021) at *A*, monitored tributaries to Lake Tahoe (table A2; fig. A1); and *B*, at the two monitoring stations, Lake Tahoe profiling (LTP) and mid-Lake Tahoe profiling (MLTP) stations (table A3; fig. A1). Mean monthly values were averaged to determine seasonal averages. In-lake values are vertically averaged for the top 50 meters of the lake.

Particle data for most sites were typically available only twice per month; as a result, peak inflows could be missed or overemphasized in the total. Greater temporal resolution of data describing particles in streams is needed to improve estimates of actual sediment loading. Another option to improve sediment-loading estimates is to convert the more frequent turbidity data to suspended-sediment concentration data and collect field samples to quantify the fine fraction. Quantifying sediment loading to the lake from streams also would be helpful but was not possible with the available data.

In winter, Upper Truckee River and Trout Creek have the highest correlation coefficients and are the best predictors of particle counts at the LTP and MLTP in-lake observation stations. Trout Creek particle counts are the best predictors of particle counts at the LTP and MLTP lake-profiling stations for summer and annual periods. The presented correlation analysis compares simultaneous values, with no accounting for time that might be required for particles introduced at streams to reach the observation stations. Moreover, the particle counts at the in-lake stations include *Cyclotella* cells, whereas it is assumed that the stream counts do not.

**Table D2.**     Correlation coefficients (linear regression) among in-lake particle counts and Lake Tahoe Interagency Monitoring Program (LTIMP) tributary particle counts in the 1.00–4.76-micrometer-size range, 2009–19 (Watanabe and Schladow, 2021; U.S. Geological Survey, 2021).

[For example, the first number of 0.44 in the table is the correlation coefficient when comparing particle counts observed at Incline Creek in winter to the count observed at the mid Lake Tahoe profiling station (MLTP) in winter. In the last column, BL+WRD+GN represents the sum of counts for Blackwood Creek (BL), Ward Creek (WRD), and General Creek (GN), which are proximal to the Lake Tahoe profiling station (LTP). **Abbreviation**: LTIMP, Lake Tahoe Interagency Monitoring Program]

| Location | Incline Creek | Third Creek | Upper Truckee River | Trout Creek | Blackwood Creek | Ward Creek | General Creek | All LTIMP streams | BL+WRD+GN |
|---|---|---|---|---|---|---|---|---|---|
| | | | | Winter season | | | | | |
| MLTP | 0.44 | 0.44 | 0.63 | 0.73 | 0.27 | 0.30 | 0.08 | 0.39 | 0.27 |
| LTP | 0.56 | 0.50 | 0.68 | 0.77 | 0.28 | 0.31 | 0.04 | 0.41 | 0.27 |
| | | | | Summer season | | | | | |
| MLTP | 0.74 | 0.80 | 0.89 | 0.96 | 0.39 | 0.61 | 0.44 | 0.77 | 0.65 |
| LTP | 0.76 | 0.82 | 0.90 | 0.95 | 0.36 | 0.69 | 0.42 | 0.81 | 0.72 |
| | | | | Annual | | | | | |
| MLTP | 0.71 | 0.73 | 0.88 | 0.93 | 0.59 | 0.63 | 0.33 | 0.76 | 0.61 |
| LTP | 0.69 | 0.69 | 0.88 | 0.94 | 0.57 | 0.62 | 0.37 | 0.73 | 0.60 |

## Urban Fine-Sediment Loads

The analysis described in the last section did not explicitly consider fine-sediment loading to the lake from urbanized areas, although urban areas do contribute runoff to LTIMP streams and directly to the lake. Urban loading estimates are discussed in more detail later, but the correlations observed between particle abundance in streams and abundance in the lake indicates either that (a) stream loading is dominant in controlling in-lake particle abundance, (b) urban loading is closely synchronized in time with stream loading, or (c) lake hydrodynamic processes are mixing or attenuating the relative influence of sediment sources. Figure D3 indicates that the timing of urban loads is similar to stream loading in the Upper Truckee River, as would be expected if urban loading is driven by the same hydrologic events that lead to high particle counts in the monitored river. Urban runoff is typically more variable than stream runoff, however, and the drainage area represented by urban monitoring is sparse. Only about 1.5 percent of total urban area in the Lake Tahoe basin is monitored by the RSWMP, whereas the Upper Truckee River represents 18 percent of total land area in the Lake Tahoe basin and about 25 percent of annual stream streamflow to the lake (California Regional Water Quality Control Board and Nevada Division of Environmental Protection, 2010).

A major conclusion of the TMDL Technical Report (California Regional Water Quality Control Board and Nevada Division of Environmental Protection, 2010) was that urban fine-sediment particle (FSP) contributions represented about 72 percent of the total fine-particle flux. Coincident with the large runoff year in 2017 and continuing in the two following years, there has been a pronounced increase in stream particle concentrations (figs. D1, D2), which manifests as a large absolute and relative increase in FSP loading from the Upper Truckee River compared to urban sites (fig. D3). Also, many urban best management practices (BMPs) were implemented during the years following the 2003–04 TMDL stormwater calibration, and benefits from these BMPs are now implicitly represented in RSWMP data collected from 2013 through 2019. Furthermore, precipitation during the 2003 and 2004 water years (WY) was below average (approximately 83 percent of WY 1981–2019).

## Contributions by Runoff from Urbanized Areas

The RSWMP was developed to coordinate urban runoff monitoring across the Lake Tahoe basin for consistency of data acquisition, analysis, and reporting. Specifically, the RSWMP was implemented in support of the Lake Tahoe TMDL and is used to meet jurisdictional permit requirements for the TMDL. Lake clarity credits are a TMDL progress tracking tool based on modeled annual average load reductions acquired from aggregate best management practice (BMP) implementations by each of the seven basin jurisdictions. These results are reported each year as part of the Lake Clarity Crediting Program (LCCP), which focuses on load reductions in the urban upland source category.
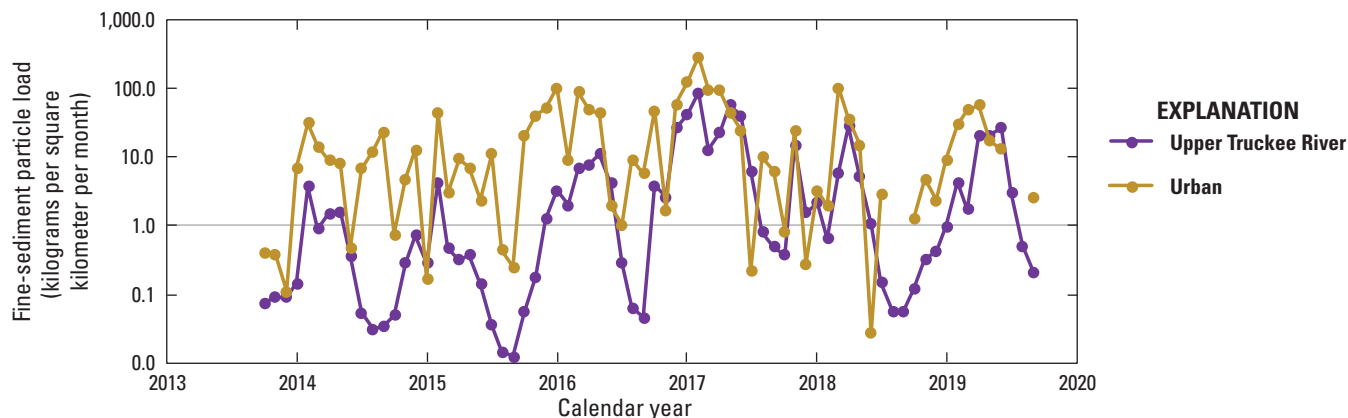
**Figure D3.**  Fine-sediment particle (FSP) loading to Lake Tahoe, 2013–19, based on Upper Truckee River measurements and urban loading derived from the seven Tahoe Resource Conservation District Regional Stormwater Monitoring Program (RSWMP) monitoring locations identified in table D2 (Tahoe Regional Planning Agency, 2021; U.S. Geological Survey, 2021). Data are presented in terms of sediment mass, as consistent with reported FSP (0.5–16 micrometers) loads from RSWMP urban sites, normalized to drainage areas shown in table D2.

The most recent LCCP report summarizes TMDL implementation accomplishments through 2019 (Nevada Division of Environmental Protection and the California Regional Water Quality Control Board, 2020). The report presents progress with load reductions compared with baseline loading amounts, which are the 2004 loads (appendix 1). Annual load reductions are estimated from jurisdictional registrations in the LCCP "Stormwater Tools" accounting platform, which includes a "Pollutant Load Reduction Model" to calculate reduced loadings (https://clarity.laketahoeinfo.org/Home/UrbanJurisdictions). The LCCP and RSWMP report loads in pounds (for example, as pounds per year from watershed or pounds per acre per year). The LCCP estimates that 1 pound of fine sediment particles (FSP; less than 16 μm in diameter) is equivalent to $5 \times 10^{13}$ particles (appendix 1). The RSWMP calculates FSP load from samples collected at RSWMP monitoring sites and analyzed for particle-size distribution and mass (Tahoe Resource Conservation District, 2020).

Initial RSWMP monitoring sites were established in 2014, with several sites added subsequently and other sites discontinued (table D3). Sites were selected to represent runoff from a range of land-use categories and for assessment of changes associated with BMP implementations in drainages from around the Lake Tahoe basin. Given the focus of this analysis on urban runoff association with water-clarity patterns, we removed sites from analysis that have been discontinued, are inflows to BMPs, or have less than 5 years of data. The remaining seven established monitoring sites

represent a relatively short period of record (WY 2014–19) compared to Secchi disk depth and most other watershed variables. This 6-year stormwater-monitoring record starts with 2 years of severe drought, includes an extreme winter precipitation in 2017, as well as 3 years of average or above-average precipitation.

## Tahoe Regional Stormwater Monitoring Program Data Analysis

Runoff events and meteorological conditions are monitored at the RSWMP sites throughout the year (Tahoe Resource Conservation District, 2020). Volumetric flow rates are calculated from transducer- or bubbler-stage readings continuously recorded throughout the water year at 5- or 10-minute intervals. Runoff samples from selected events are collected by autosamplers at each site and used to create volume-weighted event mean composites (EMCs) for subsequent laboratory analysis of nutrient and fine-sediment concentrations. When combined with runoff volumes, nutrient and fine-sediment concentrations result in reliable estimates of event loads. The event loads are used to calculate annual, seasonal, and monthly loads for each site (https://monitoring.laketahoeinfo.org/RSWMP). Data are presented in pounds of pollutant loads per month from the drainage for total phosphorus (TP), total nitrogen (TN) and FSP (less than 16 μm). Total suspended solids (TSS) are also analyzed for loading estimates. The data were converted from pounds to kilograms for our statistical evaluations.

**Table D3.**    Tahoe Resource Conservation District Regional Stormwater Monitoring Program (RSWMP) urban monitoring sites (Tahoe Regional Planning Agency, 2021).

[The CICU category references mixed commercial, industrial, communications and utilities land use (Tahoe Resource Conservation District, 2020). **Abbreviation**: ID, identification; %, percent]

| Site name | Site ID | Latitude | Longitude | Drainage (acres) | Water years on record | Dominant land use |
|-----------|---------|----------|-----------|------------------|----------------------|-------------------|
| Contech Inflow | CI | 39.27436 | −119.946 | 0.7 | 2014–19 | Primary road (100%) |
| Contech Outflow | CO[1] | 39.27431 | −119.947 | 0.7 | 2014–19 | Primary road (100%) |
| Incline Village | IV | 39.24028 | −119.949 | 83.6 | 2014–16 | Multi-family residential (38.2%) |
| Jellyfish Inflow | JI | 39.27431 | −119.947 | 0.7 | 2014–19 | Primary road (100%) |
| Jellyfish Outflow | JO[1] | 39.27425 | −119.947 | 0.7 | 2014–19 | Primary road (100%) |
| Elks Club | EC | 38.87345 | −120.002 | 14.4 | 2018–19 | Single family residential (50.0%) |
| Lakeshore | LS | 39.24022 | −119.946 | 97.8 | 2017–19 | Multi-family residential (43.2%) |
| Pasadena Inflow | PI | 38.94443 | −119.981 | 78.8 | 2014–17 | Single family residential (52.4%) |
| Pasadena Outflow | PO[1] | 38.94468 | −119.981 | 78.8 | 2014–19 | Single family residential (52.4%) |
| Rubicon | RI | 39.01548 | −120.118 | 13.8 | 2014–15 | Single family residential (75.9%) |
| Speedboat | SB[1] | 39.2252 | −120.01 | 39 | 2015–19 | Single family residential (35.9%) |
| Tahoe Valley | TV[1] | 38.92064 | −119.998 | 338.4 | 2015–19 | CICU (20.3%) |
| Tahoma | TA[1] | 39.06744 | −120.126 | 49.5 | 2014–19 | Single family residential (41.2%) |
| Upper Truckee | UT[1] | 38.92239 | −119.99 | 10.5 | 2015–19 | CICU (39.3%) |

[1]Station selected for statistical analysis in this report.

Monthly loads were summed across RSWMP sites (appendix 1) and then totaled by month over each water year (WY) of record for comparison to annual or seasonal Secchi depth. Our analysis of trends and correlations with lake clarity and other water-quality variables was applied to these data. In addition to site precipitation measurements, we also evaluated snow telemetry (SNOTEL) data from the Tahoe City Cross (TCX) station (Natural Resources Conservation Service, National Water and Climate Center

https://wcc.sc.egov.usda.gov/nwcc/site?sitenum=809), to represent Lake Tahoe basin precipitation at a slightly higher elevation (6,797 ft). Associations among variables were evaluated using Pearson product moment correlation. Trends analysis for precipitation-normalized loading by water year was done with a rank-based non-parametric approach, using Kendall's Tau for correlation (with associated probability) and a Theil-Sen estimator for best fit lines (Helsel and others, 2020).

## Results from Urban Data Analysis

The year with highest average annual loads for RSWMP sites was WY 2017, an exceptionally high precipitation year, whereas low precipitation amounts during the drought years of 2014 and 2015 yielded correspondingly low annual loads (table D4).

Among annual average pollutant loads from RSWMP sites, the highest Pearson's correlation coefficient (r) for annual average Secchi depth (fig. D4) was with TN (r = −0.67), followed by TP (r = −0.64), TSS (r = −0.63), and FSP (r = −0.55). None of these correlations was statistically significant (p>0.05), however. An equivalent analysis with annual winter Secchi depth produced lower correlation coefficients and no statistically significant results.

Correlations of water year annual average RSWMP loads with the calendar year annual average Secchi depths are slightly stronger and are significant (p≤0.05) for TN, RSWMP precipitation, and TCX, indicating a potential carryover effect into fall (October–November). Although the correlations of monthly RSWMP data with corresponding monthly Secchi depth are not as strong as the correlations between annual averages, there are statistically significant correlations for the relative percentage change in monthly Secchi depth at a 4-month lag time to monthly FSP (r = −0.40, p<0.001) and TP (r = −0.39, p<0.01) loads.

Trend detection at monitoring sites is problematic with only six consecutive years of runoff data, especially given the variability of watershed processes among sites. Thus, it is not surprising that precipitation-normalized RSWMP results at sites through WY 2019 show no statistically significant trend (fig. D4), except at the Speedboat site (table D3;

fig. A1), where TP and TN loads have both apparently increased slightly through time (Tahoe Resource Conservation District, 2020).

Aggregating data from all seven RSWMP sites selected for statistical analysis in this report (table D3; fig. A1) provides a broader perspective on loading trends in the Lake Tahoe basin, but the ability to examine trends in loads is still limited by the short period of record and number of sites. The RSWMP-average loading rates were calculated for each water year by taking the sum of all site loads and then normalizing to total drainage area and to average water-year precipitation. These results are shown in table D5.

Although normalization helped reduce some of the influence from variability introduced by differences in land-use characteristics, drainage areas, and precipitation rates among sites, water-year data remained scattered. Therefore, trends were assessed with non-parametric Kendall Tau correlation coefficients and Theil-Sen estimators for best-fit lines (table D6), which are more resistant to outliers than standard parametric techniques (Helsel and others, 2020). Best-fit lines indicated that normalized annual average TSS and FSP loading rates decreased and TN loading rates increased through time; however, none of these results was statistically significant (fig. D5). Six data points represent a short record for this type of evaluation, even with non-parametric techniques and normalized data, so continued data collection is essential to support future trends analysis. Establishing a statistical sampling design to select and sample additional sites that appropriately represent the variability observed in the Lake Tahoe basin could also improve the quality of these analyses.

**Table D4.** Average annual loading of measured pollutants and precipitation from Regional Stormwater Monitoring Program (RSWMP; Tahoe Regional Planning Agency, 2021) urban sites by water year (WY).

[Annual precipitation from the Tahoe City Cross (TCX) snow telemetry site is also shown for these years. Abbreviations: No., number; Avg, average; TP, total phosphorus; kg, kilogram; TN, total nitrogen; TSS, total suspended solids; FSP, fine-sediment particles; precip, precipitation; in., inch; m, meter]

| WY | No. of urban sites | Avg WY TP (kg) | Avg WY TN (kg) | Avg WY TSS (kg) | Avg WY FSP (kg) | RSWMP Avg precip (in.) | TCX precip (in.) | WY Secchi depth (m) |
|---|---|---|---|---|---|---|---|---|
| 2014 | 4 | 2.2 | 3.5 | 720 | 380 | 18.3 | 24.6 | 23.8 |
| 2015 | 7 | 2.0 | 5.9 | 600 | 340 | 16.7 | 22.6 | 22.3 |
| 2016 | 7 | 7.4 | 15.9 | 1,910 | 1,500 | 25.2 | 41.8 | 21.2 |
| 2017 | 7 | 20.2 | 78.0 | 4,500 | 2,900 | 45.9 | 78.0 | 19.8 |
| 2018 | 7 | 5.9 | 21.4 | 1,600 | 680 | 21.4 | 37.1 | 20.0 |
| 2019 | 7 | 5.8 | 22.6 | 1,290 | 680 | 23.7 | 51.7 | 20.1 |
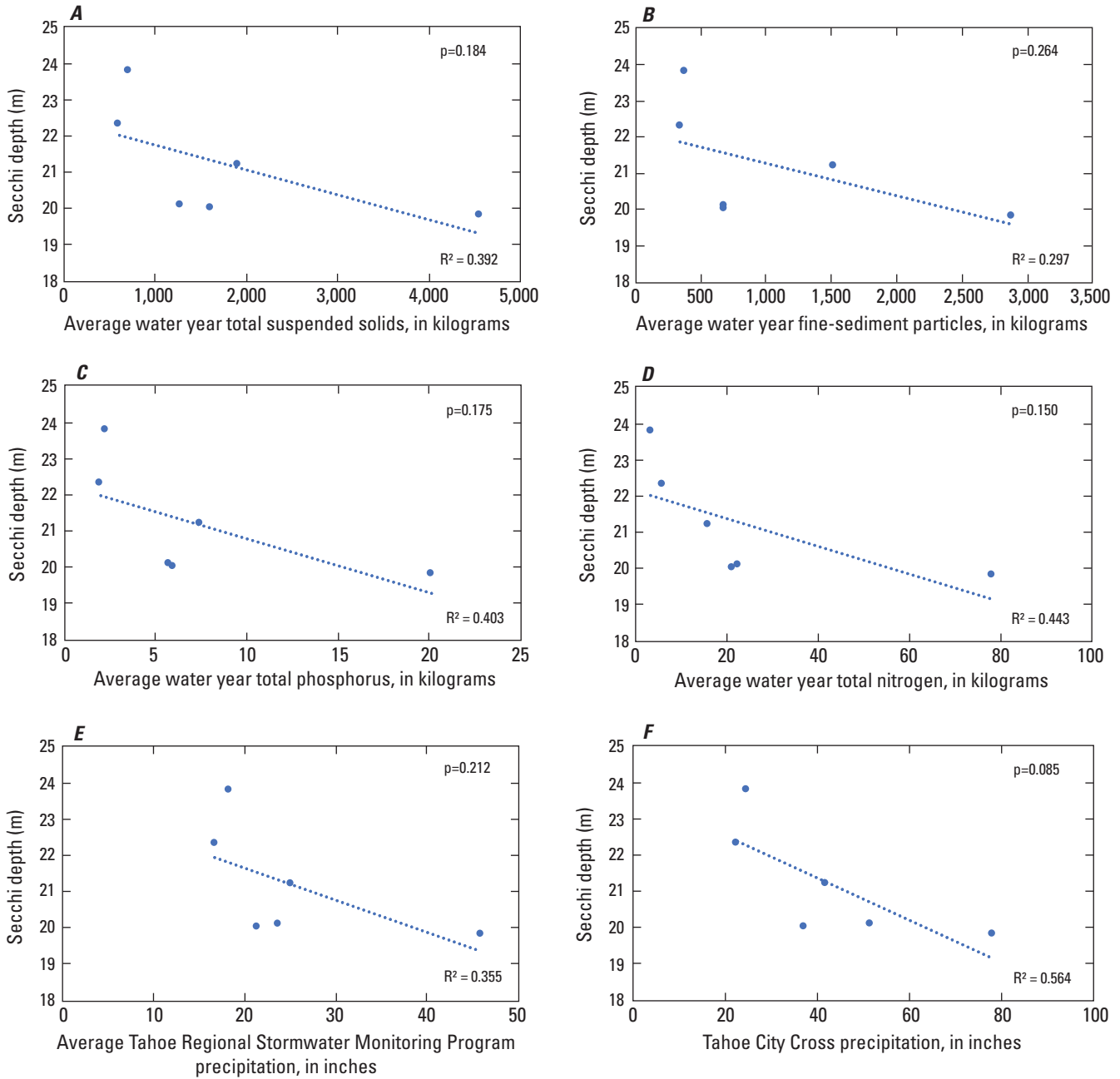
**Figure D4.**   Water year (WY) annual average Secchi depth, in meters (m), relative to water year loads and precipitation, including coefficients of determination ($R^2$) and p-values, Lake Tahoe, 2014–19: *A*, total suspended solids (TSS); *B*, Tahoe City Cross (TCX) precipitation; *C*, fine-sediment particles (FSP); *D*, Regional Stormwater Monitoring Program precipitation; *E*, total nitrogen (TN); and *F*, total phosphorus (Watanabe and Schladow, 2021; Tahoe Regional Planning Agency, 2021). Peak Secchi depth of 23.8 m was in WY 2014, during which time only four of the seven monitoring sites were operational.

**Table D5.**    Average loading rates (kilograms per acre per inch of precipitation) for measured pollutants from Regional Stormwater Monitoring Program (RSWMP; Tahoe Regional Planning Agency, 2021) urban monitoring sites normalized to area and precipitation by water year (WY).

[No., number; kg/acre/in, kilogram per acre per inch; TSS, total suspended solids; FSP, fine-sediment particles; TN, total nitrogen; TP, total phosphorus]

| WY | No. of urban sites | Drainage area (acre) | TSS (kg/ac/in) | FSP (kg/acre/in) | TN (kg/acre/in) | TP (kg/acre/in) |
|---|---|---|---|---|---|---|
| 2014 | 4 | 130 | 1.21 | 0.65 | 0.006 | 0.004 |
| 2015 | 7 | 518 | 0.49 | 0.28 | 0.005 | 0.002 |
| 2016 | 7 | 518 | 1.03 | 0.81 | 0.009 | 0.004 |
| 2017 | 7 | 518 | 1.30 | 0.85 | 0.023 | 0.006 |
| 2018 | 7 | 518 | 1.00 | 0.43 | 0.013 | 0.004 |
| 2019 | 7 | 518 | 0.73 | 0.39 | 0.013 | 0.003 |
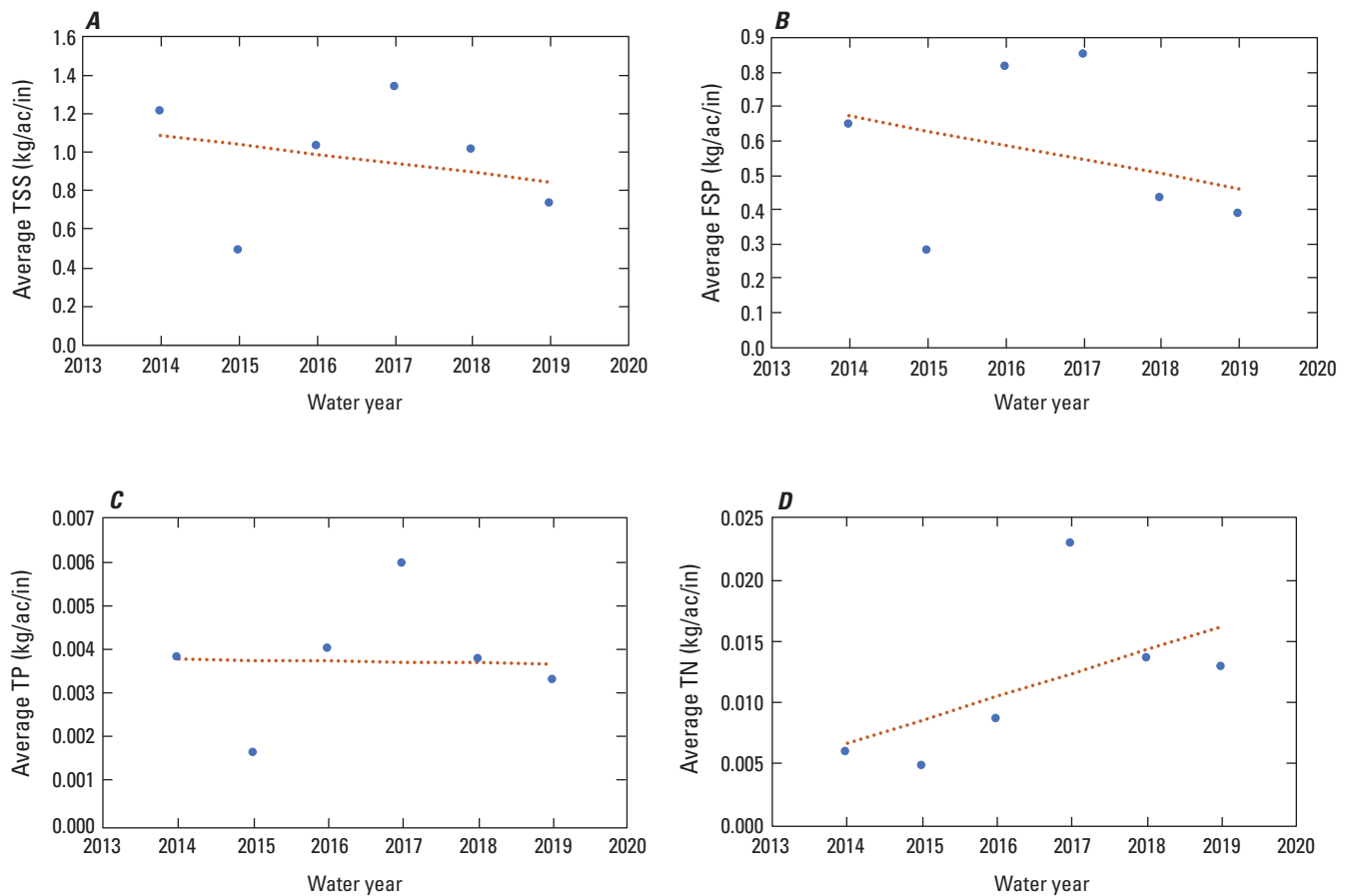


**Figure D5.**    Annual average pollutant loads from Regional Stormwater Monitoring Program (RSWMP; Tahoe Regional Planning Agency, 2021) sites, Lake Tahoe, 2014–19, for *A*, total suspended solids (TSS); *B*, fine-sediment particles (FSP); *C*, total phosphorus (TP); and *D*, total nitrogen (TN). Abbreviation: kg/ac/in, kilograms per acre per inch.

**Table D6.**    Theil-Sen estimators of trend for normalized urban runoff loads at Regional Stormwater Monitoring Program (RSWMP) sites.

[kg/acre/in., kilogram per acre per inch; TSS, total suspended solids; FSP, fine-sediment particles; TN, total nitrogen; TP, total phosphorus]

| Theil-Sen[1] (water years 2014–19) | RSWMP average (kg/ac/in) | | | |
|---|---|---|---|---|
| | TSS | FSP | TN | TP |
| Tau | −0.2 | −0.067 | 0.467 | −0.067 |
| p-value for \|Tau\|[2] | 0.573 | 0.851 | 0.189 | 0.851 |
| Slope | −0.0497 | −0.0422 | 0.0019 | −0.00003 |

[1]Theil-Sen estimator of best-fit lines (Helsel and others, 2002).

[2]The greater the absolute value of the non-parametric Kendall rank correlation coefficient (Tau), the stronger the association between two variables.

The Pollutant Load Reduction Model (PLRM) is a hydrologic and pollutant load model used to estimate annual average urban stormwater pollutant loads in the Lake Tahoe basin for the LCCP (Nevada Division of Environmental Protection and the California Regional Water Quality Control Board, 2020). Regional estimates of loading from urban catchments are derived from PLRM model simulations for each jurisdiction as they register improvements and BMP implementations for load reductions and corresponding lake clarity credits. The existing PLRM uses precipitation and temperature time-series data derived from extrapolation of local meteorological datasets from 1988 through 2006. By design, therefore, surface-runoff and pollutant-loading results from the PLRM are based on an 18-year historical meteorological average rather than on recent water-year measurements. Thus, substantial differences between PLRM estimates and measured values may be expected because annual precipitation and runoff characteristics vary from year to year. A recent evaluation of PLRM site loading estimates compared to RSWMP monitoring-site measured data for WY 2019 showed average and median differences of 899 percent and 455 percent, respectively, among the seven sites (table D3) for FSP, TN and TP loading (Tahoe Resource Conservation District, 2020).

Although time series of the RSWMP monitoring-site data are not adequate at present (2019) for reliable trends assessment, the LCCP reports that urban loads have been reduced based on PLRM estimates (table 1.1; Nevada Division of Environmental Protection and the Lahontan Regional Water

Quality Control Board, 2020). Accordingly, cumulative load reductions credited against 2004 (baseline) loading amounts estimated for the TMDL have hypothetically achieved a 19.7 percent reduction in FSP loading, a 15.5 percent reduction in TP loading, and an 11.7 percent reduction in TN loading.

We used average loading rates from the RSWMP monitoring sites (table D5) to compare total urban loadings to the 2004 baseline levels (appendix 1). This evaluation included extrapolating to a total jurisdictional catchment area of around 40,000 acres from monitored drainage areas representing less than 1.5 percent of the total catchment. As a result, the accuracy of this evaluation is likely to be poor and should be viewed more as an approximation based on measured data than a reliable estimate. Longer-term datasets and many more sites are needed to improve loading estimates (Heyvaert and others, 2011).

## Summary of Findings for Hypothesis 2

Hypothesis 2 is restated here:

The change in trend of decreasing winter clarity is a response to decreasing fine suspended-sediment concentrations resulting from load reductions.

Trend analysis of fine sediment loads from urban areas revealed no statistically significant trend. Urban load-reduction activities that have taken place in the Lake Tahoe basin have likely resulted in nutrient and fine-sediment reductions (Domagalski and others, 2021); however, the length of record for urban load reductions are insufficient to reach a statistically meaningful conclusion.

Three questions were posed at the beginning of this section:

(1)  Is there a statistically significant trend in the fine suspended sediment in Lake Tahoe?

The results presented in the discussion of hypothesis 1 indicated that although there was a large increase in the number of particles in the lake beginning in 2017, there is no statistically significant temporal trend in the number of particles observed at the two in-lake profiling stations. The fraction of *Cyclotella* cells included in the counts of particle abundance contained some uncertainty and was not continuously available, and we did not attempt to subtract *Cyclotella* counts from the total to determine a sediment-only time series.

(2)  Is there a trend in the loading of fine sediment to Lake Tahoe? Potential sources include tributary streams, runoff from urbanized areas, and direct atmospheric deposition onto the lake's surface.

The available data did not allow for a definitive answer to this question. Data describing particle abundance at selected tributaries showed correlation with in-lake particle abundance, but these data were only available for selected periods that were insufficient to determine loading to the lake. Fine sediment loads from LTIMP streams were not available and the scope of this study did not include computing monthly and annual fine sediment loads. Fine sediment loads are needed to track seasonal inputs to Lake Tahoe from LTIMP streams. A majority of the watershed draining to Lake Tahoe remains unmonitored. As described later in the report, climate change is altering lake stratification, hydrology, and the timing of inflows such that fine-sediment loads could be introduced at different depths in the lake thereby altering the effect of sediment loads on clarity.

The temporal period and resolution of urban loading data are limited, so uncertainties in the available data are high. Also, much of the urbanized area is not monitored. Consequently, the length of the record is not yet sufficient for trend analysis, and extrapolation of limited monitoring sites would result in high uncertainty even in the absence of other concerns. Moreover, data are not yet available to estimate the relative importance of atmospheric deposition of insoluble particles directly onto the lake's surface.

(3)  Is the fine sediment concentration in the lake correlated with in-lake clarity time-series data?

Figure C8 shows the correlation between the inverse of the Secchi depth and the particle abundance, for different size classes. Clarity tended to decrease when particle abundance was high, and the number of particles greater than 1 μm was a better predictor than the total number of particles (>0.5 μm).

# E. Hypothesis 3: Changing Hydrodynamic Conditions in the Lake are Increasing Thermal Stability and Resistance to Mixing

## Background

A lake's hydrodynamic characteristics and patterns depend on several factors, including size, shape, hydrology, and meteorological conditions. The latter two factors have been altered by climate change and are expected to continue changing at an accelerating rate for the same reason (Sahoo and others, 2015). Hydrodynamic processes and forcing, including thermal stratification, wind-shear stress, vertical circulation, inflows and outflows, and gyres and seiches, play an important role in Lake Tahoe's hydrodynamics. Changes in hydrodynamic characteristics affect the distribution of chemical and biological solutes and particles, such as nutrients (nitrogen, phosphorous) and chlorophyll, among other things (Hutchinson, 1957).

## Datasets

We used physical, chemical, and biological long-term time series of in-lake parameters measured by UC Davis at the two long-term sites from 1968 through 2019 (table E1). We utilized data from the top 50 m of the water column at both sites, meaning we analyzed data from nine depths at LTP (0, 2, 5, 10, 15, 20, 30, 40, 50 m) and three depths at MLTP (0, 10, 50 m).

## Approach

To examine hypothesis 3, we first characterized the changes in thermal stratification (timing, intensity, and duration) using long-term time series of lake temperatures to calculate indices that quantify the resistance to mixing across the thermocline and related the results to water clarity. Secondly, we evaluated trends of in-lake physical, chemical, and biological variables (temperature, nutrients, chlorophyll, and fine particles), as well as streamflow, and related these trends to clarity. Thirdly, we examined the periodicity of the different long-term time series described in this section and explored correlations with thermal stratification and clarity. Finally, we proposed potential explanations for the different periodicities in the time series and mechanisms underlying the variability in stratification and clarity.

We quantify the resistance to mixing across the thermocline using two indexes: stability index (SI, in kilograms per square meter) and the buoyancy frequency (N; in per second). The stability index measures the energy required to mix the upper 120 m of the lake when it is stratified (Sahoo and others, 2015) and is computed as follows:

**Table E1.**     Long-term time series used to characterize the changes in hydrodynamic conditions in Lake Tahoe (Watanabe and Schladow, 2021).

[MLTP, mid Lake Tahoe profiling station (460 meters, m); LTP, Lake Tahoe profiling station (120 m)]

| Parameter | Site(s) | Period of record | Frequency |
|---|---|---|---|
| Physical | | | |
| Secchi depth | MLTP; LTP | 4/1969–12/2019; 1967–2019 | Variable; typically, 1–2x/month |
| Water temperature (T) | MLTP; LTP | 1969–96; 1967–96 | Monthly; every 10 days |
| Profiling temperature | MLTP; LTP | 1996–2006 | Monthly; every 10 days |
| Profiling temperature (Sea-Bird) | MLTP; LTP | 2005–19 | Monthly; every 10 days |
| Fine-particle size distribution (FSD) | MLTP; LTP | 2008–19 | Monthly; every 10 days |
| Chemical | | | |
| Nitrate ($NO_3$) | MLTP; LTP | 1970–2019; 1968–2019 | Monthly; every 10 days |
| Total Kjeldahl nitrogen (TKN) | MLTP | 1989–2019 | Monthly |
| Total hydrolyzable phosphorus (THP) | MLTP; LTP | 1972–2019; 1968–2019 | Monthly; every 10 days |
| Total phosphorus (TP) | MLTP | 1989–92, 2000–19 | Monthly |
| Biological | | | |
| Chlorophyll-a (Chl-a) | LTP | 1984–2019 | 1984–2006: monthly profiles with composites every 10 days; monthly (profile + composite) since 2007 |
| — | MLTP | 1984–2019 | Monthly |

$$SI = \sum_{z=z_0}^{z=z_1}(z - \bar{z})\rho_z \qquad (1)$$

where

 $z$  is the depth of the water column from the surface,

 $z_0$  is the depth of the surface water (for example, 0.5 m),

 $z_1$  is the maximum depth of the study water column, and

 $\bar{z}$  is the centroid or center of mass of the water column.

Water density at depth $z$ is $\rho_z$. A positive value for SI indicates stable stratification, and greater positive values indicate more stable stratification. The buoyancy frequency can be interpreted as the vertical-frequency response excited by a displacement of a fluid parcel (that is, resistance to mixing) and is calculated as follows:

$$N = \sqrt{\frac{g}{\rho_z}\frac{\partial \rho_z}{\partial z}} \qquad (2)$$

where

 $\delta\rho/\delta z$  is the vertical-density gradient, and

 $g$  is the acceleration due to gravity.

A larger density gradient results in a higher buoyancy frequency, which indicates greater resistance to mixing. For this report, we evaluated the maximum values of SI and N to characterize changes in hydrodynamic conditions in the upper waters of Lake Tahoe by first calculating these variables from the measured temperature profiles and then identifying the depths of the maxima.

We quantified trends of the different datasets using the least square method to fit the time series to the best linear model (Molugaram and Rao, 2017). T-tests were used to evaluate the statistical significance (p-values) of these trends. Correlation coefficients were calculated using the approach described in Press and others (1992).

We computed the power spectrum for all the available long-term time series of parameters and depths above 50 m at the two sampling sites. We computed power spectral density (PSD) in the frequency domain using a fast Fourier transform and smoothing results with a cosine taper window [1,16] and a 95-percent confidence interval based on the chi-squared distribution (Bendat and Piersol, 1986). Results from this analysis indicated the dominant periodicity or periodicities as peaks of the PSD expressed in years or fraction of year for each parameter. This analysis provides insight to the possible causes of the variance of specific time series.

## Results

Changes in the thermal stratification of Lake Tahoe are the most straightforward observation of changes in the hydrodynamic conditions in the lake since 1968 (fig. E1).
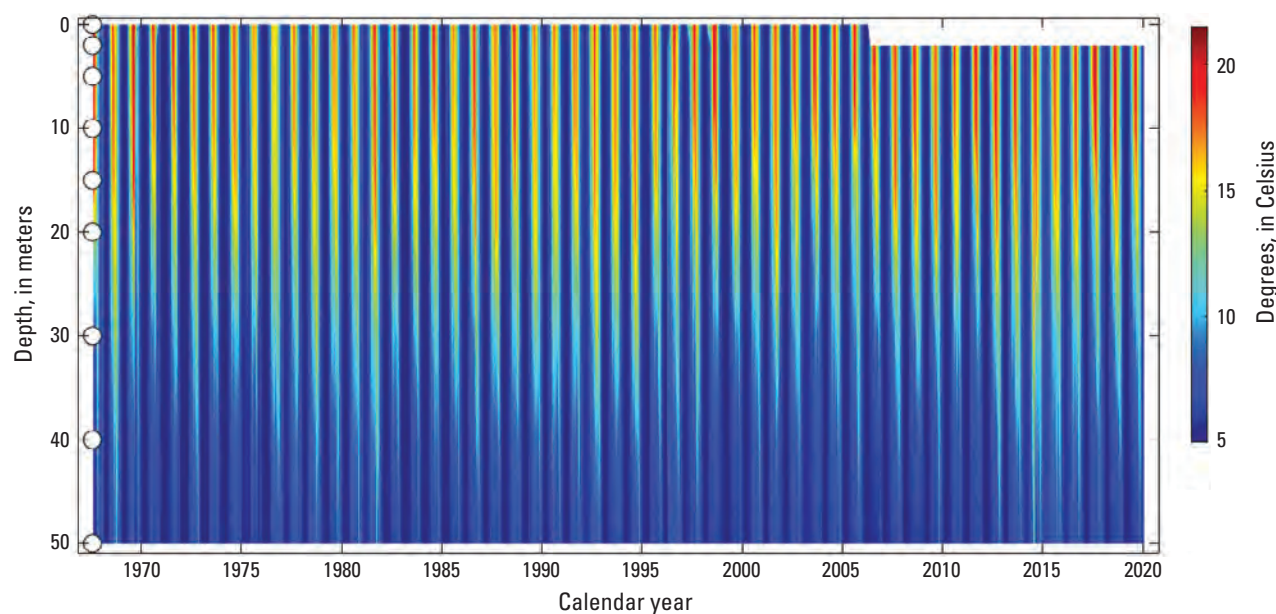


Figure E1.   Time series of water temperature by depth at the Lake Tahoe profiling station (LTP), 1970–2019 (Watanabe and Schladow, 2021). The circles next to the x-axis indicate depths at which samples for water-quality determination were collected. See table E1 of this report for period of record and frequency.

The maximum annual values of indices that quantify the resistance to mixing across the thermocline show a trend of linear increases from 2000 to 2019 (fig. E2). These maxima were always reached during the summer season (June to September). The linear trends of stability index (SI) and buoyancy frequency (N) computed by the least-squares method using data from 2000 to 2019 show increases on the order of thousandths of kilograms per square meter and hundredths of seconds annually ($R^2 = 0.54$ and $0.83$, $p<0.001$), respectively. We can infer several conclusions from these results: (1) stability index and buoyancy frequency define magnitude of stratification and are both increasing through time, indicating that water column density differences are becoming greater, (2) buoyancy frequency may be a better index to quantify the changing hydrodynamic conditions in Lake Tahoe in the context of lake clarity because trend and the coefficient of determination $R^2$ are stronger than for SI, and (3) suppressed mixing could be affecting water clarity, particularly observed reductions in summer clarity.
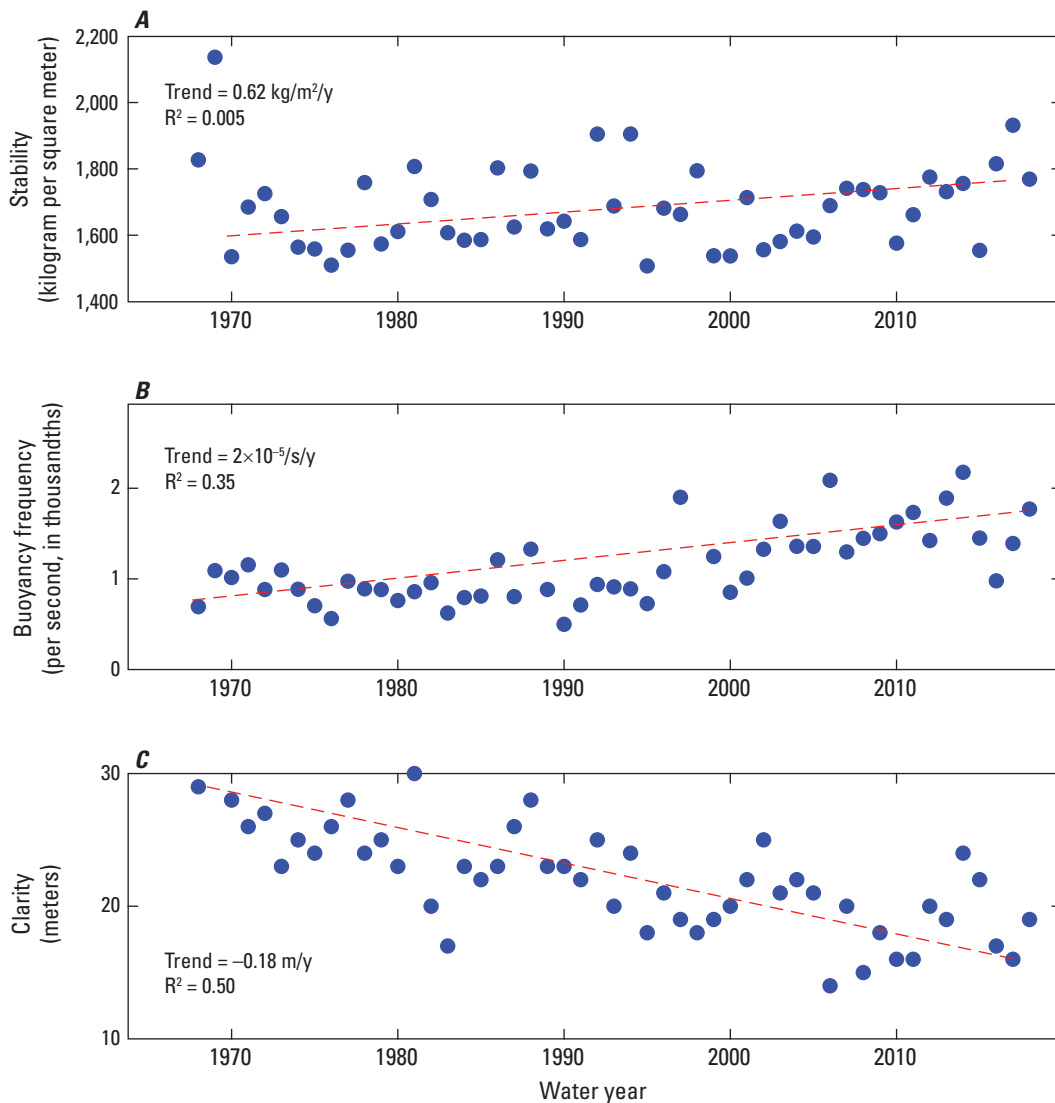


**Figure E2.** Linear regression trend analyses of annual maximum values, along with computed trend values and coefficients of determination ($R^2$ values) for variables describing hydrologic conditions and characteristics at the Lake Tahoe profiling station (LTP), 1968–2019 (Watanabe and Schladow, 2021): *A*, stability index; *B*, buoyancy frequency; and *C*, mean summer clarity (June–September). All trends are statistically significant ($p<0.001$). Abbreviations: kg/m²/y, kilograms per square meter per year; s/y, seconds per year; m/y, meter per year.

We also found a weak trend to an earlier occurrence in the time of deepest mixing ($R^2$=0.1, $p$=0.028, fig. E3). This could indicate that deep mixing starts earlier in spring, although the evaluation of the maximum mixing depth can only be made once per month; therefore, there is considerable uncertainty about the precise date (±15 days). Deep mixing is known to be complex and believed to be strongly influenced by three-dimensional convective cooling from the relatively shallow shelves that are present at the northern and southern ends of the lake (Schladow, 2019). The analysis needed to understand that process is beyond the scope of this report.

We used statistical analyses to assess the timing and duration of lake stratification to complement our evaluation of stratification strength or resistance to mixing. We found statistically significant trends ($R^2$ = 0.71−0.83, $p$<0.001) showing that earlier, prolonged, and more intense stratification could be contributing to the decline in summer clarity (fig. E4). These trends are consistent with those presented in Sahoo and others (2015) and shown by Winder and others (2008); such climate mediated effects are linked to an increasing abundance of *Cyclotella*.

Figure E4 contains plots with all the long-term time series used in our analysis of trends. Clarity decreased through time (table E2). Total phosphorous at the MLTP station showed a trend of increasing overall, but for the first half of the record, it was decreasing. Chlorophyll shows a negligible trend; however, this overall trend could obscure the fact that smaller species (that affect clarity) have been increasing in concentration relative to larger species that do not affect clarity. The actual change in chlorophyll concentration is small, thus disguising what might be an important trend. Trends for the variables in table E2 from different depths had less than 2 percent variability from the mean. The upper lake concentration of fine particles showed a large peak in 2017, the year of record high inflows. Fine-particle concentrations in the lake increased by a factor of 3–4 (see also fig. C3). The values remained elevated for the next 2 years. During this 3-year period, concentrations appeared to increase, but the trend was not significant. Prior to this time, fine-particle concentrations were relatively unchanged, if not decreasing, although the available record is relatively short. Trends for the other variables were negligible over the same period, although visually trends appeared to show interannual periodicity in multiyear cycles.
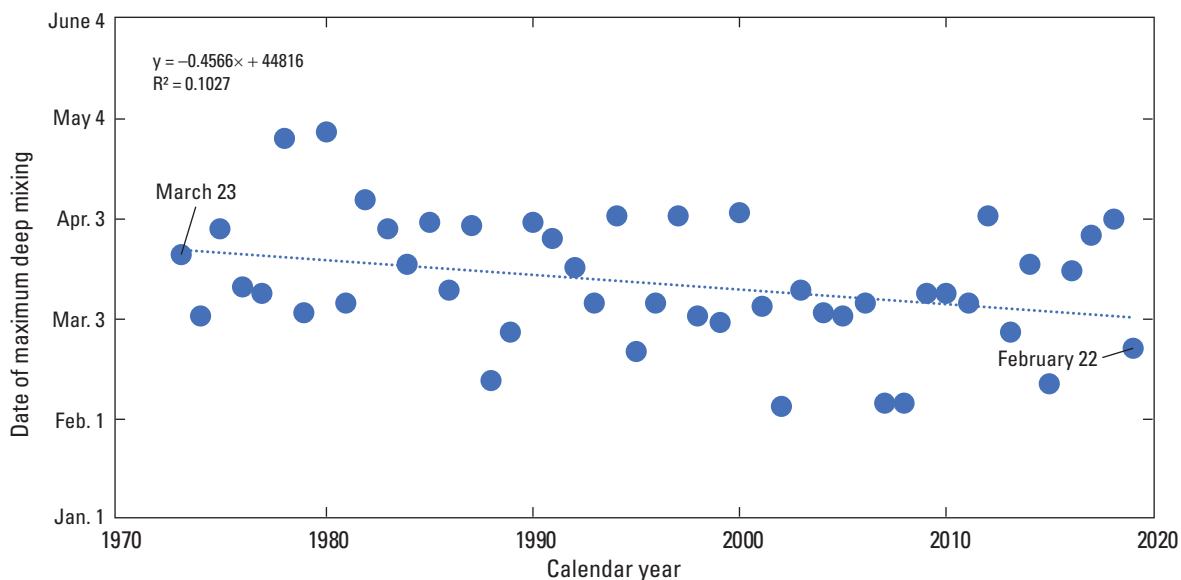


**Figure E3.** Linear regression analysis and computed coefficient of determination ($R^2$) for the date of maximum deep mixing at the Lake Tahoe profiling station (LTP), 1973–2019 (Watanabe and Schladow, 2021; $p$<0.05).
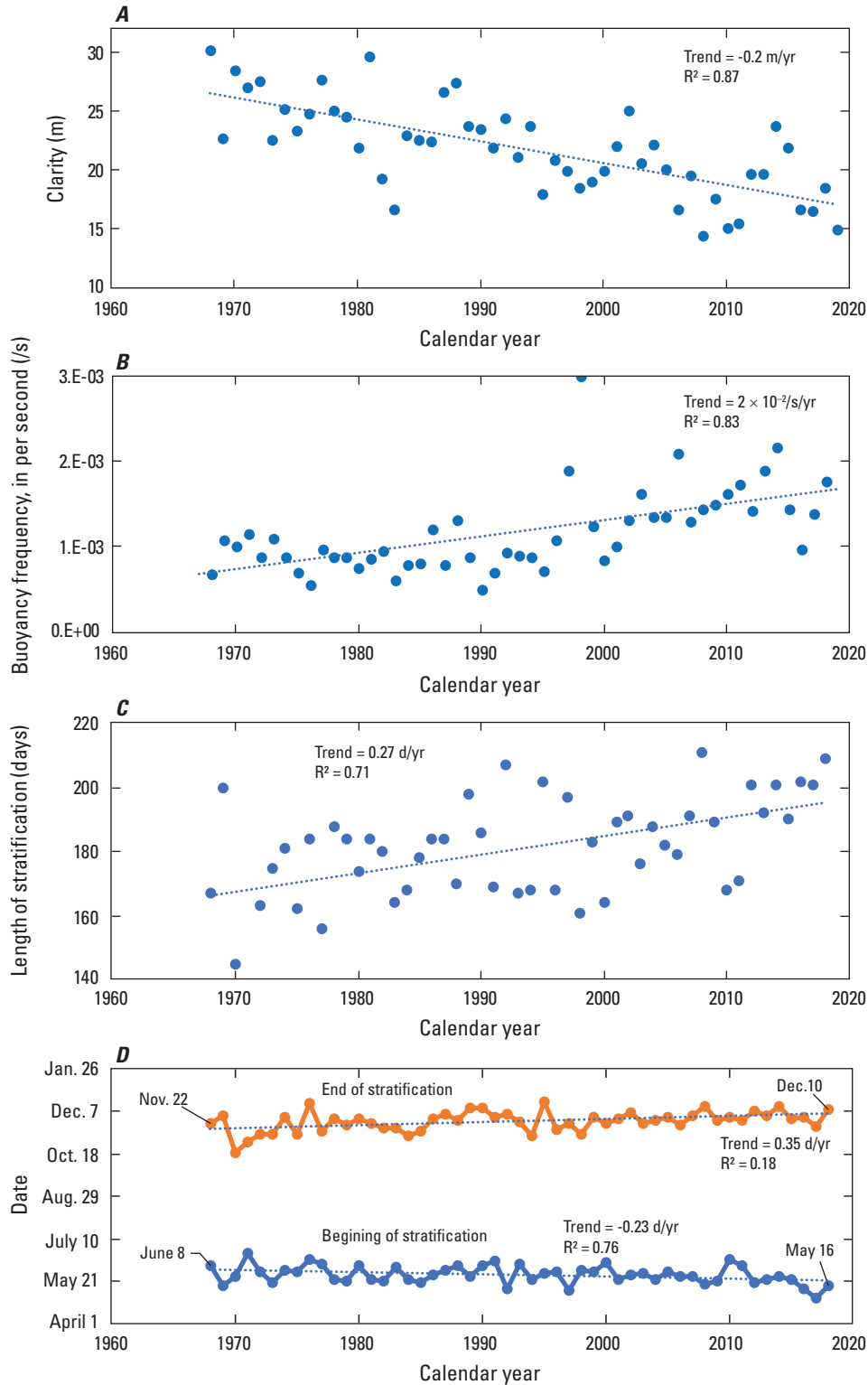
**Figure E4.**   Linear regression analyses withcomputed trends values and coefficients of determination (R² values) for variables characterizing Lake Tahoe during the summer (June–September), 1968–2019: *A*, clarity; *B*, buoyancy frequency; and *C*, period of stratification at the Lake Tahoe profiling station (LTP); and *D*, dates of stratification beginning and ending (Watanabe and Schladow, 2021). Abbreviations: m, meter; m/yr, meter per year; s/yr, seconds per year; d/yr, day per year.

**Table E2.** Linear trends of water-quality variables for Lake Tahoe computed by the least square method, coefficient of determination ($R^2$) values, and standard deviation of the mean values in depth (Watanabe and Schladow, 2021). Variables with $R^2$ values less than 0.15 were negligible.

[Each in-lake variable was measured at two stations in the lake [Lake Tahoe profiling station (LTP) and mid-Lake Tahoe profiling station (MLTP)] albeit at different depths. Variables in bold are showing negative trends. All trends were statistically significant (p-value<0.001) with different measurement depths. Trend Units: clarity in meters per year, fine-sediment particle concentration (FSP) in counts per year, and total phosphorous (TP) concentration in micrograms per liter per year. **Abbreviations**: std dev, standard deviation; ×, times; —, no data; NT, no trend; P, phosphorus]

| Variable | Site | Trend | $R^2$ | Std dev in depth (percent) |
|---|---|---|---|---|
| **Annual clarity** | **LTP** | **$-4 \times 10^{-4}$** | **0.21** | — |
| **Annual clarity** | **MLTP** | **$-4 \times 10^{-4}$** | **0.17** | — |
| **Summer clarity** | **LTP** | **$-2 \times 10^{-1}$** | **0.89** | — |
| **Summer clarity** | **MLTP** | **$-2 \times 10^{-1}$** | **0.85** | — |
| Lake temperature | LTP | NT | Negligible | — |
| Lake temperature | MLTP | NT | Negligible | — |
| Fine-sediment particles | LTP | NT | Negligible | 1 |
| Fine-sediment particles | MLTP | NT | Negligible | 2 |
| Chlorophyll-a | LTP | NT | Negligible | — |
| Chlorophyll-a | MLTP | NT | Negligible | — |
| Nitrate | LTP | NT | Negligible | — |
| Nitrate | MLTP | NT | Negligible | — |
| Total hydrolyzable P | LTP | NT | Negligible | — |
| Total hydrolyzable P | MLTP | NT | Negligible | — |
| Total Kjeldahl nitrogen | MLTP | NT | Negligible | — |
| Total phosphorus | MLTP | $6 \times 10^{-4}$ | 0.15 | 1 |
| Blackwood flow | USGS 1033660 Blackwood C NR Tahoe City, CA | NT | Negligible | — |

We examined the periodicity in the long-term time series and explored the relations with thermal stratification and clarity (fig. E5). Results from the power spectral analysis provided the dominant periodicity or periodicities as peaks of the PSD expressed in years or fraction of year for each parameter along with 95-percent confidence intervals for the peaks as a function of periodicity. Where a peak is smaller than the range indicated, it is below the 95-percent confidence level. The peaks indicated by the red dots exceed the magnitude at their respective periods. Some of the smaller peaks do not exceed this range and are not considered statistically significant. Periodicity results from the power spectral analysis provide some insights into the processes that could be driving change. For example, the periodicity of lake temperatures at LTP was dominated by 1-year periodicity ($10^0$) at all depths down to 50 m. A 6-month periodicity was apparent at the water surface, whereas longer than 6-year periodicity was only evident at 50 m (fig. E6). Such differences among combinations of periodicity and depth suggest that different parts of the water column are subject to different processes. Thus, it seems that deep mixing events that occur only in some years affect temperature at a depth of 50 m, but surface-heat fluxes which vary seasonally dominate temperatures at shallower depths. Summer clarity had a range of periodicity varying from 1 to 10 years, depending on the measurement site. The longer periodicities indicate that sub-decadal meteorological changes as well as long-term climate change could be playing a role. The 6-month periodicity represents seasonality. Further analysis of periodicity was beyond the scope of this project.

The periodicities of all variables from LTP and MLTP are summarized in figure E6. Periodicities of clarity appear to be similar to those for the load of fine particles (flow multiplied by number of fine particles), nitrate, and lake temperature values. The relation between periodicity and load of fine particles does not establish causality; rather, it points to a common set of drivers that could be explored further. Thus, changes in lake stratification (for example, more resistance to mixing) and higher concentrations of fine particles (organic and inorganic) appear to be affecting clarity in Lake Tahoe.
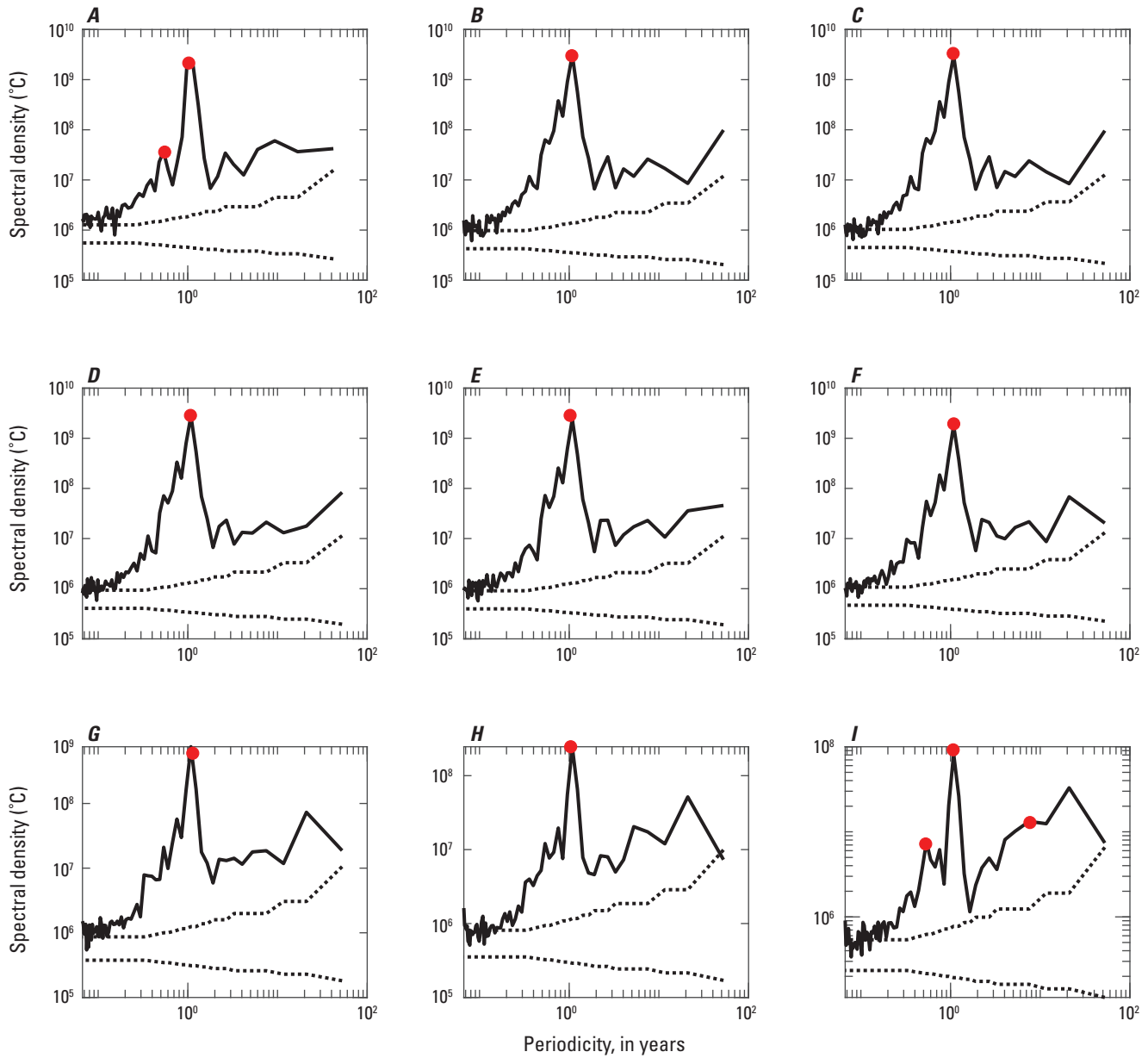
**EXPLANATION**

● Statistically significant periodicity or peaks in frequency, in years

····· 95-percent confidence intervals outside which we identify peaks in frequency content

**Figure E5.** Power spectral density (PSD) of lake temperature, in degrees Celsius (°C), for nine depths at the Lake Tahoe profiling station (LTP), 1968–2019 (Watanabe and Schladow, 2021): *A*, water surface; *B*, 2 meters deep; *C*, 5 meters deep; *D*, 10 meters deep; *E*, 15 meters deep; *F*, 20 meters deeps; *G*, 30 meters deep; *H*, 40 meters deep; and *I*, 50 meters deep. The dashed lines correspond to the 95-percent confidence interval for the peaks as a function of periodicity. Where a peak is smaller than the range indicated, it is below the 95-percent confidence level. The peaks indicated with the red dots exceed the magnitude at their respective periods.
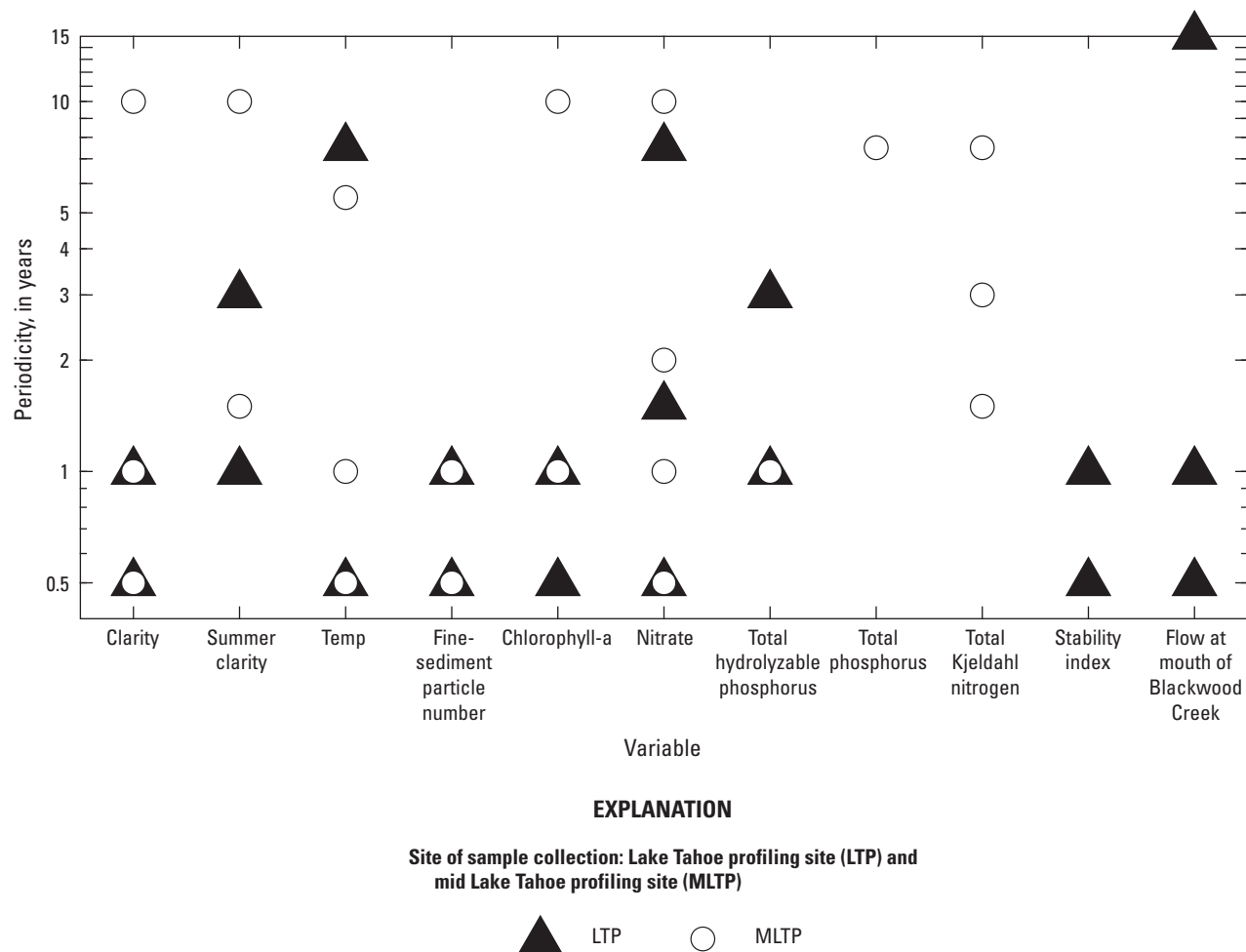
**Figure E6.** Periodicity (in years) for the long-term time-series variables for Lake Tahoe representing a range of qualities and characteristics (Watanabe and Schladow, 2021).

## Summary of Findings for Hypothesis 3

Hypothesis 3 is repeated here:

Changing hydrodynamic conditions within the lake are increasing thermal stability and resistance to mixin*g.*

A statistical evaluation of the trends in thermal stratification variables was used to test this hypothesis. We found statistically significant trends that support earlier, prolonged, and more intense stratification as factors that have contributed to the decline in summer clarity ($R^2 > 0.71$, $p<0.001$). These factors have been linked to climate change (Winder and others, 2008; Sahoo and others, 2015). Our analysis shows that the maximum annual values of buoyancy frequency and resistance to mixing show a linear trend of increasing values on the order of two one-hundredths per second per year ($R^2 = 0.83$, $p<0.001$). Winder and others

(2008) linked this trend to an increase in *Cyclotella* and, hence, to the clarity of the lake. The next chapter looks at the effect of these changing stratification conditions on the insertion depth of inflows, another potential cause of clarity decline.

Periodicity of long-term time series of in-lake variables reveals patterns (0.5- and 1-year periods) driven by annual and seasonal changes in meteorological conditions and hydrological conditions. Longer periodicities, such as 3, 7, and 10 years, are present in our long-term records. Some potential explanations for periods of more than one year include climatological phenomena such as the El Niño–Southern Oscillation (ENSO), among others, and their hydrological consequences, interactions between different trophic levels and nutrients, and ecological effects of invasive species introductions (Sahoo and others, 2013b).

# F. Hypothesis 4: The Trend in Summer Clarity is a Result of Earlier, Prolonged, and More Intense Stratification

## Background

The previous chapter indicated long-term increasing trends in stability index, buoyancy frequency, duration of stratification, and shift toward earlier onset of stratification. Hypothesis 4 is focused on summer clarity and its relation to stratification.

Table F1 presents the relations between summer clarity and the stratification variables buoyancy frequency (N), the date of onset of stratification, and the duration of stratification. Results are consistent with the expectation that earlier stratification would lead to stronger (higher buoyancy frequency), longer duration stratification in most cases.

Summer clarities were negatively correlated with buoyancy frequencies and durations of stratification. Earlier stratification was correlated with reduced summer clarity. The correlations indicated that when stratification was stronger, commenced earlier, or extended longer, summer clarity was reduced. Similar correlations were identified by Sahoo and others (2015). These correlations do not necessarily indicate cause and effect. Changes in stratification are more likely affecting other processes that influence clarity.

Considering "summer" to be the period of stratification and "winter" to be the period of no stratification, the counterpart to longer summers is a reduction in the length of the winter period of vertical mixing that affects water quality throughout the water column. Through the process of deep mixing, there is a vertical transfer of temperature, nutrients, and particles. The deep water (also referred to as the "hypolimnion") is typically high in nutrients (for example, nitrate) but low in particle concentration. Data indicated that shorter winter periods did not directly affect clarity, however. Clarity during winter tended to decline at faster rates

until early 2000, but winter clarity slightly increased from 2000 to 2020 (fig. B2*B*). Deep mixing may, however, affect summer clarity because nutrients transferred to the euphotic zone can be used to stimulate spring algal blooms, and deep mixing is immediately followed by the onset of stratification. Understanding the process of vertical mixing in Lake Tahoe during the winter would be useful for developing robust correlations with clarity but is beyond the scope of this report.

Earlier onset and changes in magnitude and duration of stratification could alter other in-lake processes that affect lake clarity. Longer and stronger stratification periods have the potential to alter particle settling rates. Results of trend analysis of in-lake solutes and particles in the upper 50 m, however, indicate little spatial variability in the vertical direction (normalized standard deviation less than 7 percent, table F1). These results do not indicate changed settling rates in the water column as a result of stronger stratification.

The interaction of the stream water with the ambient lake stratification could affect the stream insertion depth (depth of stream insertion in the lake once its level of neutral buoyancy has been attained) and dilution of fine particles and nutrients from streams (and urban discharges from culverts). Interactions between inflowing stream water and ambient lake stratification were recently shown to be important and highly responsive to climate change by Roberts and others (2018). Changes in the onset and duration of the summer stratification period (in combination with changing stream temperatures) affect the stream intrusion depth. Streams entering a stratified water body can form plunging flows when the inflowing stream is denser than the ambient water or form overflows near the lake surface when stream water is less dense than the ambient water (fig. F1). The distribution of lake water density changes throughout the day and throughout the summer stratified period. Stream temperatures can vary by up to 8 degrees Celsius (°C) during the day–night cycle. Given the potential for stream loads to affect clarity if they insert at shallow depths, we explored the effects of the depth distribution on stream load insertion.

Overflows reduce clarity because river-borne fine particles are trapped in the near-surface, whereas plunging flows or underflows that are inserted below the Secchi depth might not affect the measured clarity. Here, we describe a simplified analytical model to evaluate overflow timing, interannual variability, and relation with lake clarity. This simplified model only requires basic stream and lake physical properties.

**Table F1.** Correlation coefficients (r) and p-values for the relation between decreasing summer clarity and the stratification variables buoyancy frequency, date of onset of stratification, and duration of stratification in Lake Tahoe, (1968–2019; Watanabe and Schladow, 2021).

| Variable | Correlation coefficient | p-value |
|---|---|---|
| Buoyancy frequency | −0.46 | 0.0007 |
| Onset of stratification date | 0.26 | 0.0426 |
| Duration of stratification | −0.34 | 0.0167 |
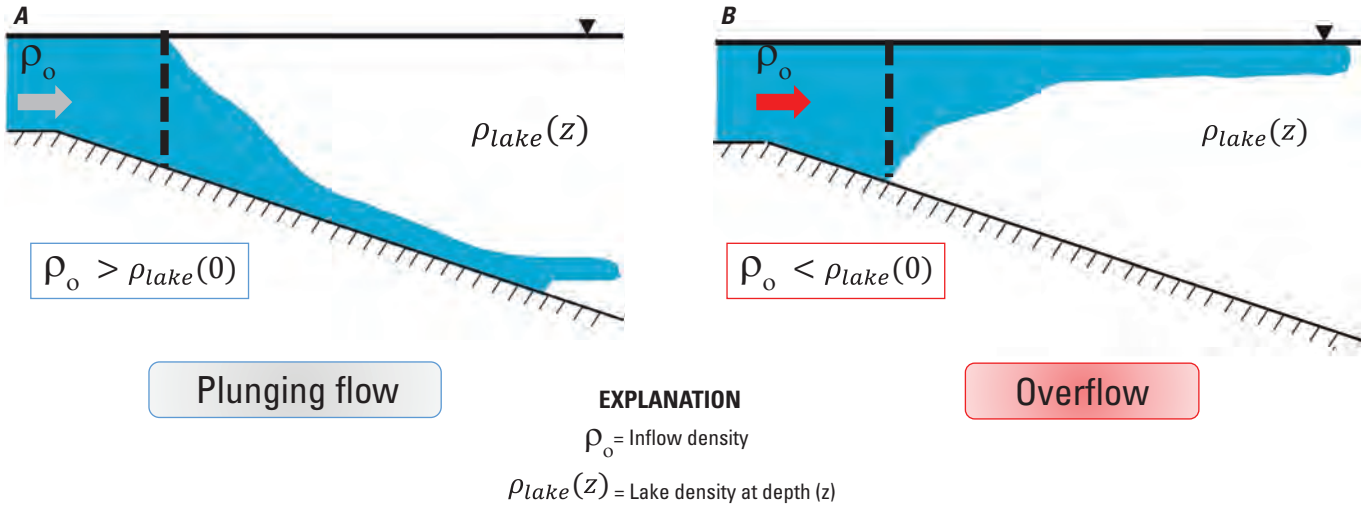
**Figure F1.** Idealized inflow dynamics of streams entering a stratified water body: A, plunging flow beneath less dense lake water; and B, overflow above denser lake water.

## Datasets

We used the lake temperature time series measured in the top 5.5 m every 2 minutes at the NASA-UC Davis buoys deployed in Lake Tahoe. Sensors were vertically spaced every 0.5 m in depth. Our period of analysis is from January 2015 to May 2020.

We also used 15-minute stream temperature, streamflow, and stage data provided by the U.S. Geological Survey (2021) at two of the inflowing streams (Upper Truckee River at South Lake Tahoe, Calif., and Blackwood Creek near Tahoe City, Calif.; table A3) for the same period. These sites were selected given the availability of data and their contributions to sediment loads to Lake Tahoe. For each stream, we computed a continuous time series of width at the mouth as a function of streamflow.

## Approach

We developed a dimensionless number to characterize the nature of the overflows entering Lake Tahoe as a function of time, using a balance between the strength of the inflow and the strength of the lake stratification in the upper 5.5 m. This "buoyancy number" (BN) is defined by the following equation:

$$BN = \frac{IBF_0^{2/3}}{(NH)^2} \qquad (3)$$

where

    $IBF_0$    is the inflow buoyancy flux per unit width,
    H    is the thickness of the upper lake layer

(assumed to be 5.5 m), and
    N    is the buoyancy frequency.

The inflow buoyancy flux per unit width (cubic meters per cubic seconds [m³/s³]) can be estimated as follows:

$$IBF_0 = \frac{gp_0 Q_0}{W_0} \qquad (4)$$

where

    $Q_0$    is the streamflow,
    $W_0$    is the stream width at the mouth, and
    $gp_0$    is the reduced gravity (m/s²), which is calculated as follows:

$$gp_0 = g\frac{\rho_0 - \rho_{lake}(0)}{\rho_{lake}(0)} \qquad (5)$$

where

    $\rho_0$    is the stream density,
    $\rho_{lake}(0)$    is the lake-surface density, and
    $g$    is the acceleration due to gravity.

Finally, we characterize the strength of the lake stratification in the top 5 m using the buoyancy frequency (N; in per second, 1/s):

$$N = \frac{g}{\rho}\frac{d\rho}{dz} \qquad (6)$$

where

    $d\rho/dz$    is the vertical density gradient, and
    $\rho$    is the surface density.

The stratification in the top 5.5 m was evaluated because high spatial and temporal resolution temperature data were only available for the buoy sites.

The physical significance of the buoyancy number is that it indicates the likelihood of overflows as opposed to plunging inflows. If the BN is greater than 5, the inflow buoyancy flux dominates, and the streamwater overflows at the lake surface. If the BN is less than, lake stratification dominates; inflow momentum gets impeded by the ambient stratification and plunges below the surface flowing down the lakebed as a plunging flow or underflow before insertion at its level of neutral buoyancy.

## Results

Changes in surface-water temperature and buoyancy frequency were delineated at time scales that ranged from hourly to interannually from 2015 to 2020. These results show the effect of the warmer summers after 2017 (fig. F2). Buoyancy frequency (N) indicates the strength of the

stratification was as high as 0.06 per second in the summer and approached zero per second in the winter. Hourly values of N can show large departures from the daily values at all times of year, however, indicating the propensity for short-term thermal stratification to affect the fate of stream-borne particles and nutrients throughout the year. Hourly values of N were almost double the daily mean values.

Stream variables were delineated on an hourly, daily, seasonal, and annual basis (fig. F3). Generally, stream temperatures were colder than the lake surface, except for short periods during summers. These temperature differences produced large density differences between the stream and lake surface (that is, large $gp_0$). Stream temperatures oscillated up to 8 °C between day and night, particularly during spring and early summer, when snowmelt was a dominant component of the streamflow. Lowest stream temperatures were early in the day, and warmest temperatures were late in the day, with precise timing varying with factors such as watershed size, aspect, and daily meteorology.
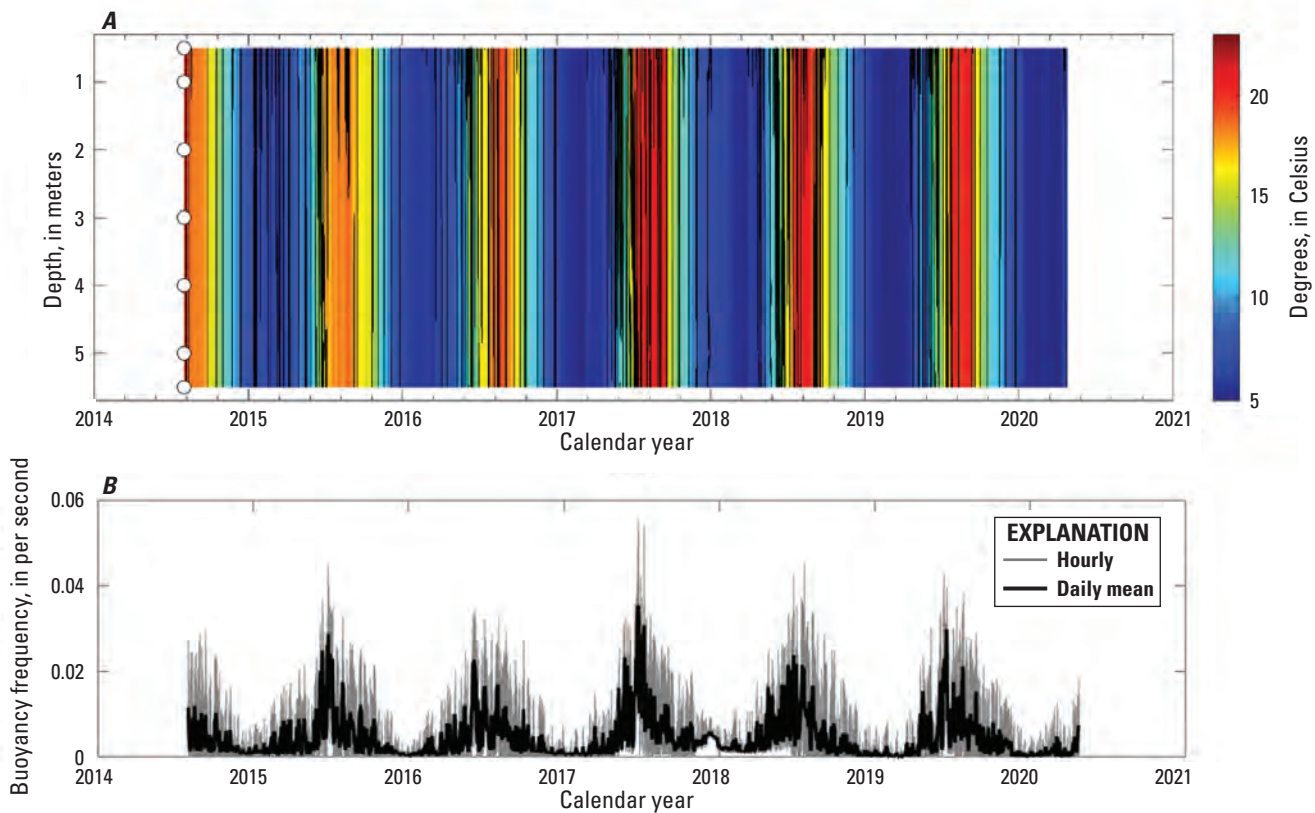


**Figure F2.**    Time series of *A*, lake temperature; and *B*, buoyancy frequency in the upper 5.5 meters of Lake Tahoe (Watanabe and Schladow, 2021). Note that we used the length scale of the layer where high resolution temperature is available (H = 5) as critical value to characterize the fate of the inflow within or below this layer. See table E1 of this report for period of record and frequency.
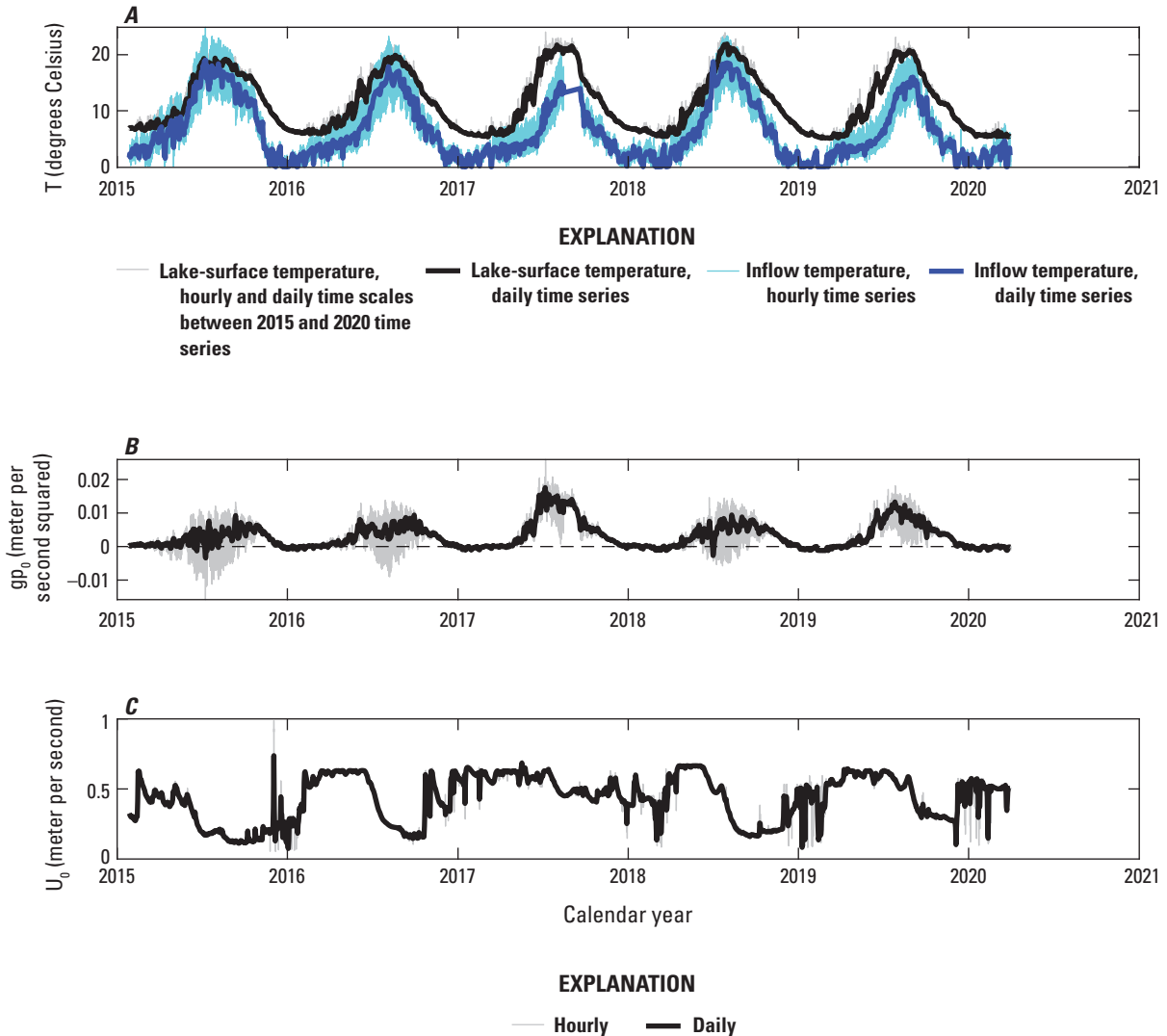
**Figure F3.** Time series at hourly and daily time scales during 2015–20 for Blackwood Creek inflows and Lake Tahoe surface water of *A*, water temperature (T) of inflows and lake surface (Watanabe and Schladow, 2021; U.S. Geological Survey, 2021); *B*, reduced gravity of the stream ($gp_0$) indicating the density difference between the stream and the lake surface; and *C*, the calculated stream velocity ($U_0$). See table E1 of this report for period of record and frequency.

The values of $gp_0$ demonstrate the difference between the stream and lake-surface densities. Daily average values indicate that the stream is generally denser (that is, colder) than the lake surface, because the values of $gp_0$ were positive; however, hourly values show that during spring and summer, the stream can become less dense during the day (negative $gp_0$), resulting in conditions that increase the possibility of overflows. In 2017 and 2019, Blackwood Creek had virtually no negative $gp_0$ conditions. Stream velocities (in meters per second; m/s) were computed by dividing the measured streamflow at a streamgage by the cross-sectional area computed from measurements of stream stage and width and were highest during peak snowmelt in the spring. In 2017,

stream velocity remained high (0.4 m/s) for much of the year because of the high snowmelt and streamflow during that year that were discussed previously.

Buoyancy numbers were computed and are shown in figure F4. Overflow conditions (BN greater than 5) were more common in winter, spring, and early summer (on a daily average and an hourly basis, whereas underflows (BN less than 5) were more common during the fall. Particle fluxes are often low in the fall. Because of the high diurnal fluctuations, the buoyancy number could change in sign throughout the year, meaning that overflows (particle fluxes introduced above the Secchi depth) can develop at any time of year depending on the specific storm event and the lake conditions.
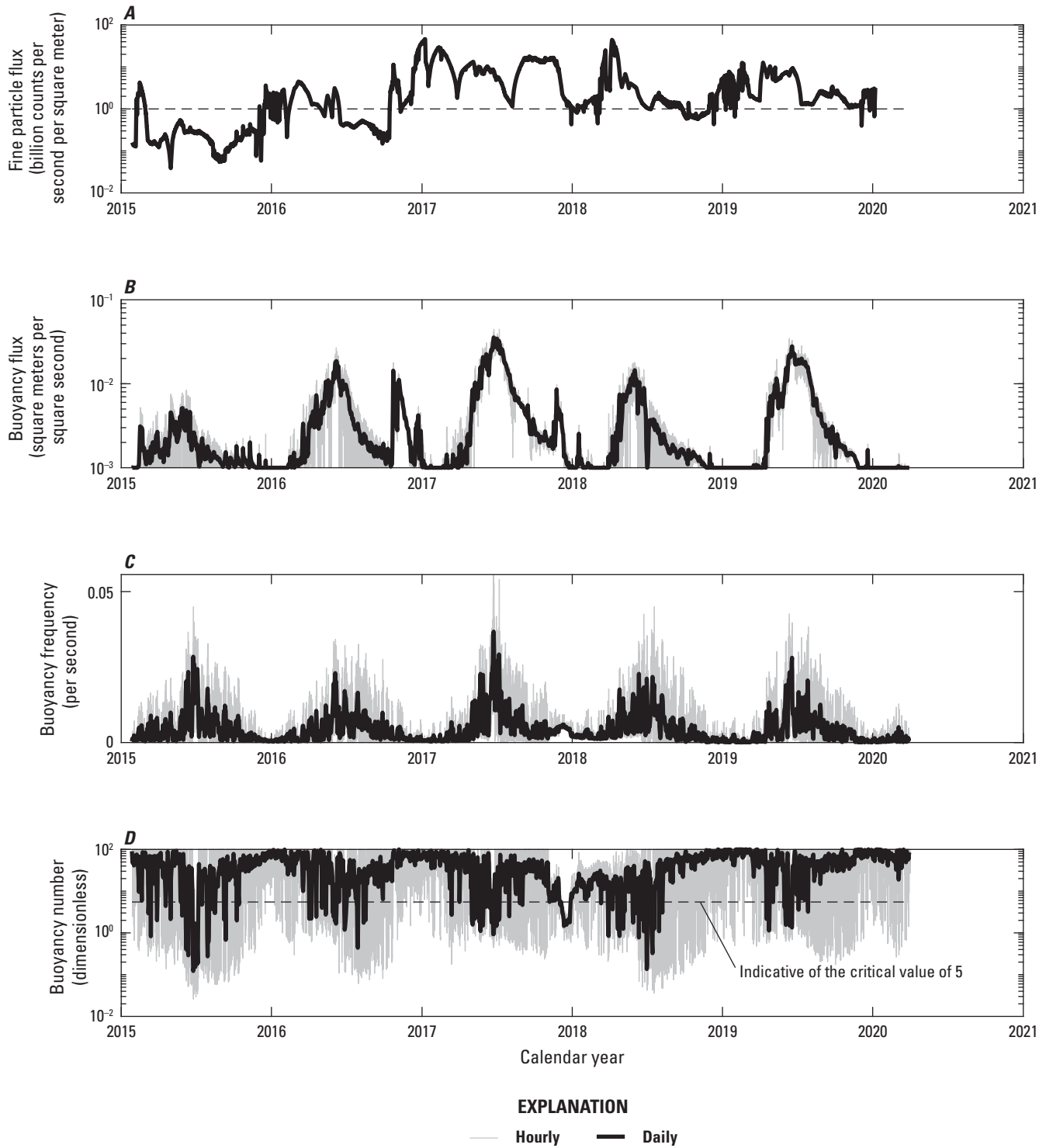
**Figure F4.**   Time series of hourly and daily mean values of variables characterizing inflow density and buoyancy dynamics from Blackwood Creek and surface water in Lake Tahoe between 2015 and 2020 (U.S. Geological Survey, 2021): *A*, inflow fine-particle flux; *B*, inflow buoyancy flux per unit width (IBF$_0$); *C*, lake buoyancy frequency (N); and *D*, buoyancy number values. See table E1 of this report for period of record and frequency.

Interannual variability was apparent in the buoyancy number values during 2015–19 (table F2). The minimum annual value of the buoyancy number was in 2015, which means that underflows were more likely in that year. Values of the buoyancy number were higher during the summer after 2016, indicating more frequent overflows at the lake surface that likely influenced summer lake clarity. In addition, the buoyancy flux ($IBF_0$) and the fine-particle flux from the stream both appear to be consistently greater after 2016 (fig. F4).

The length of this record (2015–20) and the predominant conditions during this 5-year period should be considered when interpreting the presented results. The first 2 years represent the end of a drought of historic proportion, when streamflows and accompanying particle fluxes were very low. The year 2017 had historically high precipitation, streamflows, and particle fluxes, and the 2 years after that both had above average precipitation and streamflow and well above average particle fluxes (see earlier sections of this report).

Finally, we evaluated the effect of using a different lake-surface temperature definition (0 m depth instead of mean for the top 5.5 m temperature) when computing buoyancy numbers; results only changed 0.12–0.17 percent. We also explored the effect of spatial variability comparing results from two streams (Upper Truckee River and Blackwood Creek). Upper Truckee River tended to have greater buoyancy, but buoyancy numbers only changed about 5.2 percent for both streams. The sensitivity of buoyancy number indicates that the approach taken was robust in terms of the data used and may be used as a guide to what to expect for other streams in the Lake Tahoe basin.

**Table F2.** Seasonal and annual values of buoyancy number and water clarity for Lake Tahoe, 2015–20 (Watanabe and Schladow, 2021).

| Period | 2015 | 2016 | 2017 | 2018 | 2019 |
|---|---|---|---|---|---|
| Buoyancy number (dimensionless) | | | | | |
| Winter (December–March) | 46 | 66 | 66 | 12 | 81 |
| Summer (June–September) | 20 | 24 | 30 | 31 | 39 |
| Annual | 36 | 48 | 45 | 39 | 44 |
| Clarity (meters below water surface) | | | | | |
| Winter (December–March) | 21.8 | 25.4 | 24 | 22.4 | 24.7 |
| Summer (June–September) | 22.3 | 17.2 | 16.3 | 18.8 | 16.1 |
| Annual | 22.3 | 21.1 | 18.4 | 21.6 | 19.1 |

## Summary of Findings for Hypothesis 4

Hypothesis 4 is repeated here:

The trend in summer clarity is a result of earlier, prolonged, and more intense stratification.

Declining summer clarity is correlated with earlier, prolonged, and more intense stratification; thus, factors that drive reductions in clarity are likely increasing as a result of changes in stratification. To fully test this hypothesis would require modeling of the fate of fine inorganic particles and of fine algae through time, which is beyond the scope of this report. To partially test this hypothesis, we focused on the insertion depth of streamflows for the period when high-resolution lake-surface stratification data were available. We expected that higher frequency of surface insertions compared to plunging insertions resulted in greater reductions in clarity.

We used the interannual variability and relations with overflows and lake clarity of buoyancy number to determine that higher frequency of insertion overflows coincided with reductions in clarity. Overflows with high concentrations of fine particles were more frequent in years of poorer lake clarity, particularly in summers after 2016, which had high buoyancy numbers. As a caveat on these findings, the five years available for the analysis were not "average" years. The first two were extreme drought years, and the last three were greatly affected by the extreme wet year of 2017.

The relation between overflow frequency and lake clarity described in this report is similar to the relation described by Roberts and others (2018). They explored the effects of changing snowpack conditions as well as changing lake stratification. They concluded that "…lower snowpack has caused inflows to enter Lake Tahoe earlier relative to the onset of thermal stratification and with more positive buoyancy. With projections of warming air temperatures and a reduction in snowpack, inflow mixing conditions are likely to increasingly favor nearshore and near-surface mixing."

Other processes affecting clarity that could be altered by longer, more strongly stratified summer periods include bloom dynamics of small phytoplankton cells, the depth of lake mixing in early spring (which can transfer nutrients to the euphotic zone), and changes in settling rates as density gradients increase and suppress turbulent mixing.

# G. Hypothesis 5: Ecological (Food Web) Interactions are Causing Changes in the Trends of Seasonal or Annual Clarity

## Background

Long-term data on food-web interactions at Lake Tahoe were not available, so a narrative assessment of this hypothesis is provided. This hypothesis was first examined in Schladow and others (2020). This narrative assessment was supported using data from Lake Tahoe and its embayment, Emerald Bay. We did not evaluate the relations between lake clarity and the entire Lake Tahoe food web. Rather, we focused specifically on the relations between the introduced *Mysis* shrimp, the native cladocerans (*Daphnia* and *Bosmina*) that were largely eliminated following *Mysis* introduction, and particulates in Lake Tahoe. Here particulates are defined as free-floating phytoplankton and inorganic particles of terrigenous origin based on recent observations (between 2011 and 2016) of cladocerans returning and clarity increasing by 11 m in 18 months after *Mysis* disappeared from Emerald Bay. When *Mysis* returned, the cladocerans largely disappeared again, and clarity was reduced to its previous level.

In this section, we describe the general effects of *Mysis* on lakes and the events in Emerald Bay from 2011 to 2016. The long-term Lake Tahoe phytoplankton record is reviewed considering the effects of cladocerans on fine particles, and the results are summarized. Specific questions posed by agency representatives are addressed at the end of this section.

The decline of the clarity of Lake Tahoe has been attributed to land-use change spurred by rapid development and population growth in the Lake Tahoe basin starting in the 1950s (Goldman, 1988) as well as by enhanced atmospheric deposition of nitrogen from vehicle emissions and other sources (Jassby and others, 1994). Through the TMDL studies (California Regional Water Quality Control Board and Nevada Division of Environmental Protection, 2010), it was found that fine particulates had a greater effect on lake clarity than nutrients (Jassby and others, 2003; Swift and others, 2006). Consequently, most restoration efforts have targeted legacy development projects and their effects on fine particle and nutrient additions (Tahoe Regional Planning Agency, 2019).

From 1963 to 1964, coincident with a period of rapid development, the non-native opossum shrimp, *Mysis diluviana* (formerly *M. relicta*, here referred to as *Mysis*), was introduced to Lake Tahoe and Emerald Bay. The population of newly introduced mysids took several years to become establish lake-wide, but by 1970, they were a large part of the diet of deep-living lake trout (Richards and others, 1975). Once established, *Mysis* quickly altered the aquatic food web. By selectively feeding on native cladoceran species (*Bosmina longirostris*, *Daphnia rosea*, and *D. pulex*; Cooper and Goldman, 1980; Threlkeld, 1981), *Mysis* effectively

depressed the abundances of all three species in Lake Tahoe by 1973 (Richards and others, 1975). Stomach contents' analysis of *Mysis* identified remains of all the non-cladoceran zooplankton (Threlkeld and others, 1980), highlighting the role of *Mysis* in altering the structure of the native zooplankton community. The resulting pelagic zooplankton assemblage became dominated by copepods *Epischura nevadensis, Diaptomus tyrrelli*, and the rotifer *Kellicottia longispina*.

Zooplankton community structure can assert strong selective pressure on phytoplankton assemblages. Copepods are less efficient grazers than cladocerans (Wu and Culver, 1991) and can reduce predation on smaller algae species by selectively grazing on larger forms of phytoplankton, thereby enhancing the pelagic biomass of small-sized algae (Sommer and Sommer, 2006). Evidence of such a shift was found in Lake Tahoe, where a concomitant increase in the small diatom genus *Cyclotella* spp. followed the loss of cladoceran species (Richards and others, 1975). More recently, Winder and Hunter (2008) reported a trend that among diatoms, *Cyclotella* spp. are the only genus that increased significantly in concentration during the period 1982–2006. They attributed the increased abundance primarily to climate change and increased thermal stratification (Winder and Hunter, 2008).

The shift toward an increase in small-sized planktonic diatom abundance contributes to the decline in lake clarity (Schladow, 2019). Suspended particles (organic and inorganic) attenuate a fraction of light impinging on them through scattering, with a much smaller loss due to absorption. This fraction, the attenuation efficiency, varies in a complex manner with particle size and composition. The work of Van de Hulst (1957) showed theoretically that the attenuation efficiency is maximized at particle diameter of 1.7 µm for inorganic particles, such as quartz, and a particle diameter of about 6.5 µm for organic particles. For larger particle sizes, the attenuation rapidly decreases. Diatoms are organic particles with an inorganic silica frustule and may reflect the characteristics of inorganic and organic particle types. Therefore, attenuation efficiencies of diatoms in Lake Tahoe can be expected to be between values for inorganic and organic particles.

The extent to which *Mysis* in Lake Tahoe could be linked to declines in water clarity went unreported for decades. In 2011, an unprecedented, near-total disappearance of *Mysis* was observed in Emerald Bay, leading to a large and sustained increase in water clarity for more than 3 years. Records of water clarity in Emerald Bay (1962–2021, non-continuous) confirm its clarity had always been less than that of the main body of Lake Tahoe.

Emerald Bay was sampled during the 5-year period following the decline of *Mysis* to characterize the ecosystem-level effects. The sampling results strongly indicated that the decline in water clarity in Lake Tahoe may have in part been the result of the alteration in food web structure initiated by the loss of cladocerans through the introduction of *Mysis*. The loss of cladocerans may have reduced the ability of Lake Tahoe's ecosystem to counter the effects of watershed degradation caused by rapid urban development. The data used in this analysis are indicated in table G1.

## Results

### The Emerald Bay Perturbation

The range of relevant data from Emerald Bay and Lake Tahoe are shown in figure G1. When sampled in November 2011, *Mysis* densities were less than 1 individual per square meter (ind./m$^2$; fig. G1*B*) and remained low until mid-2014, after which values increased to a peak of approximately 150 ind./m$^2$. For reference, *Mysis* densities ranged from 21 to 292 ind./m$^2$ with an average of 120 ind./m$^2$ between July 1979 and June 1985.

**Table G1.** Sampling sites, types, and date ranges and days between sample collections of long-term phytoplankton and zooplankton data, Lake Tahoe (Schladow and others, 2020; Watanabe and Schladow, 2021).

[Discrete indicates samples at specific depths. Composite indicates a prescribed mixture of water from specific depths. Profile indicates continuous measurements with depth. Station designations: EB, Emerald Bay; LTP, Lake Tahoe profiling station; MLTP, mid Lake Tahoe profiling station; SS, south shore site. **Abbreviations**: SD, standard deviation; Nov., November; Aug., August; Apr., April; Dec., December; NO$_3$+NO$_2$, nitrate and nitrite; THP, total hydrolyzable phosphorus; —, no data]

| Site | Sample type | Sampling dates | Mean days between sample collection (SD) |
|---|---|---|---|
| *Mysis* | | | |
| [1]19 Tahoe sites | Vertical tow | 1979–86 | 120–365 |
| [1]11 Tahoe sites | Vertical tow | 1987–95 | 90–365 |
| LTP | Vertical tow | Nov. 2011–Nov. 2016 | 80.1 (30.6) |
| MLTP | Vertical tow | Nov. 2011–Nov. 2016 | 84.0 (29.5) |
| SS | Vertical tow | Nov. 2011–Nov. 2016 | 82.7 (29.8) |
| EB | Vertical tow | 1979–85 | 60–365 |
| EB | Vertical tow | Nov. 2011–Nov. 2016 | 81.0 (30.6) |
| Zooplankton[2] | | | |
| LTP | Vertical tow | Aug. 1967–Nov. 2019 | 30 |
| MLTP | Vertical tow | Apr. 1980–Nov. 2019 | 30 |
| EB | Vertical tow | July 1983–Dec. 1985 | 30 |
| EB | Vertical tow | Nov. 2011–Nov. 2016 | 30 |
| Phytoplankton | | | |
| LTP | Discrete | Aug. 1967–Nov. 1989 | 13.6 (28.0) |
| LTP | Discrete | Jan. 2002–Nov. 2016 | 31.8 (14.4) |
| LTP | Composite | Oct. 1984–Nov. 1989 | 11.5 (2.31) |
| MLTP | Discrete | Sep. 1998–Dec. 2015 | 30.4 (18.2) |
| MLTP | Composite | Feb. 1992–Dec. 2014 | 32.3 (15.4) |
| EB | Discrete | Dec. 2013–Dec. 2016 | — |

| Site | Sample type | Sampling dates | Mean days between sample collection (SD) |
|---|---|---|---|
| Chlorophyll-a | | | |
| LTP | Discrete | Nov. 1983–Nov. 2016 | 32.1 (11.7) |
| MLTP | Discrete | Mar. 1992–Nov. 2016 | 31.8 (12.3) |
| EB | Surface | Dec. 2013–Nov. 2016 | 91.1 (28.8) |
| Primary productivity | | | |
| LTP | Discrete | Jun. 1970–Dec. 2006 | 11.4 (4.1) |
| LTP | Discrete | Jan. 2007–Nov. 2016 | 40.6 (32.5) |
| NO$_3$+NO$_2$ and THP | | | |
| LTP | Discrete | Aug. 1967–Dec. 1991 | 10.8 (4.1) |
| LTP | Discrete | Jan. 1992–Nov. 2016 | 31.0 (12.6) |
| MLTP | Discrete | Apr. 1980–Nov. 2016 | 28.2 (18.7) |
| Water temperature | | | |
| LTP | Profile | Aug. 1967–Nov. 2016 | 11.7 (4.9) |
| MLTP | Profile | Mar. 1969–Nov. 2016 | 27.9 (17.8) |
| EB | Profile | Jan. 2011–Nov. 2016 | 35.1 (30.1) |
| Secchi depth | | | |
| LTP | — | July 1967–Nov. 2016 | 12.8 (6.6) |
| MLTP | — | Apr. 1980–Nov. 2016 | 28.4 (12.5) |
| EB | — | Jan. 2011–Nov. 2016 | 35.1 (30.1) |

[1]Wantabe and Schladow (2021) and Schladow and others (2020).

[2]Ranges are shown because only one or two samples were collected per year, and standard deviations were not computed.

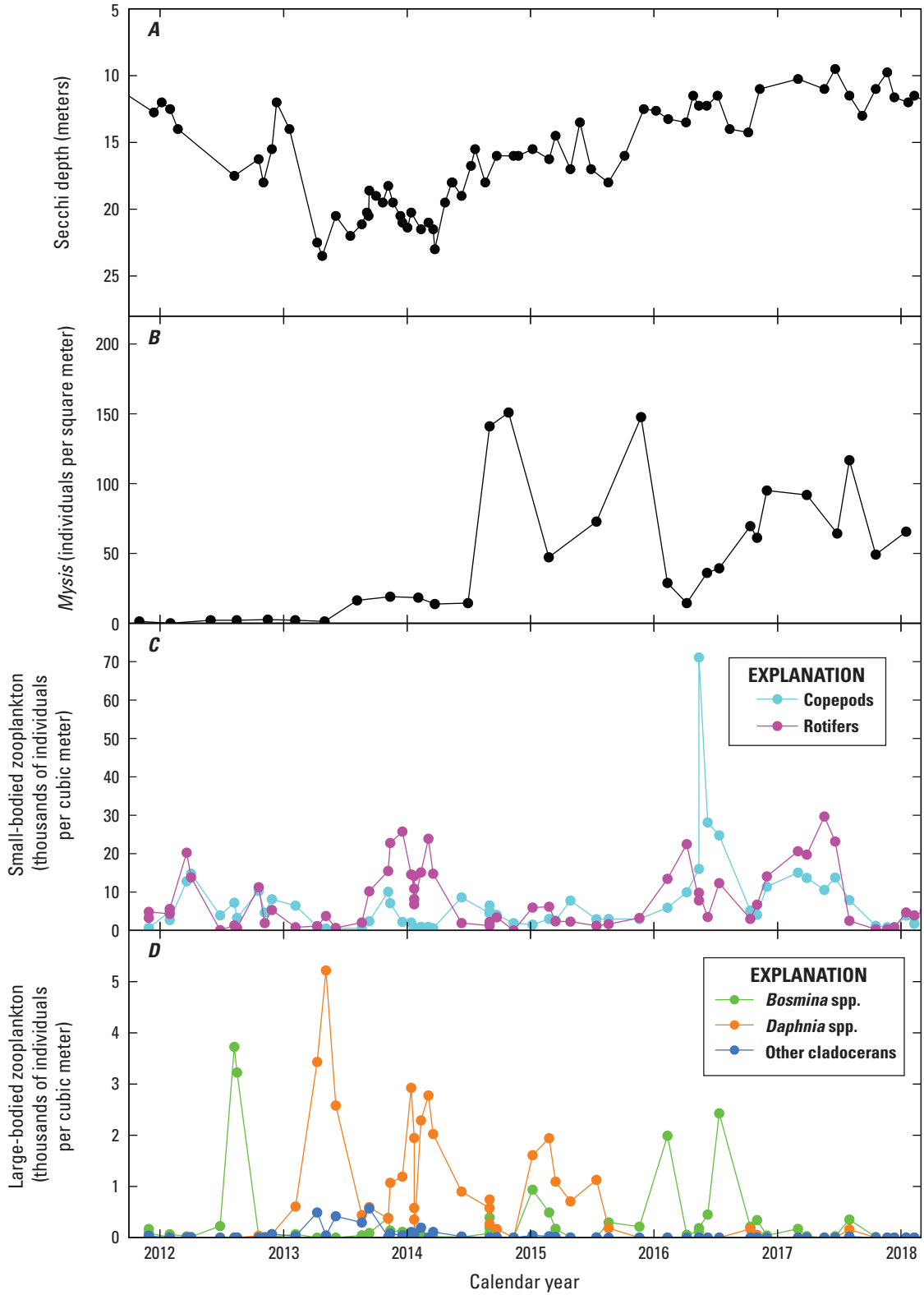**Figure G1.**    Secchi depth and abundances of *Mysis* spp. and zooplankton in Emerald Bay, Lake Tahoe, California, calendar years 2012–18 (Watanabe and Schladow, 2021): *A*, Secchi depth; *B*, *Mysis* abundance; *C*, small-bodied zooplankton; and *D*, large-bodied zooplankton. Note the y-axis ranges are different in *C* and *D*. See table G1 of this report for period of record and frequency.

Values of Secchi depth for Emerald Bay (fig. G1*A*) increased by more than 11 m during 2012–13. A positive change in clarity of this magnitude has never been observed in either Emerald Bay or Lake Tahoe, except for the response to very brief (days) upwelling events (Schladow and others, 2004) or after complete mixing to the bottom of Lake Tahoe (weeks) (Schladow and others, 2020).

Small-bodied zooplankton such as copepods and rotifers, although present in large numbers, fluctuated with no apparent relation to changes in water clarity (fig. G1*C*). Declines in small-bodied zooplankton abundance associated with increases in *Mysis* abundance indicated they were being grazed by *Mysis*. In the absence of *Mysis*, the abundance of large-bodied zooplankton increased substantially. *Bosmina* abundance responded fastest to declines in *Mysis*, with an initial peak exceeding 3,000 ind./m$^3$ in July 2012. By November 2012, *Daphnia* had become more abundant and remained the most abundant cladoceran until August 2016. The cladoceran populations fluctuated, usually 180 degrees out of phase with *Mysis* values, but from November 2012 through August 2016, the mean *Daphnia* population was 1,112 ind./m$^3$. By mid-2014, with *Mysis* abundance again increasing, cladocerans declined and Secchi depth was consistently below 20 m.

The relation between Secchi depth and *Mysis* concentration for the 2011–16 period shown was not statistically significant (r = -0.42, p = 0.434, n = 23), possibly in part due to *Mysis* samples not being collected concurrently with Secchi depth because the former are sampled at night. The relation between large-bodied zooplankton (the cladocerans) and Secchi depth was highly significant (r = 0.72, p<0.01, n = 36). The cladocerans were sampled during the day when the Secchi depth measurements were made. It is not known how much the time of sampling may have impacted the results.

The same set of measurements for Lake Tahoe for the same period (fig. G2) provide the context for the Emerald Bay data. The annual average Secchi depths in Lake Tahoe during 2012–14 were close to those of Emerald Bay, although Emerald Bay had some high Secchi depth readings in early 2012 due to periods of upwelling in the Bay. In 2013, the annual average Secchi depth in Lake Tahoe was 21.4 m, only slightly higher than what was observed in Emerald Bay (19.8 m).

*Mysis* concentrations remained high in Lake Tahoe, with the summer and fall of 2012 having exceptionally high values (about 400 ind./m$^2$), the opposite to what was being observed in Emerald Bay where Mysis abundance was near-zero. Copepods and rotifer abundances in Lake Tahoe were five times lower than values in Emerald Bay, and Cladoceran abundances in Lake Tahoe were even lower relative to abundances in Emerald Bay, with the exception of large *Bosmina* numbers in late 2012. Correlation analysis to examine relations between Secchi depth and cladoceran abundances for Lake Tahoe could not be completed in the same manner as analyses completed using data from Emerald Bay because cladoceran abundances were too low in Lake Tahoe.

## Observations from Long-Term Datasets

Since 1968, annual average clarity has generally decreased, albeit at a slowing rate in the last 20 years (fig. G3). The period of decrease, as noted earlier, coincided with rapid development in the Lake Tahoe basin (Goldman, 1988) and the introduction and establishment of *Mysis* (Richards and others, 1975).

The pre-1982 phytoplankton data record has some quantitative uncertainties relating primarily to whether both live and dead diatom cells were counted. Typically, today we find that dead cells (free floating frustules) are equivalent in abundance to living diatoms (L. Tanaka, University of California, Davis, oral commun., 2020). That uncertainty makes the full dataset unsuitable for long-term trend analysis; therefore, we only used phytoplankton data to determine presence or absence of specific algal groups. Diatoms have always been the dominant component of the phytoplankton assemblage sampled in Lake Tahoe; however, their composition and size structure changed substantially through time.
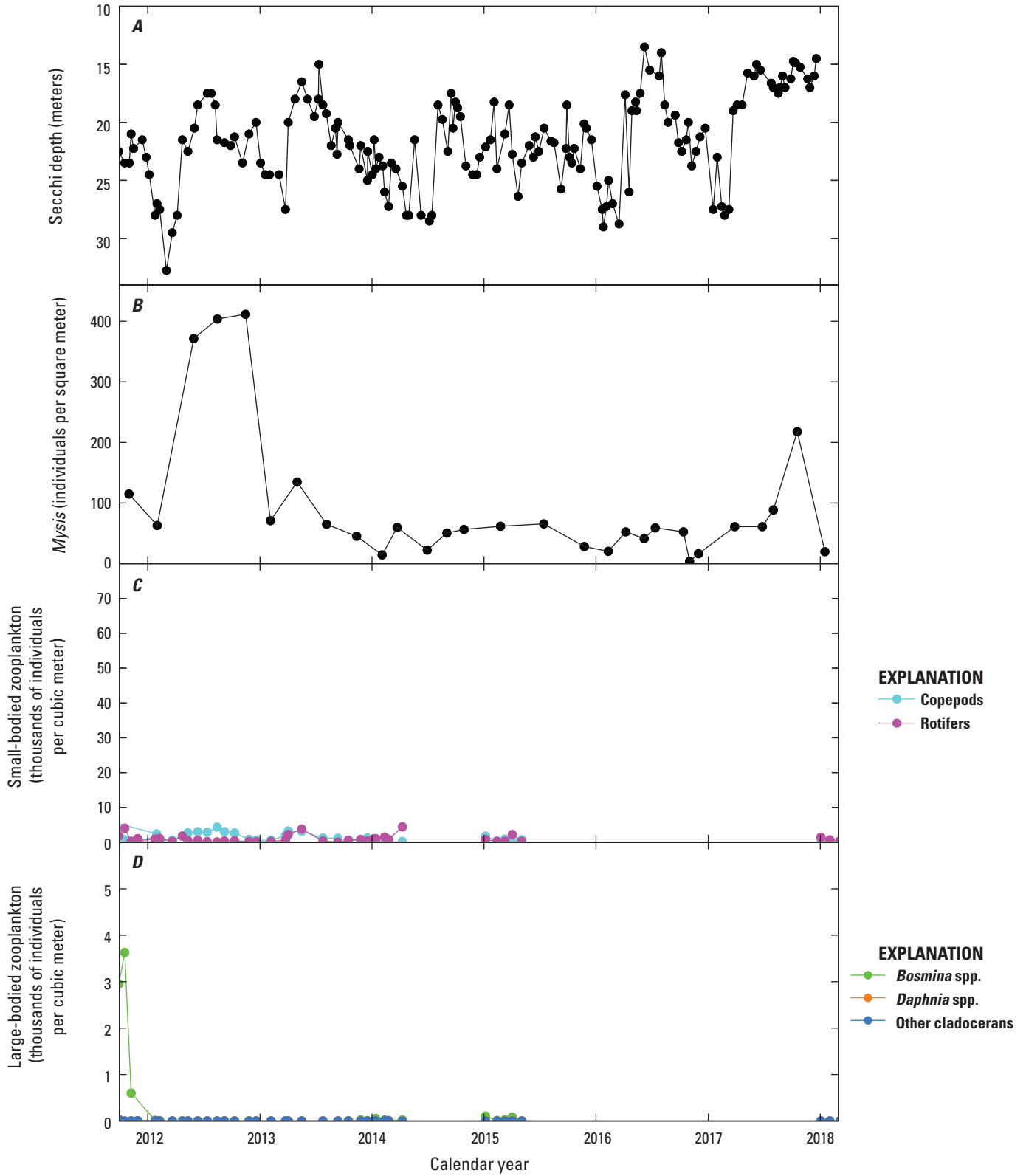
**Figure G2.**   Measurements from the Lake Tahoe profiling (LTP) station (Watanabe and Schladow, 2021). *A*, Secchi depth; *B*, *Mysis* concentration; *C*, small-bodied zooplankton; and *D*, large-bodied zooplankton. Note the y-axis ranges are different in *C* and *D*. See table G1 of this report for period of record and frequency.
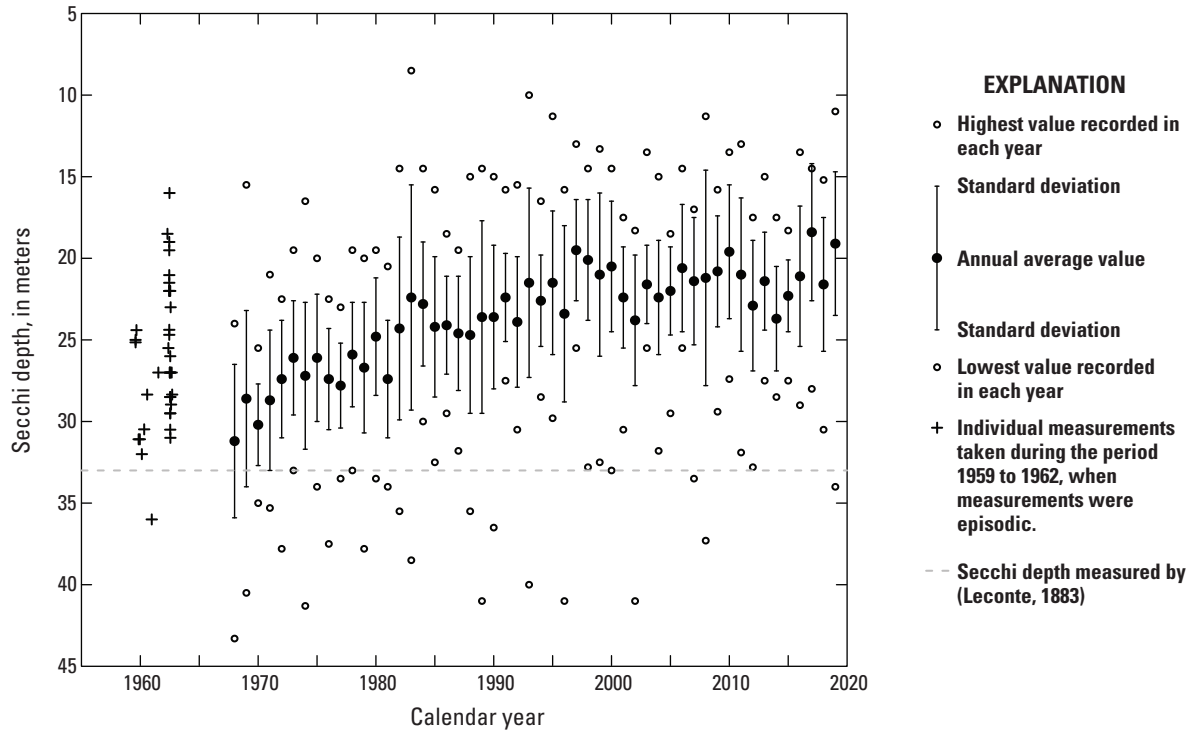
**Figure G3.**    Long-term Secchi depth data for the Lake Tahoe profiling (LTP) station, calendar years 1959–2019 (Watanabe and Schladow, 2021). See table G1 of this report for period of record and frequency.

The large-sized, colonial diatom species *Fragilaria crotonensis* was a major component of the algal community during the first years of Lake Tahoe monitoring. This species was consistently dominant in abundance (individuals per milliliter; individuals/mL) and biomass (as cell volume). Prior to 1970, the *F. crotonensis* population increased in January and February and reached peaks of over 150 cells/mL in March and April before declining to a mid-fall minimum. Time-series data from two water depths (5 m and 20 m below the surface) for *Fragilaria crotonensis* are shown in figure G4 for the 1967–2018 period (excluding 1989–2001). *F. crotonensis* lengths ranged from 60 to 72 µm, and widths ranged from 2 to 3 µm (Morales and others, 2013) and they are typically observed as contiguous colonies with a square plan form. A colony of *F. crotonensis* is shown in figure G5*A*. Since 1976, *F. crotonensis* has declined steadily to extremely low densities, and after 1980, it became an infrequent species in pelagic areas of Lake Tahoe.

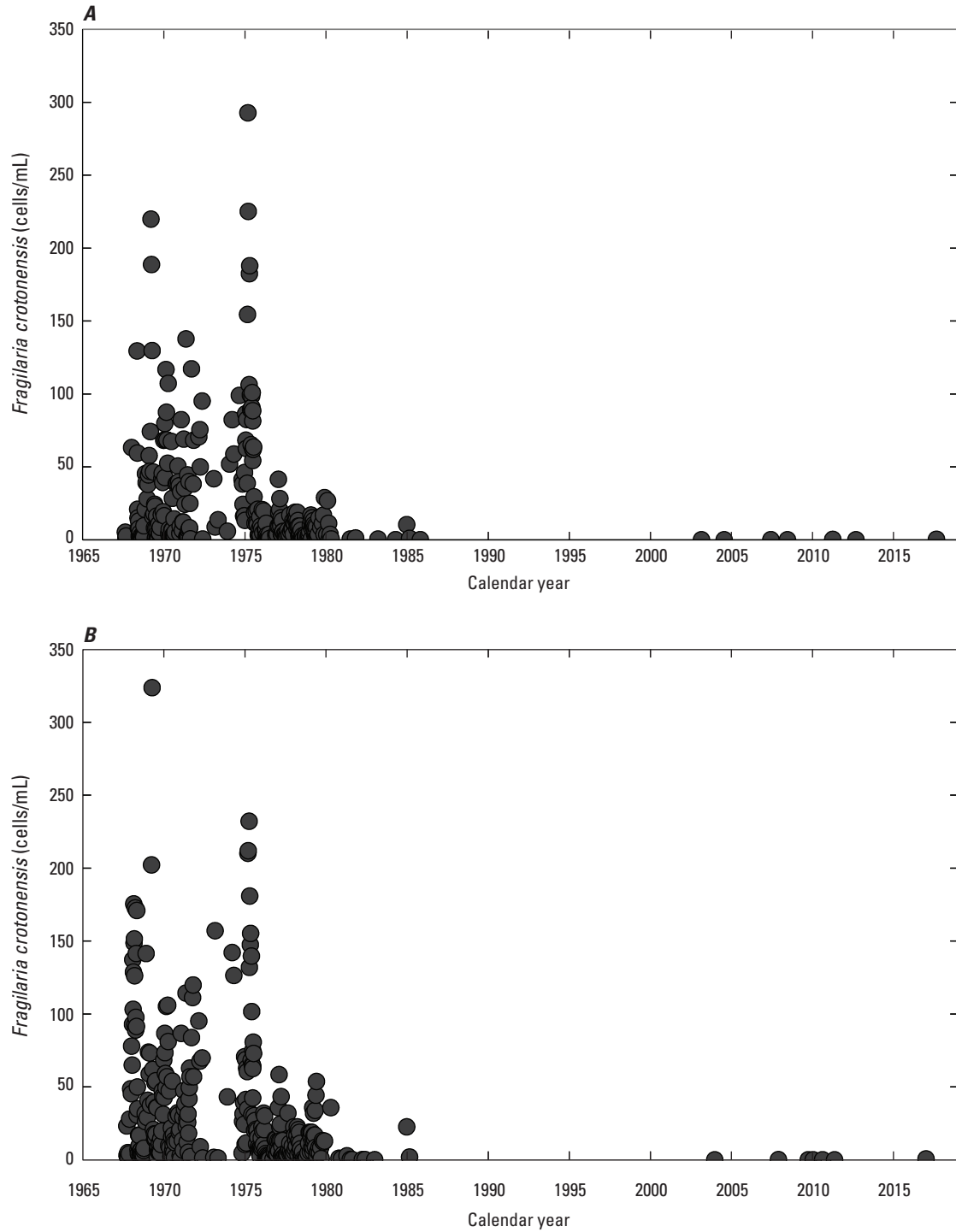**Figure G4.**   Cells per milliliter (cells/mL) of *Fragilaria crotonensis* at the Lake Tahoe profiling (LTP) station, 1967–2018 (Watanabe and Schladow, 2021), at depths of *A*, 5 meters; and *B*, 20 meters. Data were not available from 1988 through 2001; for all other years, a zero reading indicates a total absence of *F. crotonensis*. See table G1 of this report for period of record and frequency.
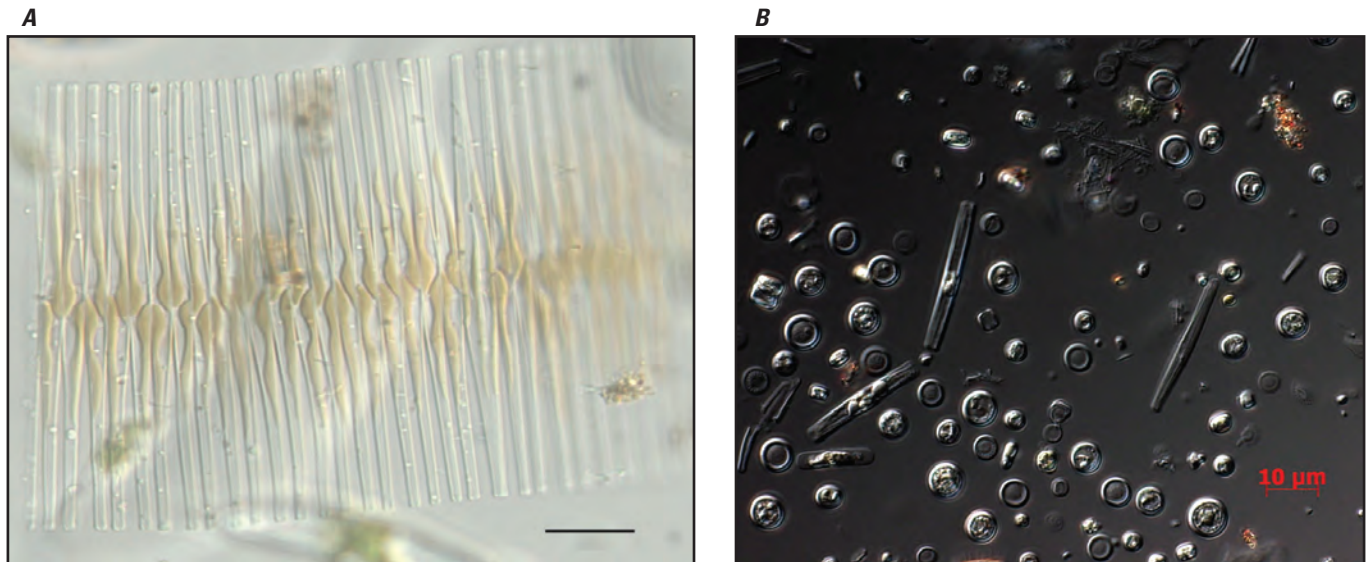
*A*

*B*

10 µm

**Figure G5.**    Diatom species living in Lake Tahoe (Watanabe and Schladow, 2021): *A, Fragilaria crotonensis* with scale bar = 20 micrometers (µm; photograph by L. Tanaka, University of California, Davis, July 2019 ); and *B, Cyclotella gordonensis* with scale bar = 2 µm (Kling and Håkansson, 1988; photograph by D. Hunter, University of California, Davis, October 2008).

Data for the unicellular, centric diatoms of the genus *Cyclotella* are shown in figure G6. *Cyclotella* in Lake Tahoe are generally small and are difficult to correctly distinguish as individual species, particularly with the lower resolution microscopes available during the early decades of the Lake Tahoe phytoplankton record. The species (and size ranges) of *Cyclotella* represented likely include *C. ocellata* (3.7–15 µm), *C. stelligera* (3.7–13.8 µm), *C. glomerata* (3–10 µm), *C. comensis* (5–12 µm), *C. meneghiniana* (6.3–16.5 µm), and *C. gordonensis* (<5 µm). Size ranges are provided by https://diatoms.org/species/ and by Kling and Håkansson (1988). Taxonomic and reference information for *C. gordonensis* can be found at https://www.algaebase.org/search/species/detail/?species_id=37757.

As discussed previously, light scattering is highest for the particulate material size range of about 1.7–6.5 µm, depending on whether the material is organic or inorganic. Diatoms possess the attributes of both material types, and the nature of their scattering properties is not well understood. The replacement of the dominant diatom with size of 70 µm, with a unicellular diatom with a diameter of between 2 and 10 µm, would have had a large effect on light scattering.

The phytoplankton community was sorted into small and large size classes for four different years (1969, 1985, 2002, and 2018; fig. G7). The small size class includes organisms smaller than 20 µm in length or diameter (excluding picoplankton, 0.2–2.0 µm), and the large size class includes all phytoplankton species larger than 20 µm. Some consistent patterns emerged after sorting the phytoplankton community data into size classes. Large species made up more than 86 percent of the phytoplankton cell counts throughout 1969 (fig. G7*A*), but this ratio changed drastically by 1985, when small species consistently accounted for 80–100 percent of the cells (fig. G7*B*). The number of cells decreased by a factor of 5 from 1985 to 2002. As shown in figure G7, there were other years when the abundance of small cells was high. For example, in 2009, 2010, and 2016 (see fig. G6), the small *Cyclotella* cell counts were in excess of 4,000 cells/mL (more than in 1985). In general, *Cyclotella* spp. account for the majority of the small-celled phytoplankton.

Looking specifically at *Cyclotella* spp. in figure G8, the evolution in total number of cells and annual distribution is evident. Concentrations of *Cyclotella* spp. were negligible throughout the year in the pre-*Mysis* period. After the initial colonization by *Mysis*, concentrations of *Cyclotella* spp. increased initially in summer only (July and August as shown for 1985). In more recent years, for example 2002 and 2018, high concentrations of *Cyclotella* spp. are observed for up to six months per year, occurring as early as May and lasting as long as November. Observed increases in *Cyclotella* spp. coincide with the recently observed declines in summer and fall clarity in Lake Tahoe (Schladow, 2019).
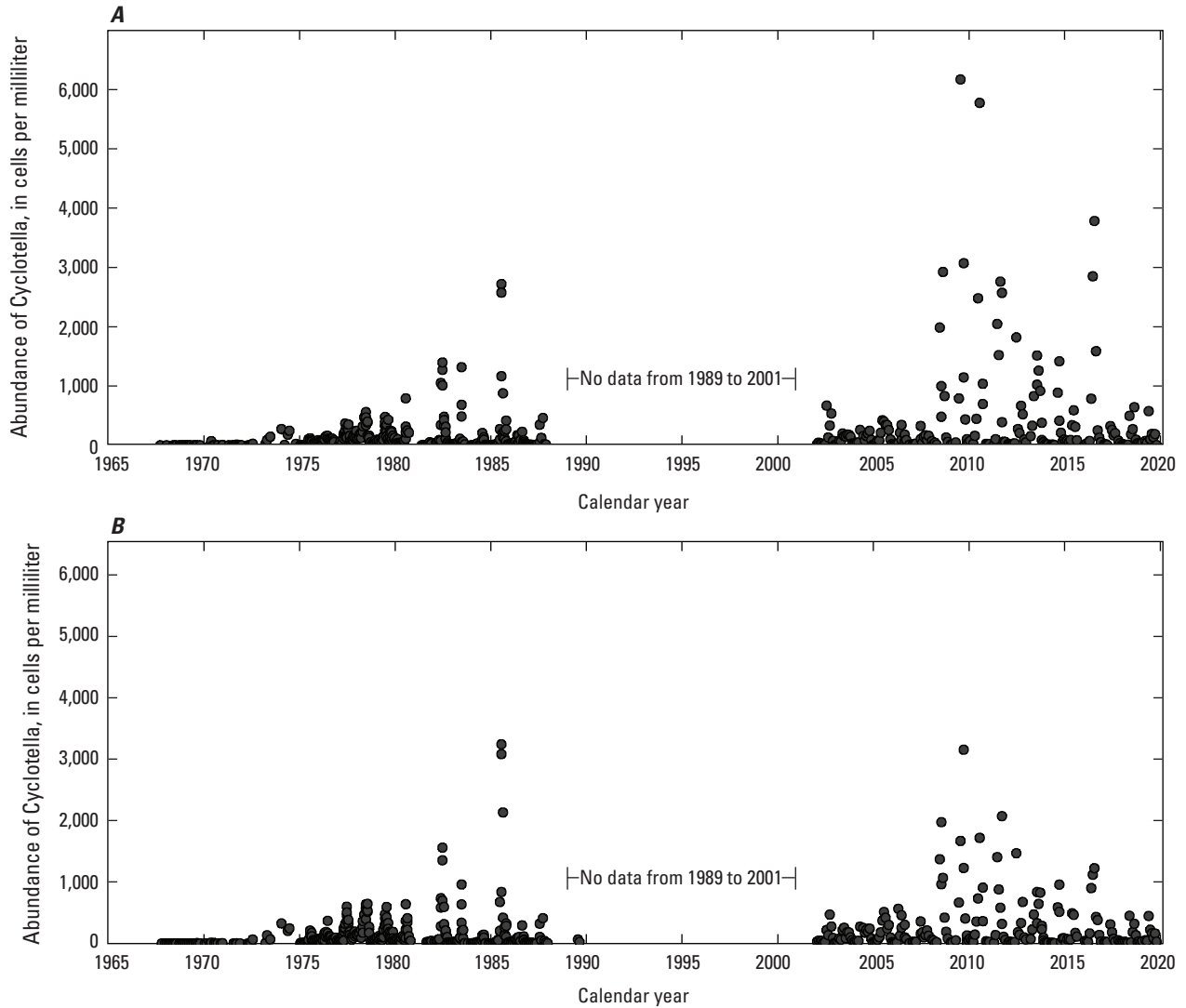
**Figure G6.**   Long-term measurements of abundance of *Cyclotella sensu lato* at the Lake Tahoe profiling (LTP) station from 1967 to 2019 (Watanabe and Schladow, 2021) for two water depths: *A*, 5 meters below the water surface; and *B*, 20 meters below the water surface. Data were not available between 1989 and 2001. See table G1 of this report for period of record and frequency.
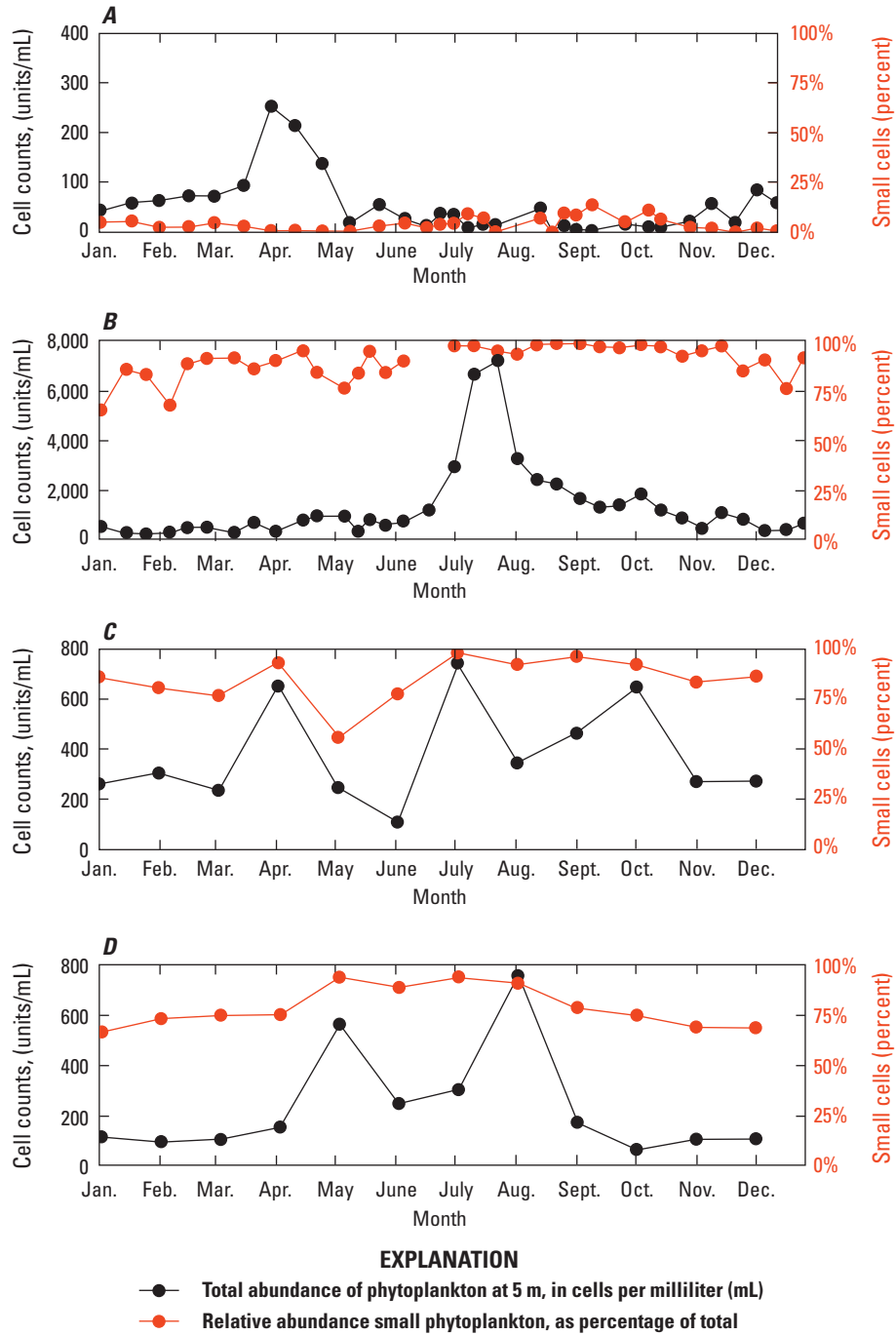
**Figure G7.** Temporal changes in abundance and distribution of phytoplankton assemblages at a depth of 5 meters during 4 years at the Lake Tahoe profiling station (Watanabe and Schladow, 2021): *A*, 1969; *B*, 1985; *C*, 2002; and *D*, 2018. Note that the left y-axis ranges differ by year. See table G1 of this report for period of record and frequency.
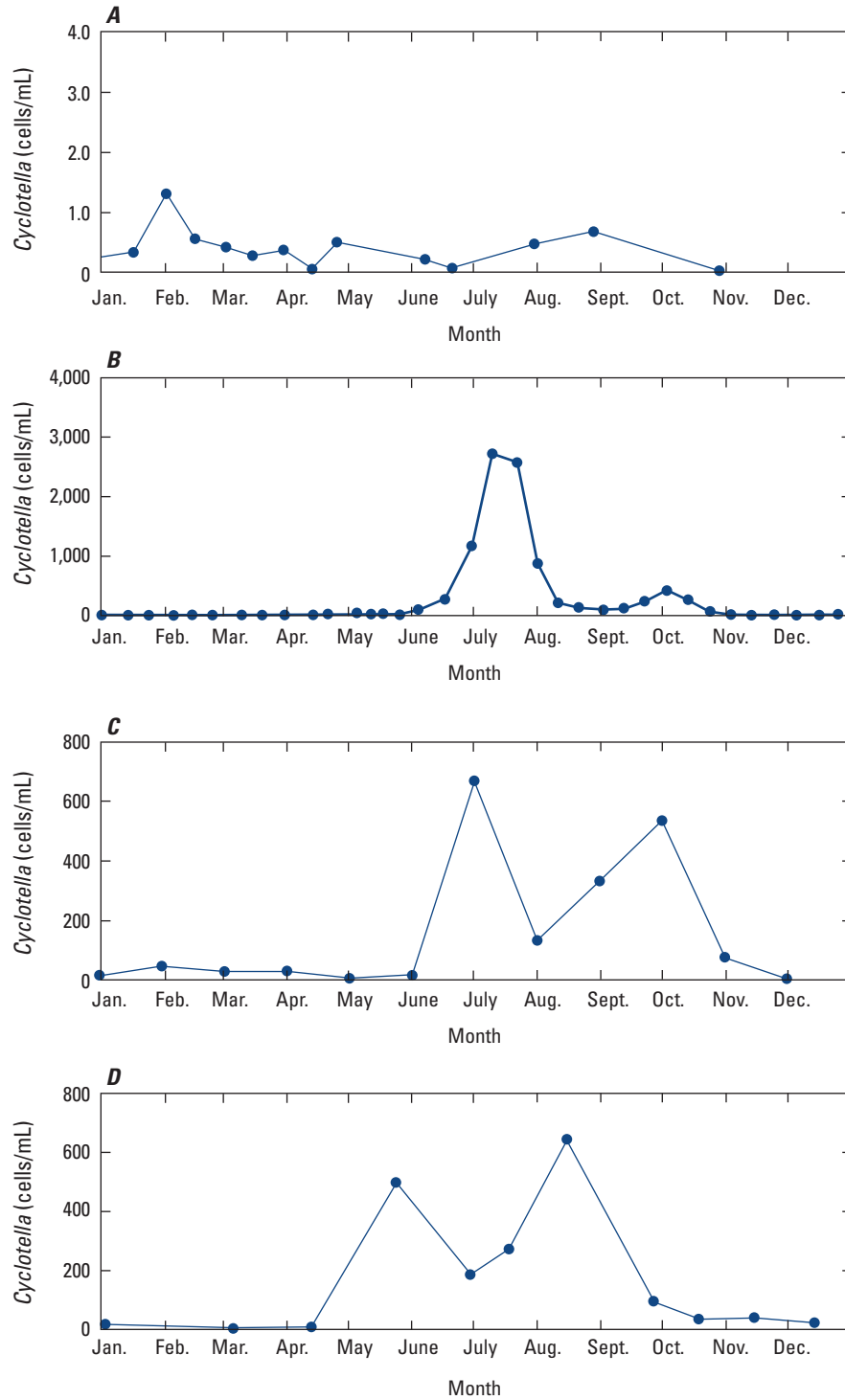
**Figure G8.**   Temporal changes in concentration of *Cyclotella* spp., in cells per milliliter (cells/mL), in Lake Tahoe at a depth of 5 meters during *A*, 1969; *B*, 1985; *C*, 2002; and *D*, 2018 (Watanabe and Schladow, 2021). See table G1 of this report for period of record and frequency.

## Discussion

The introduction of *Mysis* to Lake Tahoe and Emerald Bay altered zooplankton community structure and likely contributed to the decline of the large-bodied native cladocerans *Daphnia* and *Bosmina*. In addition, long-term Lake Tahoe phytoplankton data indicated that a substantial shift toward phytoplankton assemblage dominated by smaller cell sized species that are known to reduce clarity occurred concurrently. These shifts in phytoplankton community structure are likely to have been linked to *Mysis* grazing on larger phytoplankton species, for the reasons given below.

Stable isotope analysis and intestinal content analysis of *Mysis* in other lakes showed that diatoms or algal material formed between 25 percent and 50 percent of the assimilated diet depending on the season (Stalberg, 1933; Larkin, 1948; Johannsson and others, 2001). This is consistent with the feeding habits of *Mysis*, which can both filter feed on suspended particles and undertake raptorial feeding on larger organisms (Grossnickle, 1982). Given the feeding behavior of *Mysis* in other systems, it seems likely that larger diatoms in Lake Tahoe, such as *Fragilaria*, made up at least a part of their diet, which may fully account for the disappearance of the larger native diatoms after *Mysis* introduction. It seems highly unlikely that *Mysis* could control the emerging population of small *Cyclotella* given that observed *Mysis* gut contents typically contain organisms at least one to two orders of magnitude larger than *Cyclotella*.

Could *Daphnia* and *Bosmina* species have been effectively controlling the small-celled *Cyclotella*, and did the decline of large-bodied cladocerans in Lake Tahoe contribute to the long-term trend of decreasing water clarity? It appears that a combination of the absence of grazing cladocerans, the lack of competition for nutrients with the larger diatoms on account of *Mysis* grazing, plus the effect of climate change favoring small species (Winder and others 2008) has allowed *Cyclotella* abundance to increase through time and has likely contributed to declining water clarity, especially during the summer months when *Cyclotella* concentrations are at their highest.

Could *Daphnia* grazing rates control *Cyclotella*? Burns and Rigler (1967) showed *D. rosea* feeding rates of up to $10^5$ cells per *Daphnia* per hour (cells/*Daphnia*/hr). The cells in that case were yeast, with lengths of about 4.2 μm. As of 2020, measurements of *Cyclotella* abundance were as high as $6 \times 10^3$ cells/mL in Lake Tahoe (fig. C7).

Why wouldn't *Daphnia* have also eaten the larger diatoms that the long-term data indicate have declined since *Mysis* introduction? Burns (1968) showed that there is a linear relation between the size of filter-feeding cladocera (including *Daphnia*) and the size of their prey. *Bosmina longirostris* is 0.4–0.6 millimeters (mm) long, and *Daphnia pulex* is 0.2–3.0 mm long. Cladocerans up to 2 mm in length (the maximum size of *D. rosea*) do not prey on phytoplankton larger than 40 μm, which would eliminate *Fragileria* as *Daphnia* prey. This indicates that large diatoms were dominant before the introduction of *Mysis* because they were excluded from grazing pressure because of their size. Consequently, the subsequent decline in large diatoms was likely due to grazing by *Mysis*.

Can *Daphnia* also remove fine inorganic particles (such as those introduced by stream and urban loading) in addition to small *Cyclotella* cells? Previous studies and the findings presented in this report indicate that fine inorganic particles are contributing to declining water clarity in Lake Tahoe (California Regional Water Quality Control Board and Nevada Division of Environmental Protection, 2010). Most experiments to determine *Daphnia* filtering rates use inorganic particles, such as glass beads (Burns, 1968) and polystyrene beads (Gophen and Geller, 1984). The latter found that *Daphnia* would solely ingest polystyrene particles larger than their filter meshes (0.4–0.7 μm). They used particle concentrations of the order of $10^4$–$10^8$/mL in the size range of 0.5–5 μm, the particle-size range that is the largest contributor to light scattering and clarity loss (Van de Hulst, 1957; Davies-Colley and Smith, 2001). Thus, *Daphnia* could readily remove inorganic particles in this size range that exist at concentrations of $10^3$ to $10^5$ particles/mL in Lake Tahoe (Schladow, 2019).

## Summary of Findings for Hypothesis 5

Hypothesis 5 is repeated here:

Ecological (food web) interactions are causing changes in the trends of seasonal or annual clarity.

With the disappearance of *Mysis* from Emerald Bay and the subsequent return of cladocerans coinciding with an unprecedented increase in Secchi depth of 11 m, researchers were able to witness the potential for restoration of at least a part of the Lake Tahoe food web. Although the relation between *Mysis* and cladocerans in Lake Tahoe and elsewhere has long been known, the effect of their relation on lake clarity is new and offers an additional tool for clarity restoration.

The long-term record from Lake Tahoe indicates that a key effect of the *Mysis* introduction on Lake Tahoe's biota was the change to the phytoplankton assemblage, where larger diatoms disappeared likely due to *Mysis* grazing only to be replaced by order-of-magnitude smaller *Cyclotella* spp. Cells in this latter group were too small to be grazed by *Mysis* and other Lake Tahoe zooplankton and benefited from reduced competition for nutrients and a more density-stable water column. *Daphnia and Bosmina*, the copepods long known to have been almost eliminated by *Mysis*, are known to feed at high rates on particulates in the size range of *Cyclotella* and fine terrigenous particles. *Cyclotella* and fine inorganic particles are known to affect clarity in Lake Tahoe through their high light-scattering efficiency.

Results of analyses presented in this report support the hypothesis that "Ecological (food web) interactions are causing changes in the trends of seasonal and annual clarity." The loss of cladocerans, the "internal cleaners" of the lake, coincided with the long, sustained period of annual clarity decline starting in about 1970, and a mechanistic explanation of the process of decline exists in the published literature for numerous lakes as cited earlier.

The seasonal nature of these food-web effects is more complex. The loads of fine particles to the lake from the watershed are typically highest in spring and summer. Likewise, periodic blooms of *Cyclotella* are increasingly in the spring, summer, and fall. Thus, the loss of internal cleaners would be expected to show a maximal effect in these seasons. Other factors, such as changing meteorology, hydrology, and lake stratification further complicate the interactions. While many of these factors are beyond the control of resource management agencies, actions that restore *Daphnia* and *Bosmina* to Lake Tahoe through control of *Mysis* would complement existing actions that seek to control external loading and growth of small algae.

# H. Variables That Influence Winter and Summer Lake Clarity

This work focused on specific hypotheses and questions raised by agencies. Variables not addressed by agency hypotheses and questions likely affect clarity in Lake Tahoe. Therefore, winter and summer data were evaluated by non-parametric Spearman's rank order correlation with many additional variables beyond what agencies were requesting. This correlation analysis was used to evaluate the broad suite of measured and calculated variables related to watershed and in-lake processes that may influence lake clarity. This correlation analysis was not intended to be used draw definitive conclusions, but rather to highlight additional variables that likely contributed to changes in clarity but were not identified in hypothesis questions. We were also cautious not to conclude that strong correlation leads to causation. For example, streamflow inputs from Upper Truckee River and Blackwood Creek were used as surrogates for all stream inputs in timing of streamflow and fine sediments. A more comprehensive evaluation of stream inputs might help determine individual gaged basin influence on clarity. Variables used in winter and summer correlation assessment are defined in table 3.1.

## Winter Clarity and Summer Variables

Correlations with winter clarity were evaluated for 34 variables monitored during winter months (December–March) and summer months (fig. H1A). Variables monitored during winter months were statistically evaluated but did not provide significant correlations to winter clarity, which indicates processes in other seasons are likely controlling winter clarity. Therefore, a more comprehensive evaluation including summer variables was used to provide insight into winter clarity trends. Five summer variables were significantly correlated to winter clarity based on a level of significance ($\alpha$) of 0.05 (fig. H1B). These results indicate that winter clarity is influenced by internal lake processes and watershed processes that typically peak during seasons outside of the December to March winter period. Winter clarity was negatively correlated ($p<0.05$) with summer peak and maximum buoyancy frequency; winter clarity was positively correlated with maximum snow water equivalent (SWE), summer

total phosphorus from Blackwood Creek, and beginning stratification day. Correlations that were not statistically significant ($p>0.05$) are not shown in figure H1B.

Winter clarity improves during the winter months because winter mixing dilutes light attenuating particles (Jassby and others, 1999). The timing and influence of mixing on lake clarity, however, is difficult to describe using metrics other than mixing depth or temperature, which were found not to be statistically significant. Nevertheless, it has been widely recognized for Lake Tahoe that deep mixing brings clearer water from depth to the near surface during isothermal conditions that are common during February or March (Jassby and others, 1999). As an example, in 2019, the highest individual clarity reading of 34 m was on February 19, coincident with the onset of vertical mixing to 450 m. During mixing events, nitrate concentrations also change throughout the water column because hypolimnetic waters have higher concentrations than epilimnetic waters. Nitrate concentration was considered a better surrogate for mixing than temperature, given that isothermal conditions do not always result in mixing (Paerl and others, 1975) and because temperature instruments used before 1975 typically were only accurate to 0.01 °C. Using time-series nitrate concentrations at the 10-m lake depth as a tracer for mixing events indicated a positive visual correlation with seasonal lake clarity (fig. H2A). During seasonal periods of mixing, nitrate concentrations increase and correspond to seasonal highs in lake clarity (fig. H2B). The improvement in clarity resulting from mixing is more pronounced during spring and winter but appears less important in summer months (fig. H2C).

## Summer Clarity and Summer Variables

Correlations of 26 summer variables were evaluated to examine the potential influences of these variables on summer clarity (fig. H3A). Fifteen variables representing various watershed and lake processes were found to be negatively correlated ($p<0.05$) to summer clarity (fig. H3B). For watershed processes, peak streamflow, volume, and center of mass were found to be negatively correlated to summer clarity. In-lake variables, such as lake particles, *Cyclotella*, and resistance to mixing (MaxBF), were also negatively correlated. Additionally, streamflow nutrients such as nitrogen and phosphorous from Upper Truckee River and Blackwood Creek were also negatively correlated to summer clarity. Analysis of summer data indicates that summer clarity strongly correlates to watershed and in-lake processes (fig. H3B).
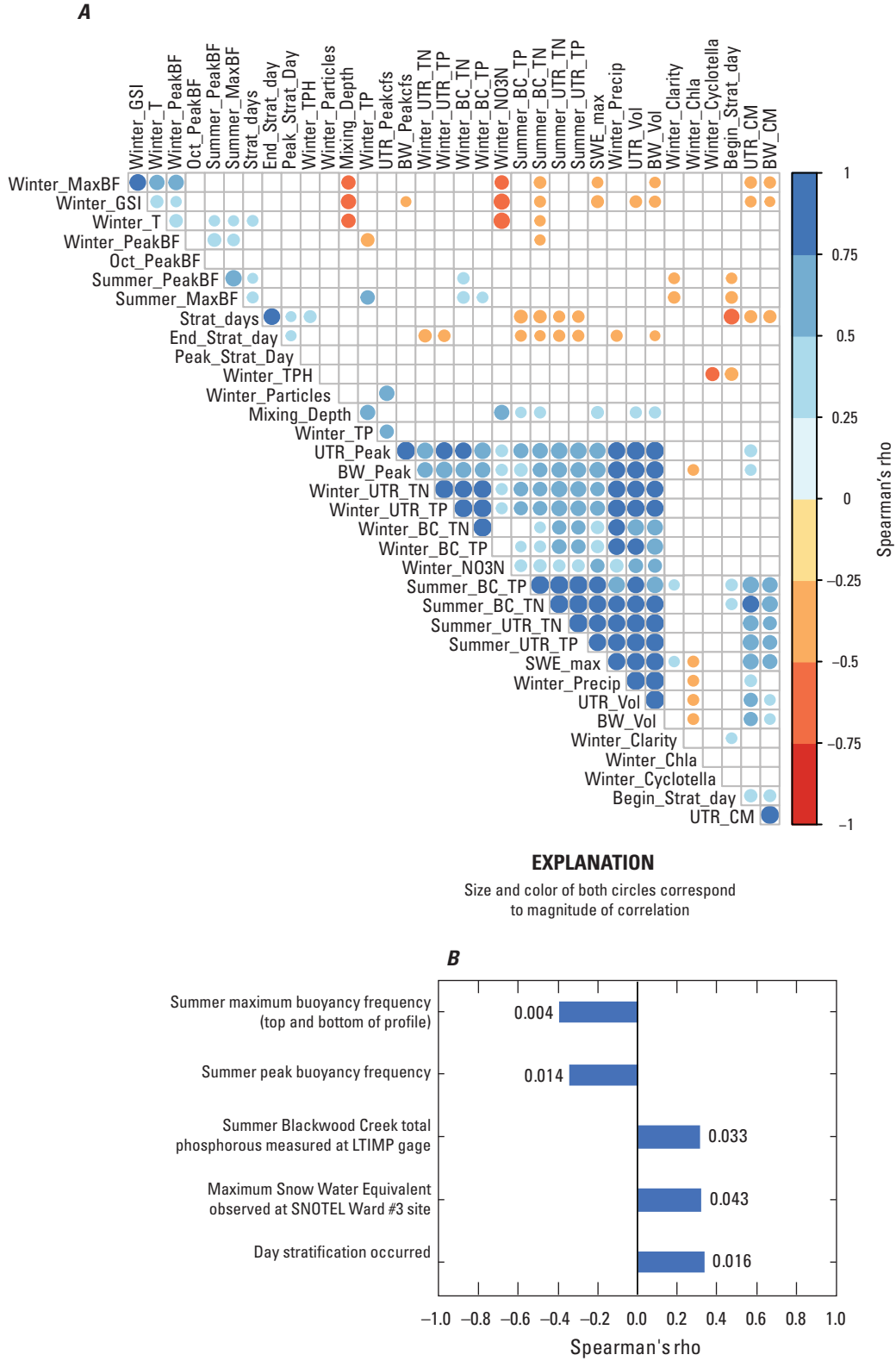
**Figure H1.** A, Spearman's rank-order correlation coefficient (Spearman's rho) for 34 variables (Watanabe and Schladow, 2021) potentially related to summer and winter processes in Lake Tahoe, water years 1967–2019; and B, Spearman's rho and p-values for summer variables that were significantly correlated ($p<0.05$) to winter clarity. Variables are defined in table 3.1 of this report.
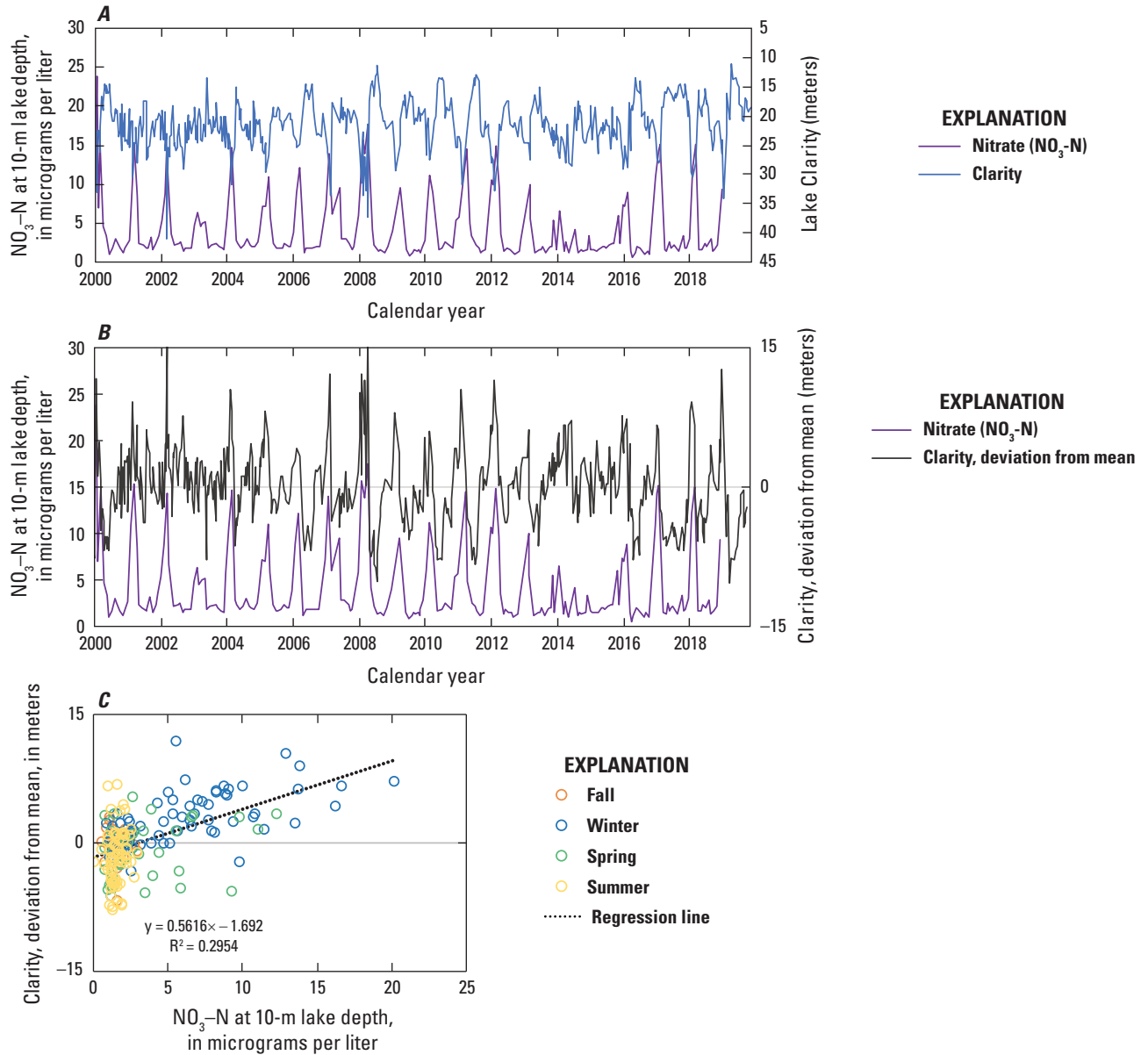
**Figure H2.**  Annual and seasonal nitrate and clarity dynamics in Lake Tahoe at 10-meter (m) lake depth, 2000–19 (Watanabe and Schladow, 2021): *A*, lake nitrate (NO$_3$–N) concentrations and clarity; *B*, lake nitrate (NO$_3$–N) concentrations and clarity deviation from mean; and *C*, linear regression equation, trend line, and associated coefficient of determination (R$^2$) between lake nitrate (NO$_3$-N) and clarity deviation from mean.
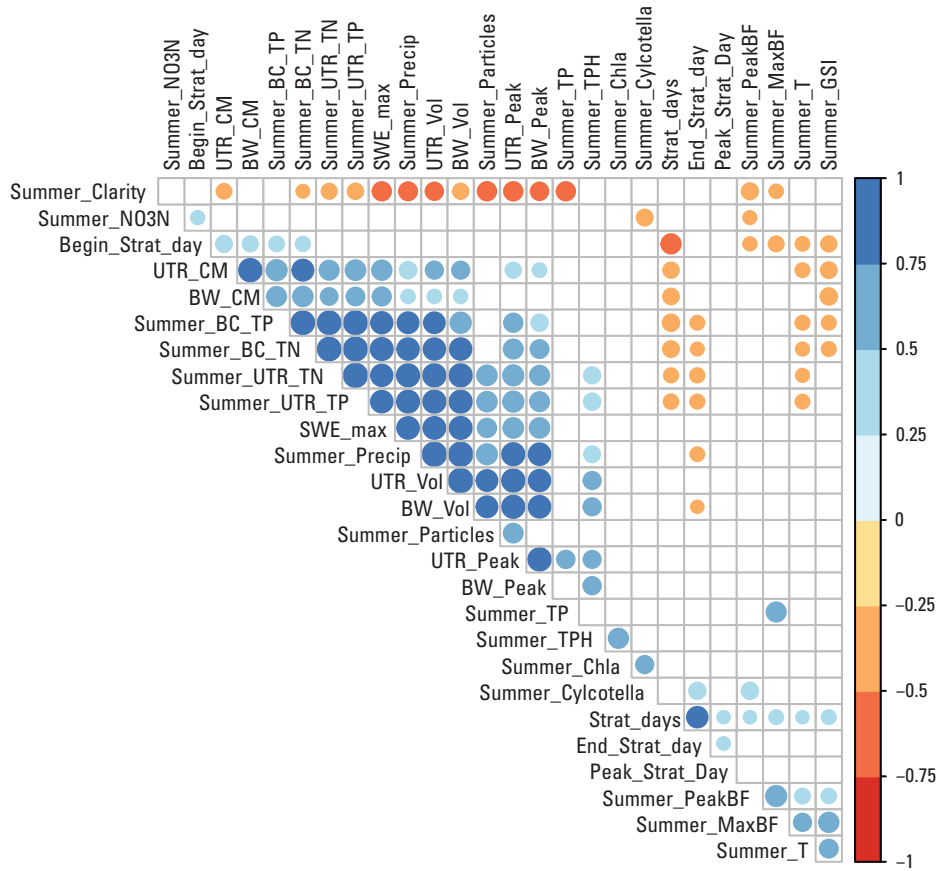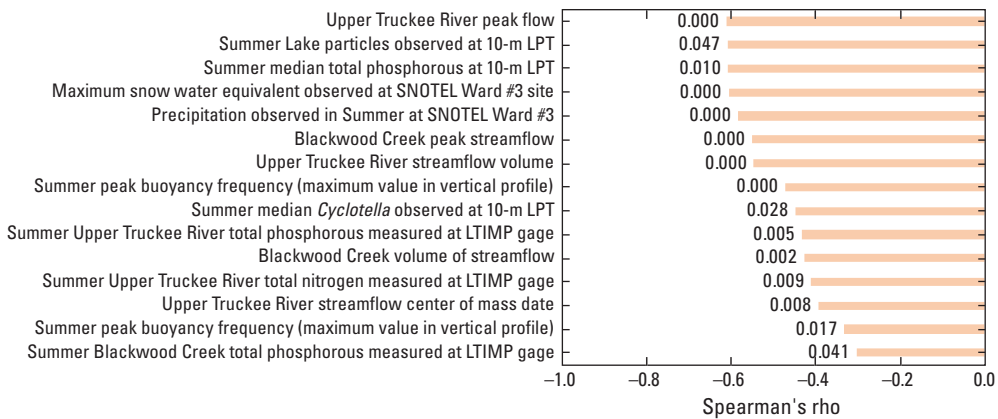
**Figure H3.**     Spearman's rank-order correlation coefficient for variables representing summer processes as related to the summer clarity of Lake Tahoe (Watanabe and Schladow, 2021): *A*, the 26 variables representing summer processes; and *B*, Spearman's rho and p-values for variables that were significantly correlated (*p*<0.05) to summer clarity. Variables are defined in table 3.1 of this report.

## Lake Clarity and Climate Change

The results of the trend analysis during 2000–19 period indicated lake clarity during fall and winter months is no longer decreasing (fig. 2.2). During this same period, the Lake Tahoe basin has experienced a series of persistent droughts followed by above average precipitation periods. Using streamflow records from the Upper Truckee River at South Lake Tahoe, Calif. (U.S. Geological Survey, 2021; table A3), lake clarity values were grouped according to streamflow timing and volume by water year and season (fig. H4). During the 2000–19 period, 50 percent of the years were drought years. Less frequent were average (30 percent) and above-average streamflow conditions (20 percent). Average water-year streamflow volumes for drought, average, and wet years were 39,000, 65,000, and 137,000 acre-ft, respectively.

Since 2000, 50 percent of the water years had less than average streamflow conditions (drought). During drought conditions, annual and season lake clarities are greater than during average or wet precipitation conditions (fig. H3). Moreover, the deepest lake clarity is during winter months of drought or wet precipitation conditions, when sediment influx to the lake is lowest. During drought years, snowpack, runoff, and associated sediment influx to the lake are less. During wet years, precipitation is stored as a high-volume snowpack or high snow–water equivalent (SWE) that usually results in less runoff during winter months and more runoff during spring and early summer months. The correlation analysis (fig. H1$A$) indicates that winter lake clarity is positively correlated to SWE ($p < 0.05$). Moreover, given that much of the last 20 years of record has been in drought, the reduction in the rate of declines in clarity identified in the trend analysis for winter and fall could be a consequence of reduced stream-sediment inflows caused by lower-than-average SWE, streamflow, and subsequent sediment influx to Lake Tahoe.



**Figure H4.**    Relations among climate conditions (drought, average, and above average conditions [wet]) based on annual (water year) and seasonal clarity values (Watanabe and Schladow, 2021) measured during 2000–19.

# I. Limitations

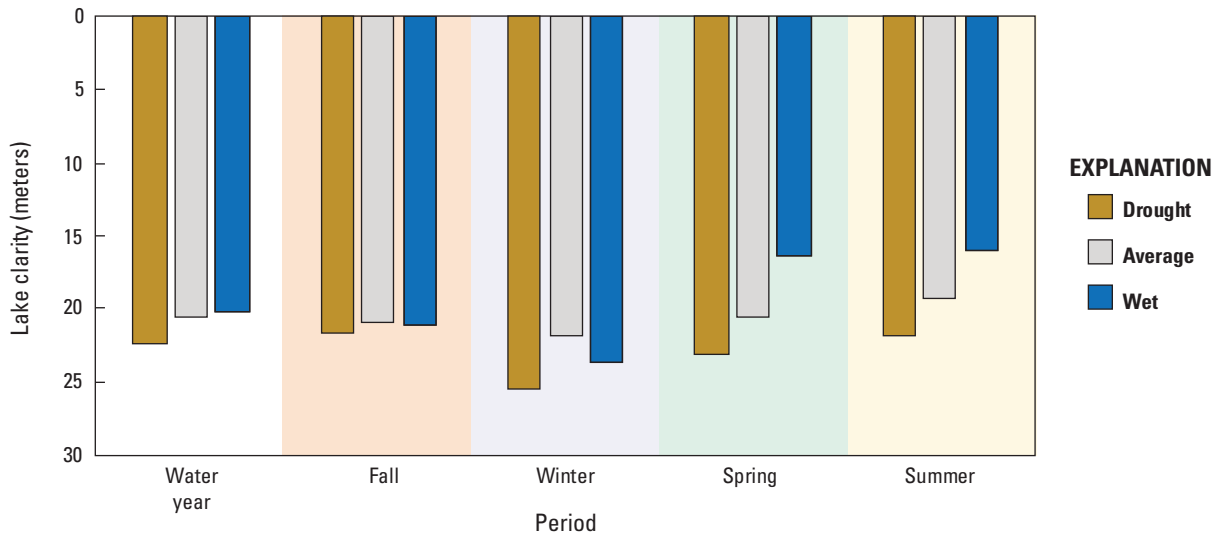Some limitations related to the available datasets and past research became apparent during this study. Limitations are listed here in no particular order for resource managers to consider when designing and prioritizing future monitoring and research efforts:

- Data on the size distribution of *Cyclotella* cells in suspension are limited, and the species present may be changing year-to-year and even season-to-season. A lack of size distribution data limits the abilities of researchers and resource managers to determine how much of the clarity problem in a particular year can be attributed to *Cyclotella* as opposed to terrigenous particles.

- Data defining the fine-particle loading to the lake from urban areas are limited, and the efficiency at which numbers of particles from 1 to 5 µm are being trapped or removed by BMPs (with a focus on particle counts in that range) is poorly understood. Current estimates of loading from monitoring sites are highly variable and only represent a fraction of the total urban watershed.

- The Pollutant Load Reduction Model was designed as a planning tool for long-term average loading estimation, but the model cannot resolve loading estimates at the higher temporal resolutions represented by typical site monitoring efforts for event, seasonal, or annual periods. Results, therefore, are not directly comparable.

- Current methods for determining proportions of fine-sediment particles may not be adequate to ensure that fine-sediment particle numbers greater than 1.0 µm are accurately represented by site monitoring and modeling results for urban and tributary loading.

- Current abilities to estimate loading of fine-sediment particles to the lake from streams are limited, and approaches have not been developed to account for loading of fine-sediment particles from streams that are not monitored.

- Data from current stream and urban monitoring programs are collected using different methods, and fine-sediment particles and nutrient-loading estimates are not directly comparable.

- Data describing atmospheric deposition of insoluble particles are currently not being collected.

- Measurements of in-lake conditions are limited to once-per-month and at a small number of discrete depths, and this complicates efforts to see the actual changes in water-column variables. Continuous sampling is now technologically feasible.

- The insertion depths of inflows from streams and stormwater culverts, and the ultimate fate of the nutrients and particle loads, are not well understood.

- Clarity data are not collected on the same day as other important variables, thereby limiting interpretations that can be made using collected data.

- Short-term, fine-sediment data from streams and urban areas are insufficient to draw conclusions on the efficacy of Environmental Improvement Program actions on load reductions.

- Climate change continues to be a factor in clarity trends given the extreme variation in seasonal runoff and sediment loads, and many of the processes that influence clarity are becoming less predictable.

# A–I. Summary

The U.S. Geological Survey, in cooperation with Nevada Division of Environmental Protection, prepared this report to describe trends in Lake Tahoe water clarity as defined by Secchi disk depth, differences between summer and winter clarity, and relations between clarity and other measured variables.

The analysis of trends in clarity indicates that during the period of record, annual mean lake clarity has declined. During the last 20 years, however, clarity reductions each year have improved from statistically significant negative trends to no trend. Since 2000, mean monthly clarity for 10 out of 12 months did not significantly decrease. This is an improvement from the 1980–99 period, during which in 1 month in every season, or 4 out of 12 months, clarity was significantly decreasing. July and August are the only months during the most recent period in which statistically significant decreases in clarity were identified.

Of the five hypotheses that were examined in this report, the first focused on the abundance of fine particles in the lake and their effect on water clarity. Particle abundance data for Lake Tahoe date from 2008 to present (2021) and have been collected two times per month. A laser diffraction device is used to collect the abundance and size distribution of suspended particles in the 0.5–20 micrometer (µm) range.

Based on light-scattering theory, the influence of particles depends on their size and composition. For inorganic (sediment) particle sizes in the range of 1.2–1.7 µm, scattering efficiency is maximized, and such particles should exert a greater effect on clarity than smaller and larger terrigenous particles. The species of *Cyclotella* most prevalent in Lake Tahoe were in the size range of 2–5 µm. Because of the presence of a silica frustule, however, the size of the alga that maximizes light scattering was not precisely determined. Available data on particle size for Lake Tahoe indicated that sizes of less than 1 µm represented at least two-thirds of the total number of particles in suspension, and these smaller particles were believed to have a negligible effect on lake clarity.

A large increase in particle abundance observed in 2016–17 may be partially attributable to an extreme winter snowpack following the end of a long period of drought. Similar increases in particle abundance were not observed in datasets for other wet years in the precipitation record.

Correlation analyses were completed to examine the relations between water clarity and several different measures of particle abundance: all particles, particles less than 1 µm, particles greater than 1 µm, and *Cyclotella* particles of all sizes. In all cases, a negative correlation was found, and these results were similar to results obtained by previous observers and to predictions based on light-scattering theory. The strongest correlation with declining lake clarity was for particles greater than 1 µm, and this finding is consistent with light-scattering theory, which indicated that terrigenous particles in the 1–2 µm range have the greatest negative effect on clarity. The analysis for *Cyclotella* particles showed a similar but less defined relation. Particle abundance and *Cyclotella* abundance were time-dependent (algal blooms tend to be highly episodic at Lake Tahoe), and this time dependence complicated efforts to assign a relative importance for each process on lake clarity; however, correlations presented in this report indicated that both processes likely influence lake clarity.

A second hypothesis focused on sediment loading to the lake, but this effort was limited by available data. Trend analysis of fine sediment loads from urban areas did not identify a statistically significant trend, but the observed lack of a significant trend could result from the short length of the monitoring dataset to date (2014-2019). Data of loading from streams are limited by temporal resolution, with fine particles measured only one or two times per month beginning in 2008. Data were sufficient for inspection of trends in particle abundance but were insufficient for quantification of loading because streamflow can vary greatly through time scales that are finer than the frequency of measurements of particle abundance.

Statistically significant trends in particle abundance were not identified in Lake Tahoe or in streams during the 2008–19 period. High correlations between particle abundances in the streams and in Lake Tahoe were observed, and a large increase in particle abundance was observed. This period marked the end of a major drought and the beginning of a very wet year (2016–17).

Hypotheses 3 and 4 considered the changes in hydrodynamics and thermodynamics of Lake Tahoe and associated effects on water clarity. The resulting analyses included trend analysis of time series describing buoyancy frequency, the date of the onset of stratification, and the duration of stratification. Statistically significant trends indicated that stratification is starting earlier and lasting longer than in the past, and the resistance to mixing is increasing. During most years, observed peak clarity is concomitant with maximum mixing. The trend of decreasing summer clarity was concluded to result from earlier, prolonged, and more intense stratification.

Periodicity of long-term time series of in-lake variables was also examined, and we identified 0.5- and 1-year periodicities corresponded to annual and seasonal changes in meteorological and hydrological conditions. Longer periodicities, such as 3, 7, and 10 years, were also present in long-term records. Some potential explanations for these longer periods of more than 1 year included climatological phenomena, such as the El Niño–Southern Oscillation (ENSO), and the hydrological consequences, interactions between different trophic levels and nutrients, and ecological effects of invasive species introductions.

Hypothesis 5 focused on the effects of ecological changes and events on clarity. Observed changes in *Mysis* abundance and clarity in Emerald Bay indicated a strong correlation between these variables.

Long-term records from Lake Tahoe indicated the disappearance of larger diatoms and their replacement by much smaller *Cyclotella* spp., closer to the particle size that maximizes light scattering in water. *Cyclotella* are unlikely to be grazed by Lake Tahoe zooplankton and benefited from reduced competition for nutrients and a more density-stable water column. The introduction of *Mysis* resulted in drastic reduction of the *Daphnia and Bosmina* populations, both of which feed on particulates in the size range of *Cyclotella* and fine terrigenous particles.

Observed ecological changes were also linked to physical changes in Lake Tahoe that influence the timing and strength of stratification, which control mixing events. *Cyclotella* blooms were typically observed in spring, summer, and fall, and stratification data indicate that the timing of these seasons is changing. The longer stratification and greater resistance to mixing indicated by the long-term dataset have physical and ecological implications.

Although not envisioned at the onset of this study, an additional analysis was performed to look at the correlation between clarity and a large set of monitored, modeled, or derived parameters and to further examine their winter and summer values. This dataset included water-chemistry parameters and atmospheric, meteorological, and hydrological variables. Results indicated that summer clarity was strongly dependent on inflow-driven and stratification-based parameters, whereas there was no clear parameter or group of parameters that exerted strong control on winter clarity.

# References Cited

Bendat, J.S., and Piersol, A.G., 1986, Random data—Analysis and measurement procedures (2d ed.): Hoboken, N.J., John Wiley and Sons, 566 p.

Burns, C.W., 1968, The relationship between body size of filter feeding *Cladocera* and the maximum size of particle ingested: Limnology and Oceanography, v. 13, no. 4, p. 675–678. [Available at https://doi.org/10.4319/lo.1968.13.4.0675.]

Burns, C.W., and Rigler, F.H., 1967, Comparison of filtering rates of *Daphnia rosea* in lake water and in suspensions of yeast: Limnology and Oceanography, v. 12, no. 3, p. 492–502. [Available at https://doi.org/10.4319/lo.1967.12.3.0492.]

California Regional Water Quality Control Board and Nevada Division of Environmental Protection, 2010, Final Lake Tahoe total maximum daily load report: California Lahontan Regional Water Quality Control Board and Nevada Division of Environmental Protection. [Available at https://www.waterboards.ca.gov/lahontan/water_issues/programs/tmdl/lake_tahoe/docs/tmdl_rpt_nov2010.pdf.]

Cayan, D.R., Maurer, E.P., Dettinger, M.D., Tyree, M., and Hayhoe, K., 2008, Climate change scenarios for the California region: Climatic Change, v. 87, no. S1, p. 21–42. [Available at https://doi.org/10.1007/s10584-007-9377-6.]

Cayan, D.R., Tyree, M., Dettinger, M., Hidalgo, H., Das, T., Maurer, E., Bromirski, P., Graham, N., and Flick, R.E., 2009, Climate change scenarios and sea level rise estimates for the California 2008 climate change scenarios assessment. Draft paper: California Climate Change Center, March 2009, CEC-500-2009-014-D, 48 p. [Available at https://escholarship.org/uc/item/22r0r5dw#main.]

Coats, R., 2010, Climate change in the Tahoe Basin—Regional trends, impacts and drivers: Climatic Change, v. 102, no. 3–4, p. 435–466. [Available at https://doi.org/10.1007/s10584-010-9828-3.]

Coats, R., Costa-Cabral, M., Riverson, J., Reuter, J., Sahoo, G., Schladow, G., and Wolfe, B., 2013a, Projected 21st century trends in hydroclimatology of the Tahoe basin: Climatic Change, v. 116, no. 1, p. 51–69. [Available at https://doi.org/10.1007/s10584-012-0425-5.]

Coats, R., Sahoo, G., Riverson, J., Costa-Cabral, M., Dettinger, M., Wolfe, B., Reuter, J., Schladow, G., and Goldman, C.R., 2013b, Historic and likely future impacts of climate change on Lake Tahoe, California–Nevada, USA, *in* Goldman, C., Kumagai, M., and Robarts, R., eds., Climatic change and global warming of inland waters—Impacts and mitigation for ecosystems and societies: Hoboken, N.J., John Wiley and Sons, p. 231–254.

Coker, J.E., 2000, Optical water quality of Lake Tahoe: Davis, California, University of California, Davis, M.S. thesis, 310 p.

Cooper, S.D., and Goldman, C.R., 1980, Opossum Shrimp (*Mysis relicta*) predation on zooplankton: Canadian Journal of Fisheries and Aquatic Sciences, v. 37, no. 6, p. 909–919. [Available at https://doi.org/10.1139/f80-120.]

Davies-Colley, R.J., and Smith, D.G., 2001, Turbidity, suspended sediment, and water clarity—A review: Journal of the American Water Resources Association, v. 37, no. 5, p. 1085–1101. [Available at https://doi.org/10.1111/j.1752-1688.2001.tb03624.x.]

Dettinger M.D., and Cayan, D.R. 1995, Large-scale atmospheric forcing of recent trends toward early snowmelt runoff in California: Journal of Climate, v. 8, no. 3, p. 606–623. [Available at https://doi.org/10.1175/1520-0442(1995)008<0606:LSAFOR>2.0.CO;2.]

Domagalski, J.L., Morway, E., Alvarez, N.L., Hutchins, J., Rosen, M.R., and Coats, R., 2021, Trends in nitrogen, phosphorus, and sediment concentrations and loads in streams draining to Lake Tahoe, California, Nevada, USA: Science of The Total Environment, v. 752, 141815. [Available at https://doi.org/10.1016/j.scitotenv.2020.141815.]

Goldman, C.R., 1981, Lake Tahoe—Two decades of change in a nitrogen deficient oligotrophic lake: SIL Proceedings, 1922–2010, v. 21, no. 1, p. 45–70. [Available at https://doi.org/10.1080/03680770.1980.11896960.]

Goldman, C.R., 1988, Primary productivity, nutrients, and transparency during the early onset of eutrophication in ultra-oligotrophic Lake Tahoe, California–Nevada: Limnology and Oceanography, v. 33, no. 6, p. 1321–1333. [Available at https://doi.org/10.4319/lo.1988.33.6.1321.]

Goldman, C.R., Morgan, M.D., Threlkeld, S.T., and Angeli, N., 1979, A population dynamics analysis of the cladoceran disappearance from Lake Tahoe, California–Nevada: Limnology and Oceanography, v. 24, no. 2, p. 289–297. [Available at https://doi.org/10.4319/lo.1979.24.2.0289.]

Gophen, M., and Geller, W., 1984, Filter mesh size and food particle uptake by *Daphnia*: Oecologia, v. 64, no. 3, p. 408–412. [Available at https://doi.org/10.1007/BF00379140.]

Grossnickle, N.E., 1982, Feeding habits of *Mysis relicta*—An overview: Hydrobiologia, v. 93, p. 101–107. [Available at https://doi.org/10.1007/BF00008103.]

Hansen, J., Sato, M., Ruedy, R., Lo, K., Lea, D.W., and Medina-Elizade, M., 2006, Global temperature change: Proceedings of the National Academy of Sciences of the United States of America, v. 103, no. 39, p. 14288–14293. [Available at https://doi.org/10.1073/pnas.0606291103.]

Helsel, D.R., Hirsch, R.M., Ryberg, K.R., Archfield, S.A., and Gilroy, E.J., 2020, Statistical methods in water resources: U.S. Geological Survey Techniques and Methods, book 4, chap. A3, 458 p. [Available at https://doi.org/10.3133/tm4A3. Supersedes U.S. Geological Survey Techniques of Water-Resources Investigations, book 4, chap. A3, version 1.1.]

Heyvaert, A., Reuter, J., and Thomas, J., 2011, Quality Assurance Project Plan (QAPP)—Tahoe regional stormwater monitoring program: Final report submitted to the U.S. Department of Agriculture Forest Service, 129 p. [Available at https://tahoercd.org/wp-content/uploads/2013/03/RSWMP-QAPP-110510.pdf.]

Hutchinson, G.E., 1957, A treatise on limnology, volume I—Geography, physics, chemistry: Hoboken, N.J., John Wiley and Sons, Inc., p. 108–114.

Jassby, A.D., Goldman, C.R., Reuter, J.E., and Richards, R.C., 1999, Origins and scale dependence of temporal variability in the transparency of Lake Tahoe, California–Nevada: Limnology and Oceanography, v. 44, no. 2, p. 282–294. [Available at https://doi.org/10.4319/lo.1999.44.2.0282.]

Jassby, A.D., Reuter, J.E., Axler, R.P., Goldman, C.R., and Hackley, S.H., 1994, Atmospheric deposition of nitrogen and phosphorus in the annual nutrient load of Lake Tahoe (California–Nevada): Water Resources Research, v. 30, no. 7, p. 2207–2216. [Available at https://doi.org/10.1029/94WR00754.]

Jassby, A.D., Reuter, J.E., and Goldman, C.R., 2003, Determining long-term water quality change in the presence of climatic variability—Lake Tahoe (USA): Canadian Journal of Fisheries and Aquatic Sciences, v. 60, no. 12, p. 1452–1461. [Available at https://doi.org/10.1139/f03-127.]

Johannsson, O.E., Leggett, M.F., Rudstam, L.G., Servos, M.R., Mohammadian, M.A., Gal, G., Dermott, R.M., and Hesslein, R.H., 2001, Diet of *Mysis relicta* in Lake Ontario as revealed by stable isotope and gut content analysis: Canadian Journal of Fisheries and Aquatic Sciences, v. 58, no. 10, p. 1975–1986. [Available at https://doi.org/10.1139/f01-118.]

Kling, H., and Håkansson, H., 1988, A light and electron microscope study of *Cyclotella* species (Bacillariophyceae) from Central and Northern Canadian lakes: Diatom Research, v. 3, no. 1, p. 55–82. [Available at https://doi.org/10.1080/0269249X.1988.9705017.]

Larkin, P.A., 1948, *Pontoporeia* and *Mysis* in Athabaska, Great Bear, and Great Slave Lakes: Bulletin—Fisheries Research Board of Canada, v. 78, p. 1–33.

LeConte, J., 1883, Physical studies of Lake Tahoe—I: Overland Monthly and Out West Magazine, v. 2, no. 11, accessed March 01, 2021, at https://tahoe.ucdavis.edu/sites/g/files/dgvnsk4286/files/inline-files/LeConte_PhysicalStudiesOfLakeTahoe_I_1883.pdf.

Molugaram, K., and Rao, G.S., 2017, Statistical techniques for engineers (2d ed.): Amsterdam, Elsevier, 554 p.

Morales, E., Rosen, B., and Spaulding, S., 2013, *Fragilaria crotonensis, in* Diatoms of North America: accessed December 28, 2019, at https://diatoms.org/species/fragilaria_crotonensis.

Nevada Division of Environmental Protection and the California Regional Water Quality Control Board, 2020, Lake Tahoe TMDL Program 2019 Performance Report, 2 p. [Available at https://clarity.laketahoeinfo.org/FileResource/DisplayResourceAsEmbeddedPDF/c5b5f31f-655b-4423-96d5-29d6ecec017f.]

Paerl, H.W., Richards, R.C., Leonard, R.L., and Goldman, C., 1975, Seasonal nitrate cycling as evidence for complete vertical mixing in Lake Tahoe, California–Nevada: Limnology and Oceanography, v. 20, no. 1, p. 1–8. [Available at https://doi.org/10.4319/lo.1975.20.1.0001.]

Pollutant Load Reduction Model Development Team, 2009, Pollutant Load Reduction Model (PRLM) User's Manual: accessed December 2009 at https://www.casqa.org/sites/default/files/effectiveness_assessment/sp-32_14_plrm_users_manual_december_2009.pdf.

Press, W.H., Teukolsky, S.A., Vetterling, W.T., and Flannery, B.P., 1992, Numerical recipes in C (2d ed.): Cambridge, United Kingdom, Cambridge University Press,194 p.

Rabidoux, A.A., 2005, Spatial and temporal distribution of fine particles and elemental concentrations in suspended sediments in Lake Tahoe streams, California–Nevada: Davis, University of California, M.S. thesis, 164 p.

Richards, R.C., Goldman, C.R., Frantz, T.C., and Wickwire, R., 1975, Where have all the *Daphnia* gone? The decline of a major cladoceran in Lake Tahoe, California–Nevada: SIL Proceedings, 1922–2010, v. 19, p. 835–842.

Riverson, J., Coats, R., Costa-Cabral, M., Dettinger, M., Reuter, J., Sahoo, G., and Schladow, G., 2013, Modeling the transport of nutrients and sediment loads into Lake Tahoe under projected climatic changes: Climatic Change, v. 116, p. 35–50. [Available at https://doi.org/10.1007/s10584-012-0629-8.]

Roberts, D.C., Forrest, A.L., Sahoo, G.B., Hook, S.J., and Schladow, S.G., 2018, Snowmelt timing as a determinant of lake inflow mixing: Water Resources Research, v. 54, no. 2, p. 1237–1251. [Available at https://doi.org/10.1002/2017WR021977.]

Rowe, T.G., 2000, Lake Tahoe interagency monitoring program—Tributary sampling design, sites, and periods of record: U.S. Geological Survey Fact Sheet 138–00, 4 p. [Available at https://doi.org/10.3133/fs13800.]

Sahoo, G.B., Forrest, A.L., Schladow, S.G., Reuter, J.E., Coats, R., and Dettinger, M., 2015, Climate change impacts on lake thermal dynamics and ecosystem vulnerabilities: Limnology and Oceanography, v. 61, no. 2, p. 496–507. [Available at https://doi.org/10.1002/lno.10228.]

Sahoo, G.B., Nover, D.M., Reuter, J.E., Heyvaert, A.C., Riverson, J., and Schladow, S.G., 2013a, Nutrient and particle load estimates to Lake Tahoe (CA–NV, USA) for total maximum daily load establishment: The Science of the Total Environment, v. 444, p. 579–590. [Available at https://doi.org/10.1016/j.scitotenv.2012.12.019.]

Sahoo, G.B., Schladow, S.G., and Reuter, J.E., 2010, Effect of sediment and nutrient loading on Lake Tahoe optical conditions and restoration opportunities using a newly developed lake clarity model: Water Resources Research, v. 46, no. 10, 20 p. [Available at https://doi.org/10.1029/2009WR008447.]

Sahoo, G.B., Schladow, S.G., Reuter, J.E., Coats, R., Dettinger, M., Riverson, J., Wolfe, B., and Costa-Cabral, M., 2013b, The response of Lake Tahoe to climate change: Climatic Change, v. 116, no. 1, p. 71–95. [Available at https://doi.org/10.1007/s10584-012-0600-8.]

Schladow, S.G., 2019, Tahoe—State of the Lake Report—2019: Report of the U.C Davis Tahoe Environmental Research Center, available at https://tahoe.ucdavis.edu/sites/g/files/dgvnsk4286/files/inline-files/SOTL2019_reduced.pdf.

Schladow, S.G., 2020, Tahoe—State of the Lake Report—2020: Report of the UC Davis Tahoe Environmental Research Center, accessed December 7, 2020, at https://tahoe.ucdavis.edu/state-lake-archive.

Schladow, G., Forrest, A., Sadro, S., Allen, B., Senft, K., Cardoso, L., Tanaka, L., Watanabe, S., Daniels, B., Trommer, S., Cheng, Y., Chandra, S., and Bess, Z., 2020, A Lake Tahoe *Mysis* Control Plan: Final Report to Nevada Division of Environmental Protection and California Tahoe Conservancy, available at https://tahoe.ucdavis.edu/sites/g/files/dgvnsk4286/files/inline-files/Mysid_FinalReport_SUBMITTED.pdf.

Schladow, S.G., Palmarsson, S.Ó., Steissberg, T.E., Hook, S.J., and Prata, F.E., 2004, An extraordinary upwelling event in a deep thermally stratified lake: Geophysical Research Letters, v. 31, no. 15, 4 p. [Available at https://doi.org/10.1029/2004GL020392.]

Sommer, U., and Sommer, F., 2006, Cladocerans versus copepods—The cause of contrasting top-down controls on freshwater and marine phytoplankton: Oecologia, v. 147, no. 2, p. 183–194. [Available at https://doi.org/10.1007/s00442-005-0320-0.]

Stalberg, G., 1933, Beitrag zur Kenntnis der Biologie von *Mysis relicta* des Vättern: Arkiv för Zoologi, v. 26A, p. 1–29.

Sunman, B., 2004, Spatial and temporal distribution of particle concentration and composition in Lake Tahoe, California–Nevada: Davis, University of California, M.S. thesis, 646 p.

Swift, T.J., Perez-Losada, J., Schladow, S.G., Reuter, J.E., Jassby, A.D., and Goldman, C.R., 2006, Water clarity modeling in Lake Tahoe—Linking suspended matter characteristics to Secchi depth: Aquatic Sciences, v. 68, no. 1, p. 1–15. [Available at https://doi.org/10.1007/s00027-005-0798-x.]

Tahoe Regional Planning Agency, 2019, Environmental Improvement Program, 2018 Accomplishments and a look ahead: Tahoe Regional Planning Agency, 19 p. [Available at https://eip.laketahoeinfo.org/FileResource/DisplayResource/d098819e-8ea6-4595-bc6e-b99cf73fcd8a.]

Tahoe Regional Planning Agency, 2021, Lake Tahoe Info Monitoring Dashboard: stormwater, accessed August 20, 2021, at https://monitoring.laketahoeinfo.org/RSWMP.

Tahoe Resource Conservation District, 2020, Annual stormwater monitoring report, water year 2019: Prepared for the Implementers' Monitoring Program component of the Regional Stormwater Monitoring Program, submitted to the Lahontan Regional Water Quality Control Board and the Nevada Division of Environmental Protection, available at https://tahoercd.org/wp-content/uploads/2021/02/Water-Year-2019.pdf.

Threlkeld, S.T., 1981, The recolonization of Lake Tahoe by Bosmina longirostris—Evaluating the importance of reduced *Mysis relicta* populations: Limnology and Oceanography, v. 26, no. 3, p. 433–444. [Available at https://doi.org/10.4319/lo.1981.26.3.0433.]

Threlkeld, S.T., Rybock, J.T., Morgan, M.D., Folt, C.L., and Goldman, C.R., 1980, The effects of an introduced invertebrate predator and food resource variation on zooplankton dynamics in an oligotrophic lake, *in* Kerfoot, W.C., ed., Evolution and ecology of zooplankton communities: Hanover, N.H., Univ. Press of New England, p. 555–556.

U.S. Geological Survey, 2021, USGS water data for the Nation: U.S. Geological Survey National Water Information System database, accessed August 19, 2021, at https://doi.org/10.5066/F7P55KJN.

Van de Hulst, H.C., 1957, Light scattering by small particles: New York, N.Y., Wiley, available at https://doi.org/10.1063/1.3060205.

Watanabe, S., and Schladow, G., 2021, Limnological data for Lake Tahoe seasonal and long-term clarity trend analysis report: Dryad, Dataset, accessed July 27, 2021, at https://doi.org/10.25338/B83P8B.

Watanabe, S., Vincent, W.F., Reuter, J., Hook, S.J., and Schladow, S.G., 2016. A quantitative blueness index for oligotrophic waters—Application to Lake Tahoe, California–Nevada, Limnology and Oceanography Methods, v. 14, no. 2, p. 100–109. [Available at https://doi.org/10.1002/lom3.10074.]

Winder, M., and Hunter, D.A., 2008, Temporal organization of phytoplankton communities linked to physical forcing: Oecologia, v. 156, no. 1, p. 179–192. [Available at https://doi.org/10.1007/s00442-008-0964-7.]

Winder, M., Reuter, J.E., and Schladow, S.G., 2008, Lake warming favours small-sized planktonic diatom species: Proceedings. Biological Sciences, v. 276, no. 1656, p. 427–435. [Available at https://doi.org/10.1098/rspb.2008.1200.]

Wood, S.N., 2006, Generalized additive models—An Introduction with R: CRC Press, Boca Raton, FL, v. 66, 410 p. [Available at https://doi.org/10.1201/9781420010404.]

Wu, L., and Culver, D.A., 1991, Zooplankton grazing and phytoplankton abundance—An assessment before and after invasion of *Dreissena Polymorpha*: Journal of Great Lakes Research, v. 17, no. 4, p. 425–436. [Available at https://doi.org/10.1016/S0380-1330(91)71378-6.]

# Appendix 1.    Supplemental Information About Hypothesis 2 for Lake Tahoe Water-Clarity Trends

## Seasonal Variations in Inorganic Particles, Organic Particles, and Lake Clarity

Seasonal variations in lake particles (inorganic) and *Cyclotella* (organic particles) and lake clarity are shown by 5th, 50th (median), and 95th percentiles (fig. 1.1). Seasonally, median lake particles are relatively constant at 1,000 counts per milliliter (counts/mL) during fall (October–November) and winter (December–March) periods. The number of median particles increases during spring (April–May) and summer months (June–September) to about 5,000 particles. Median *Cyclotella* counts decreased from 100 cells/mL during the fall to a seasonal low of 20 cells/mL during the winter months. This decrease is then followed by an increase through late summer to 300 cells/mL, close to measured fall *Cyclotella* counts. Clarity is relatively constant during the fall, then increases during the winter months (note y-axis is reversed). Median clarity values decrease during the spring and remain relatively constant during summer months at around 20 meters deep.
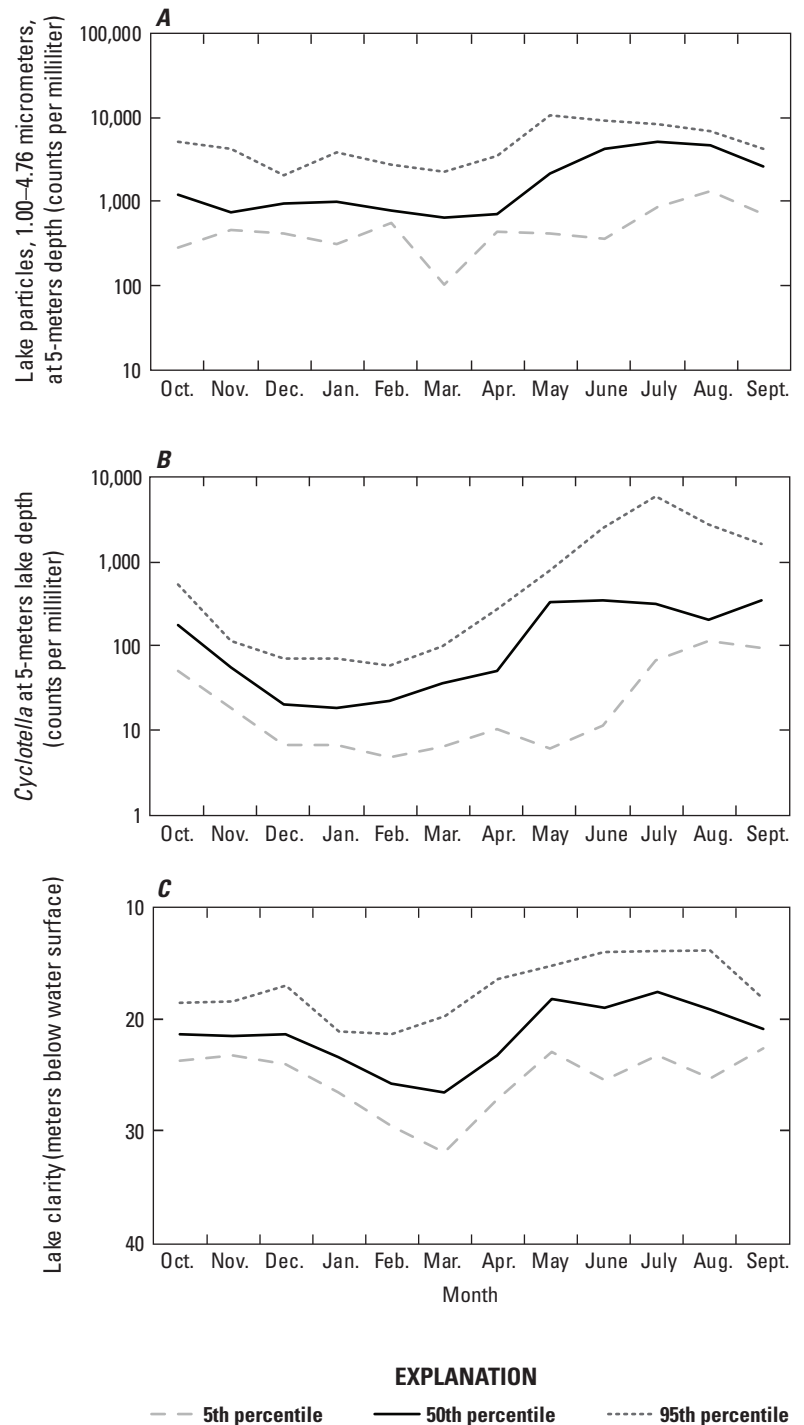


**Figure 1.1.**    Seasonal variation for Lake Tahoe in *A*, lake particles (2008–19); *B*, *Cyclotella* (1981–2019); and *C*, lake clarity (2000–19; Watanabe and Schladow, 2021).

# Urban Loading Data for Lake Tahoe

The Lake Clarity Crediting Program (LCCP) for Lake Tahoe was established as a pollutant load reduction accounting system in support of the Lake Tahoe Total Maximum Daily Load (TMDL; Lahontan Regional Water Quality Control Board and Nevada Division of Environmental Protection, 2021). Urban implementers from seven Lake Tahoe basin jurisdictions implement pollutant control practices to reduce loading from urban areas and then document these accomplishments through the LCCP. These jurisdictions include Douglas, El Dorado, Placer, and Washoe counties; the City of South Lake Tahoe; the California Department of Transportation (Caltrans); and the Nevada Department of Transportation (NDOT). The Pollutant Load Reduction Model (PLRM) was developed to provide a consistent method for estimating the average annual amount of stormwater pollution contributed to Lake Tahoe from urban catchments (NHC, Geosyntec Consultants, and 2NDNATURE, 2009). The PLRM is used by each jurisdiction to establish their baseline loads (table 1.1) and to estimate cumulative load reductions (fig. 1.2). Regulators review these estimated load reductions annually to award lake clarity credits (fig. 1.3), which correspond to load reduction targets in California stormwater permits and Nevada interlocal agreements, based on guidelines laid out in the LCCP Handbook (Lahontan Regional Water Quality Control Board and Nevada Division of Environmental Protection, 2021).

Average loading rates from urban sites (shown in table D5) can be used to evaluate basin-wide loading against baseline levels, although this approach may over-extrapolate the data, given the small total drainage area represented by the Regional Stormwater Monitoring Program (RSWMP) monitoring sites (Tahoe Regional Planning Agency, 2021). Extrapolating to a total jurisdictional catchment area, estimated at around 40,000 acres (per jurisdictional calculations), the average annual urban loading for fine-sediment particles (FSP) represents about 54 percent of the baseline from 2004. Accounting for an additional cumulative 18 percent modeled reduction (from PLRM, table 1.2) would yield 73 percent of the baseline annual loading amount, which is fairly close, considering the limited data and extrapolation. Similarly, using measured loadings for total phosphorus (TP) and total nitrogen (TN), then adding in the model-estimated reductions, yields 38 and 335 percent, respectively, of baseline annual loadings (table D5). Although the RSWMP drainages used in this analysis represent only 518 acres, less than 2 percent of urban jurisdictional catchments, they are representative of land uses and runoff characteristics for the Lake Tahoe basin (table D3), and results are at least within a few hundred percent of values expected from the basin-wide average baseline annual loading rates. Interestingly, the TN loading estimated from measured values is substantially more than baseline, whereas FSP and TP are both less than baseline, indicating that TN loading may be much higher than PLRM projections and has been increasing from baseline levels (fig. D5). The Regional Stormwater Monitoring Program was originally designed with the intention of completing a statistical assessment of basin-wide urban loading rates to the lake each year (Heyvaert and others, 2011), but longer-term data, additional sites, and a stratified randomized design are needed to complete the intended statistical assessments.

**Table 1.1.** Baseline average annual pollutant loads into Lake Tahoe representing conditions as of water year 2004 (October 1, 2003–September 30, 2004).

[Note: 1 pound of fine-sediment particles (FSP<16 micrometers) is approximately equivalent to 5E+13 particles (Nevada Division of Environmental Protection and the Lahontan Regional Water Quality Control Board, 2020). There are four county jurisdictions: Douglas, El Dorado, Placer, and Washoe. **Abbreviations**: FSP, fine-sediment particles; #particles/yr, number of particles per year; lbs/yr, pounds per year; TP, total phosphorus; TN, total nitrogen; CalTrans, California Department of Transportation; CSLT, City of South Lake Tahoe; NDOT, Nevada Department of Transportation; —, no data]

| Jurisdiction | FSP (#particles/yr) | FSP (lbs/yr) | TP (lbs/yr) | TN (lbs/yr) |
|---|---|---|---|---|
| CalTrans | 3.10E+19 | 6.17 E+05 | 1,720 | 5,370 |
| CSLT | 2.44E+19 | 4.88 E+05 | 2,060 | 8,180 |
| Douglas County | 4.80E+18 | 9.60 E+03 | 374 | 1,530 |
| El Dorado County | 1.63E+19 | 3.26 E+05 | 1,170 | 4,170 |
| NDOT | 1.03E+19 | 2.05 E+05 | 564 | 1,700 |
| Placer County | 2.64E+19 | 5.28 E+05 | 2,280 | 8,860 |
| Washoe County | 1.45E+19 | 2.90 E+05 | 1,230 | 4,720 |
| Basinwide | 1.28E+20 | 2.55 E+06 | — | — |

**Table 1.2.** Cumulative average annual pollutant load reductions achieved for Lake Tahoe, 2016–19 (from Nevada Division of Environmental Protection and the Lahontan Regional Water Quality Control Board, 2020).

[Water year is defined as the 12-month period October 1, for any given year through September 30, of the following year. **Abbreviations**: FSP, fine-sediment particles; lbs/yr, pounds per year; TP, total phosphorus; TN, total nitrogen]

| Water year | FSP (lbs/yr) | TP (lbs/yr) | TN (lbs/yr) |
|---|---|---|---|
| 2016 | 278,000 | 810 | 2,300 |
| 2017 | 302,000 | 890 | 2,600 |
| 2018 | 444,000 | 1,130 | 3,800 |
| 2019 | 477,000 | 1,450 | 4,200 |

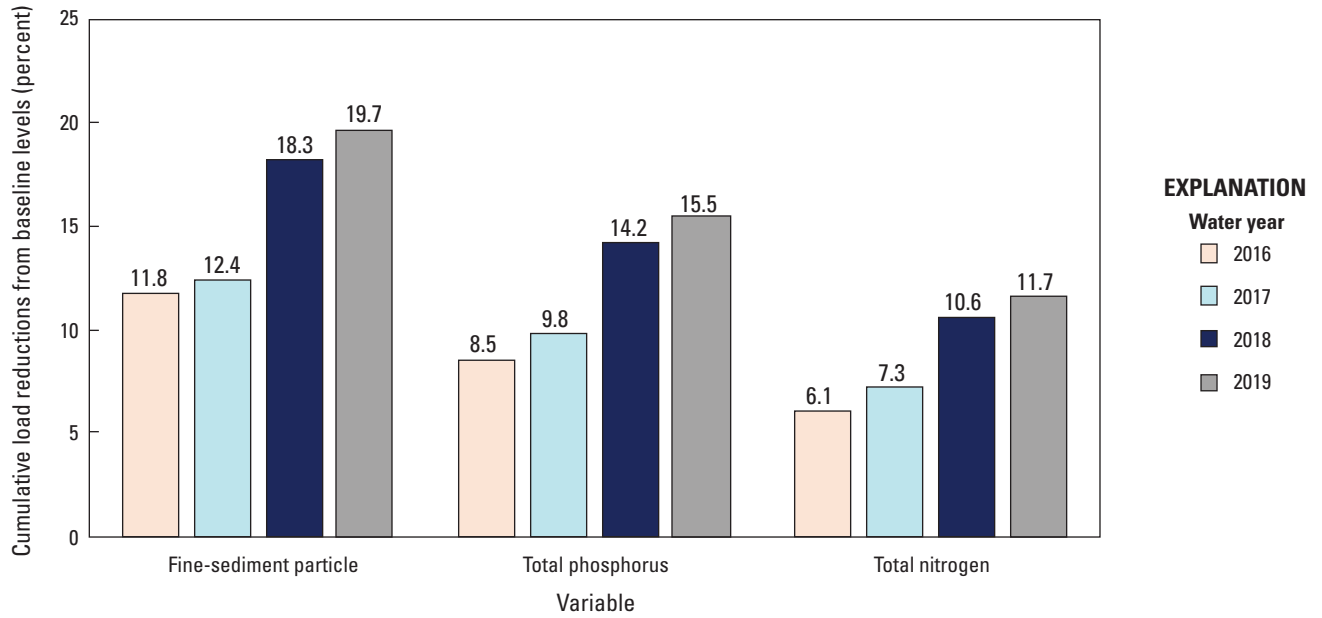**Figure 1.2.**    Cumulative load reductions into Lake Tahoe achieved against baseline levels for water years 2016–19 (adapted from Nevada Division of Environmental Protection and the Lahontan Regional Water Quality Control Board, 2020).
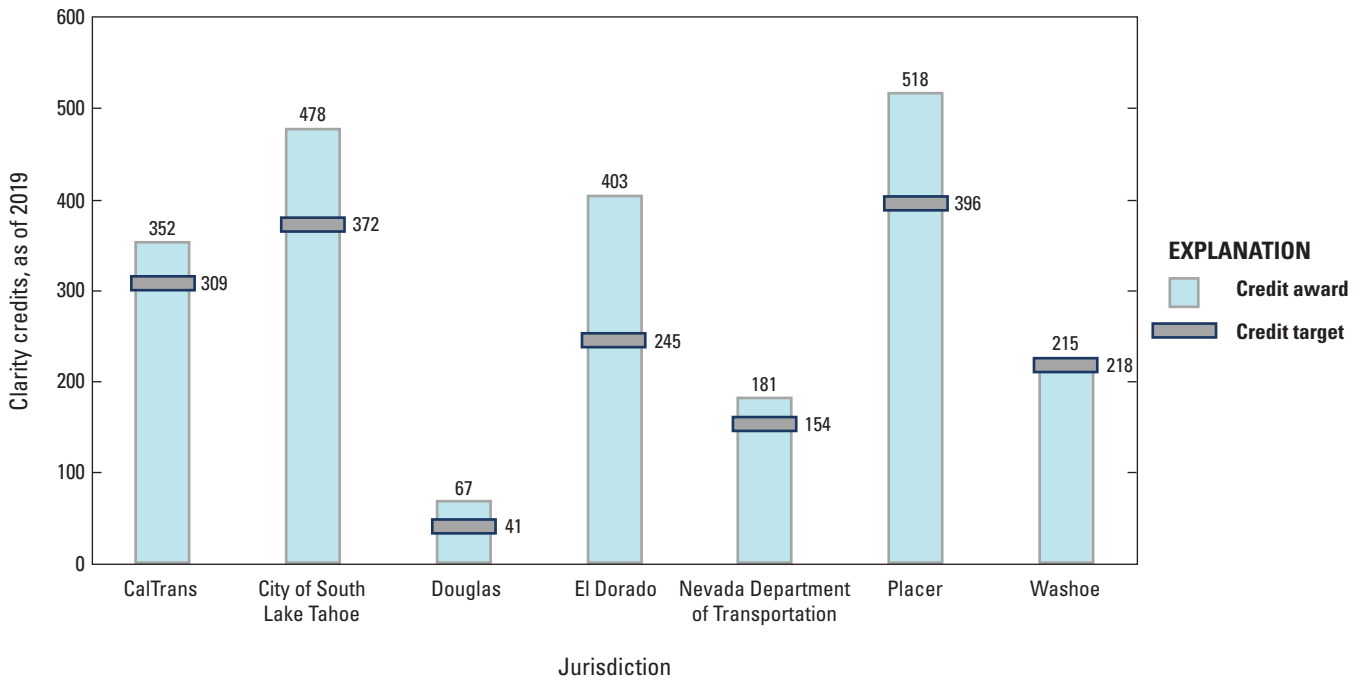


**Figure 1.3.**    Clarity credits awarded through 2019 by jurisdiction for Lake Tahoe (from Nevada Division of Environmental Protection and the Lahontan Regional Water Quality Control Board, 2020).

**Table 1.3.**    Monthly loads summed across Tahoe Resource Conservation District Regional Stormwater Monitoring Program (RSWMP) sites identified in table D3 for the RSWMP statistical analyses represented in this document.

[TSS, total suspended solids; kg, kilogram; FSP, fine-sediment particle; TN, total nitrogen; TP, total phosphorus; in., inch]

| Year-month | TSS (kg) | FSP (kg) | TN (kg) | TP (kg) | Average precipitation (in.) |
|---|---|---|---|---|---|
| 2013-10 | 11 | 6 | 0.0 | 0.0 | 0.5 |
| 2013-11 | 10 | 6 | 0.0 | 0.0 | 0.5 |
| 2013-12 | 3 | 1 | 0.0 | 0.0 | 0.5 |
| 2014-01 | 180 | 100 | 0.8 | 0.5 | 1.9 |
| 2014-02 | 780 | 460 | 4.2 | 2.7 | 6.9 |
| 2014-03 | 220 | 160 | 1.2 | 0.8 | 1.8 |
| 2014-04 | 140 | 100 | 0.7 | 0.5 | 0.6 |
| 2014-05 | 120 | 90 | 0.6 | 0.4 | 1.5 |
| 2014-06 | 20 | 10 | 0.1 | 0.0 | 0.1 |
| 2014-07 | 225 | 100 | 1.3 | 0.6 | 1.6 |
| 2014-08 | 390 | 175 | 1.7 | 1.1 | 1.2 |
| 2014-09 | 780 | 340 | 3.2 | 2.2 | 1.3 |
| 2014-10 | 26 | 20 | 0.1 | 0.1 | 0.4 |
| 2014-11 | 177 | 120 | 1.0 | 0.6 | 1.6 |
| 2014-12 | 520 | 330 | 4.3 | 1.7 | 2.7 |
| 2015-01 | 6 | 4 | 0.0 | 0.0 | 0.2 |
| 2015-02 | 1,910 | 1,120 | 17.7 | 6.8 | 4.8 |
| 2015-03 | 90 | 80 | 1.0 | 0.3 | 0.3 |
| 2015-04 | 340 | 240 | 4.8 | 1.3 | 1.7 |
| 2015-05 | 220 | 180 | 2.0 | 0.7 | 2.1 |
| 2015-06 | 100 | 50 | 2.3 | 0.4 | 0.8 |
| 2015-07 | 800 | 250 | 7.1 | 1.9 | 1.3 |
| 2015-08 | 20 | 10 | 0.4 | 0.1 | 0.2 |
| 2015-09 | 10 | 10 | 0.2 | 0.0 | 0.7 |
| 2015-10 | 610 | 520 | 4.5 | 2.3 | 1.7 |
| 2015-11 | 1,260 | 1,035 | 9.5 | 5.1 | 2.6 |
| 2015-12 | 1,570 | 1,300 | 14.3 | 6.6 | 5.5 |
| 2016-01 | 3,260 | 2,610 | 26.6 | 13.6 | 5.2 |
| 2016-02 | 280 | 230 | 2.0 | 1.1 | 0.8 |
| 2016-03 | 2,490 | 2,270 | 19.3 | 9.2 | 4.9 |
| 2016-04 | 1,350 | 1,250 | 8.9 | 4.6 | 2.4 |
| 2016-05 | 1,200 | 1,100 | 8.1 | 4.2 | 1.5 |
| 2016-06 | 210 | 40 | 2.8 | 0.8 | 0.1 |
| 2016-07 | 75 | 15 | 1.0 | 0.3 | 0.0 |
| 2016-08 | 660 | 135 | 9.0 | 2.5 | 0.2 |
| 2016-09 | 411 | 80 | 5.5 | 1.6 | 0.1 |

**Table 1.3.**    Monthly loads summed across Tahoe Resource Conservation District Regional Stormwater Monitoring Program (RSWMP) sites identified in table D3 for the RSWMP statistical analyses represented in this document.—Continued

[TSS, total suspended solids; kg, kilogram; FSP, fine-sediment particle; TN, total nitrogen; TP, total phosphorus; in., inch]

| Year-month | TSS (kg) | FSP (kg) | TN (kg) | TP (kg) | Average precipitation (in.) |
|---|---|---|---|---|---|
| 2016-10 | 2,020 | 1,230 | 23.1 | 7.9 | 6.4 |
| 2016-11 | 80 | 40 | 0.5 | 0.2 | 1.4 |
| 2016-12 | 2,500 | 1,520 | 31.6 | 10.3 | 6.3 |
| 2017-01 | 4,840 | 3,120 | 73.6 | 21.8 | 12.5 |
| 2017-02 | 10,900 | 7,260 | 174.6 | 49.7 | 12.0 |
| 2017-03 | 4,110 | 2,450 | 85.7 | 18.2 | 2.4 |
| 2017-04 | 3,810 | 2,370 | 84.0 | 17.2 | 2.6 |
| 2017-05 | 1,700 | 1,160 | 28.6 | 7.5 | 0.8 |
| 2017-06 | 1,070 | 640 | 29.4 | 5.4 | 0.2 |
| 2017-07 | 12 | 5 | 0.1 | 0.0 | 0.0 |
| 2017-08 | 490 | 250 | 10.6 | 2.1 | 0.5 |
| 2017-09 | 310 | 140 | 3.9 | 0.9 | 0.9 |
| 2017-10 | 50 | 20 | 0.9 | 0.2 | 0.4 |
| 2017-11 | 2,150 | 630 | 64.4 | 9.8 | 6.1 |
| 2017-12 | 20 | 10 | 0.5 | 0.1 | 0.3 |
| 2018-01 | 230 | 82 | 5.0 | 0.9 | 2.3 |
| 2018-02 | 160 | 50 | 4.0 | 0.7 | 0.4 |
| 2018-03 | 5,640 | 2,610 | 46.5 | 19.6 | 7.3 |
| 2018-04 | 2,060 | 920 | 18.7 | 7.1 | 1.7 |
| 2018-05 | 815 | 390 | 5.9 | 2.5 | 2.0 |
| 2018-06 | 1 | 0 | 0.0 | 0.0 | 0.0 |
| 2018-07 | 160 | 50 | 3.8 | 0.7 | 0.9 |
| 2018-08 | 0 | 0 | 0.0 | 0.0 | 0.0 |
| 2018-09 | 0 | 0 | 0.0 | 0.0 | 0.0 |
| 2018-10 | 70 | 30 | 1.4 | 0.4 | 0.8 |
| 2018-11 | 250 | 120 | 5.5 | 1.4 | 2.9 |
| 2018-12 | 140 | 60 | 3.2 | 0.9 | 1.5 |
| 2019-01 | 510 | 230 | 13.2 | 2.6 | 4.2 |
| 2019-02 | 1,820 | 770 | 53.3 | 12.6 | 7.8 |
| 2019-03 | 2,010 | 1,230 | 28.5 | 8.1 | 2.9 |
| 2019-04 | 2,690 | 1,480 | 36.9 | 9.9 | 1.1 |
| 2019-05 | 690 | 440 | 8.9 | 2.9 | 1.7 |
| 2019-06 | 690 | 330 | 6.4 | 1.3 | 0.1 |
| 2019-07 | 0 | 0 | 0.0 | 0.0 | 0.0 |
| 2019-08 | 0 | 0 | 0.0 | 0.0 | 0.0 |
| 2019-09 | 140 | 65 | 1.4 | 0.3 | 0.6 |

# References Cited

Heyvaert, A., Reuter, J., and Thomas, J., 2011, Quality Assurance Project Plan (QAPP)—Tahoe regional stormwater monitoring program: Final report submitted to the U.S. Department of Agriculture Forest Service, 129 p. [Available at https://tahoercd.org/wp-content/uploads/2013/03/RSWMP-QAPP-110510.pdf.]

Lahontan Regional Water Quality Control Board and Nevada Division of Environmental Protection, 2021, Lake clarity crediting program handbook, ver. 2.2: Lahontan Regional Water Quality Control Board and Nevada Division of Environmental Protection, 75 p. [Available at https://clarity.laketahoeinfo.org/FileResource/DisplayResourceAsEmbeddedPDF/6fa6e7fe-ad67-416b-aa5d-8113daec4992.]

Nevada Division of Environmental Protection and the Lahontan Regional Water Quality Control Board, 2020, Lake Tahoe TMDL Program 2019 Performance Report, 2 p. [Available at https://clarity.laketahoeinfo.org/FileResource/DisplayResourceAsEmbeddedPDF/c5b5f31f-655b-4423-96d5-29d6ecec017f.]

NHC, Geosyntec Consultants, and 2NDNATURE, 2009, Pollutant Load Reduction Model (PLRM) Model Development Document, 95 p., downloaded from https://clarity.laketahoeinfo.org/FileResource/DisplayResourceAsEmbeddedPDF/9b99f866-a107-4273-98ec-628dc8505de8

Tahoe Regional Planning Agency, 2021, Lake Tahoe Info Monitoring Dashboard—Stormwater: Tahoe Regional Planning Agency, accessed August 20, 2021, at https://monitoring.laketahoeinfo.org/RSWMP.

Watanabe, S., and Schladow, G., 2021, Limnological data for Lake Tahoe seasonal and long-term clarity trend analysis report: Dryad, Dataset, accessed July 27, 2021, at https://doi.org/10.25338/B83P8B.

# Appendix 2.    Supplemental Information on Hypothesis 3
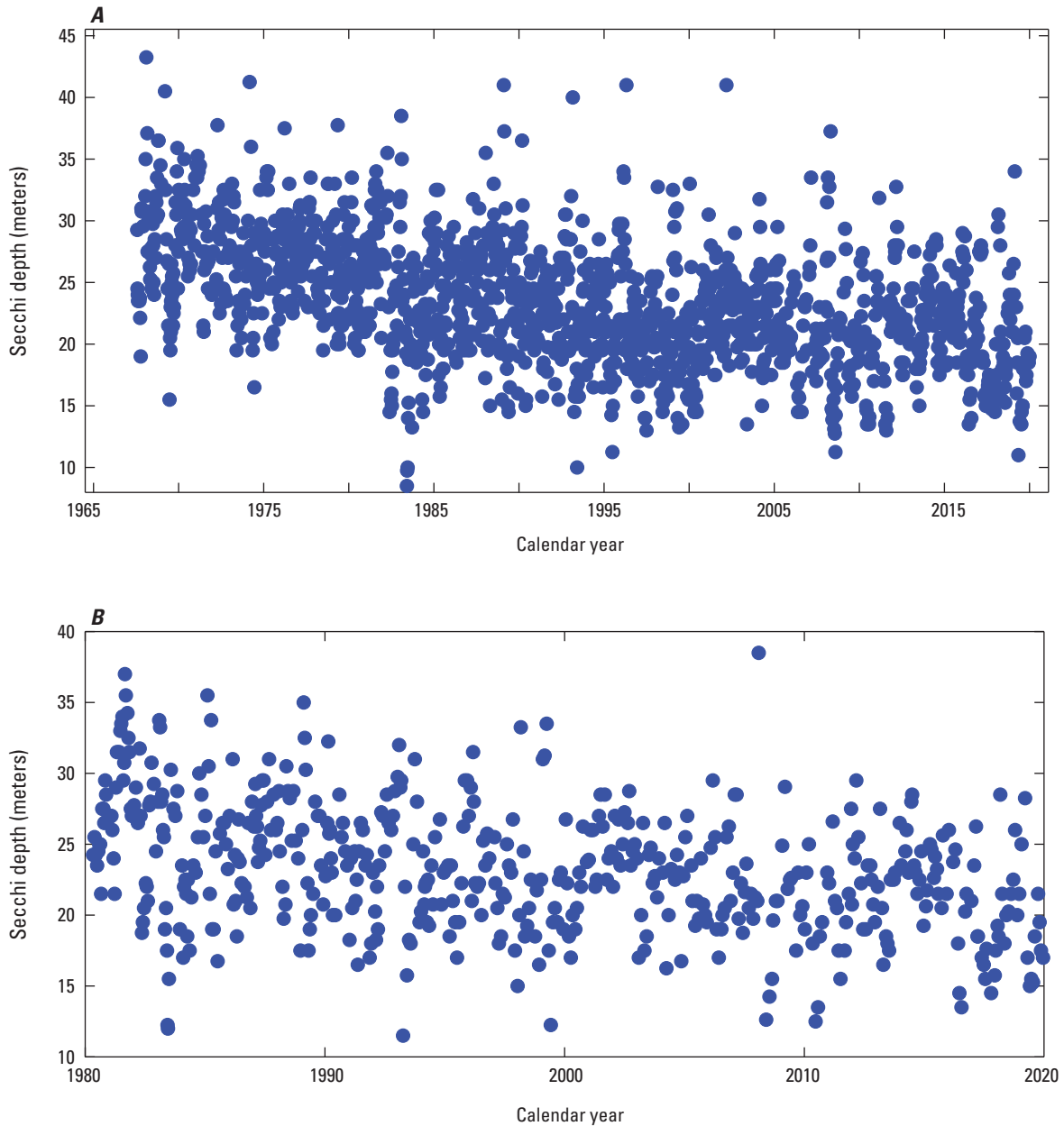
## Time-Series Data



**Figure 2.1.**    Measured Secchi depths for two sites at Lake Tahoe: *A*, the Lake Tahoe profiling station (LTP), 1967–2019; and *B*, the mid-Lake Tahoe profiling station (MLTP) 1980–2019 (Watanabe and Schladow, 2021). See table A1 of this report for period of record and frequency.
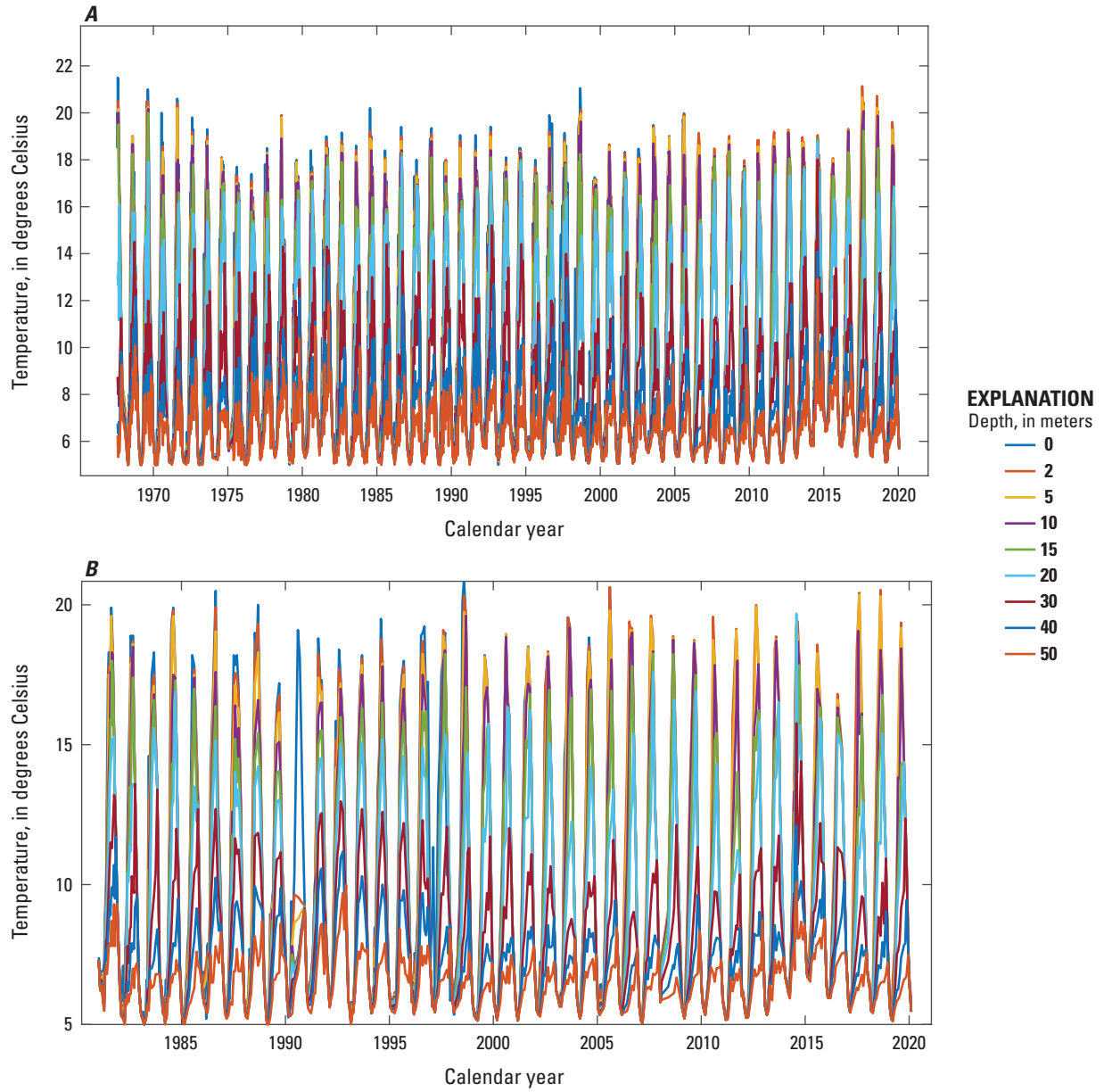
**Figure 2.2.**    Measured water temperatures at nine depths for two sites at Lake Tahoe, 1967–2019: *A*, the Lake Tahoe profiling station (LTP), 1968–2019; and *B*, the mid-Lake Tahoe profiling station (MLTP), 1981–2019 (Watanabe and Schladow, 2021). See table A1 of this report for period of record and frequency.
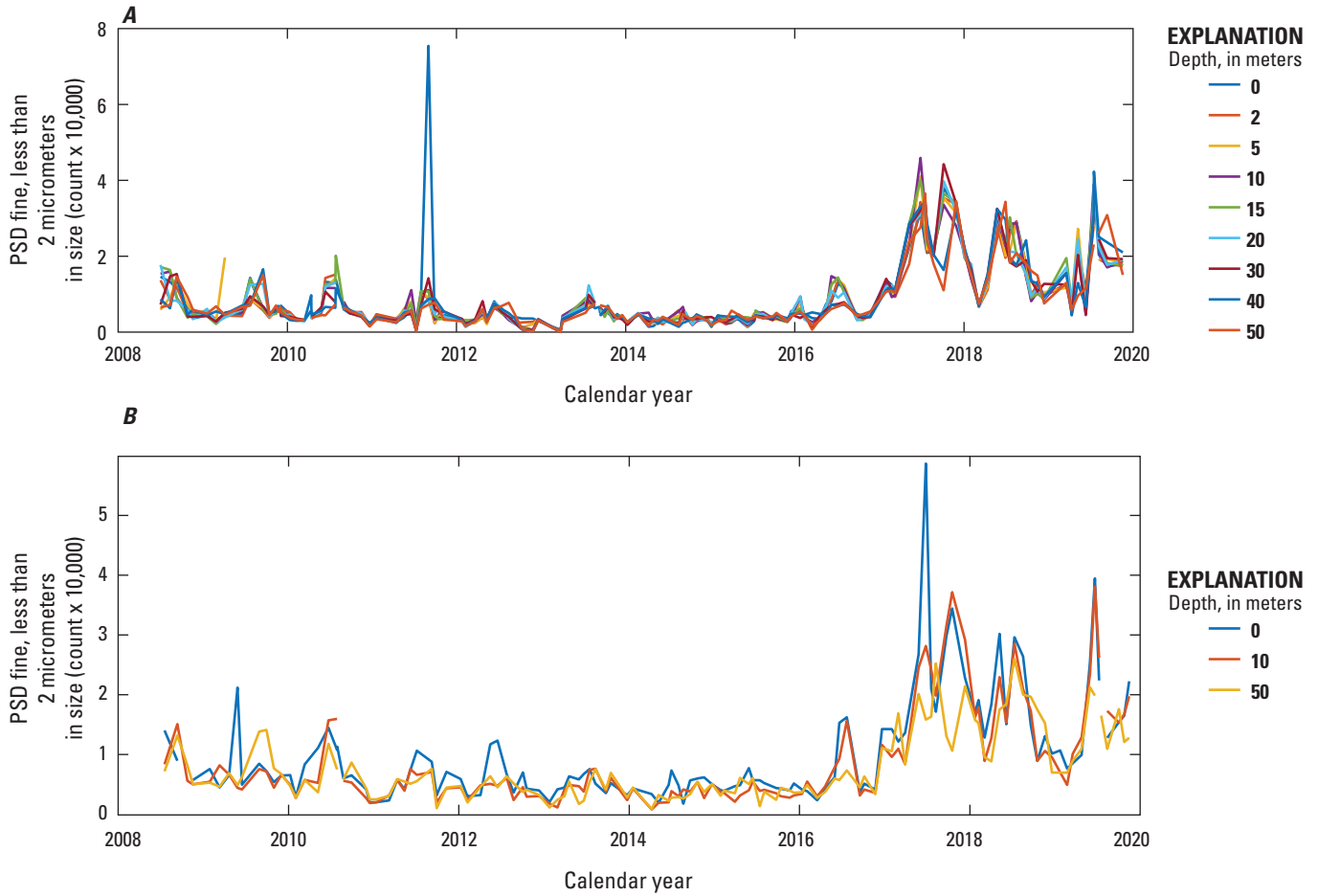
**Figure 2.3.**    Time series of particle-size distributions (PSD) of fine particles at three depths for two sites at Lake Tahoe, 2008–19: *A*, the Lake Tahoe profiling station (LTP); and *B*, the mid-Lake Tahoe profiling station (MLTP). See table A1 of this report for period of record and frequency.
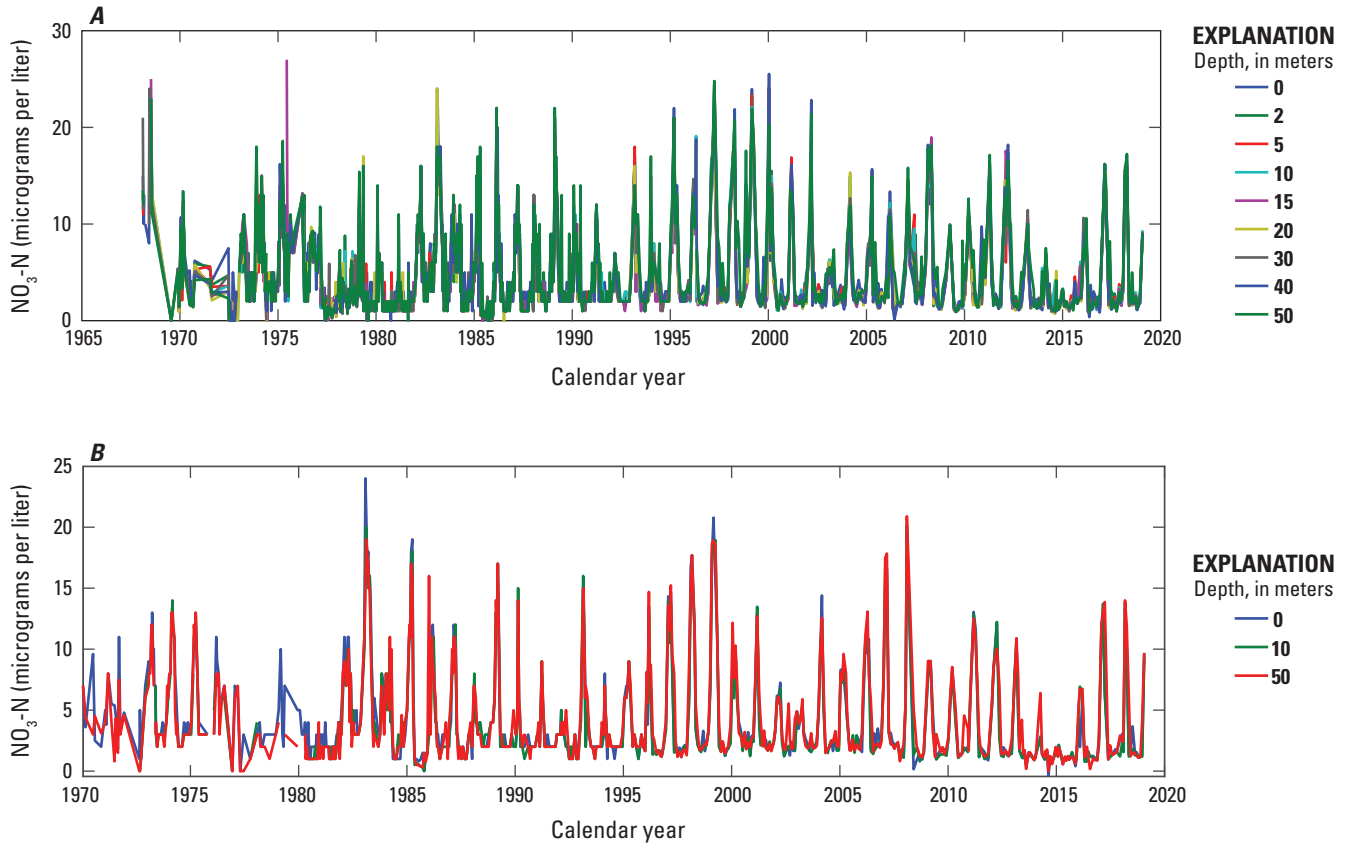
**Figure 2.4.**   Time series of nitrate as nitrogen (NO₃-N) at nine depths for two sites at Lake Tahoe: *A*, the Lake Tahoe profiling station (LTP), 1968–2018; and *B*, the mid-Lake Tahoe profiling station (MLTP), 1970–2018. See table A1 of this report for period of record and frequency.
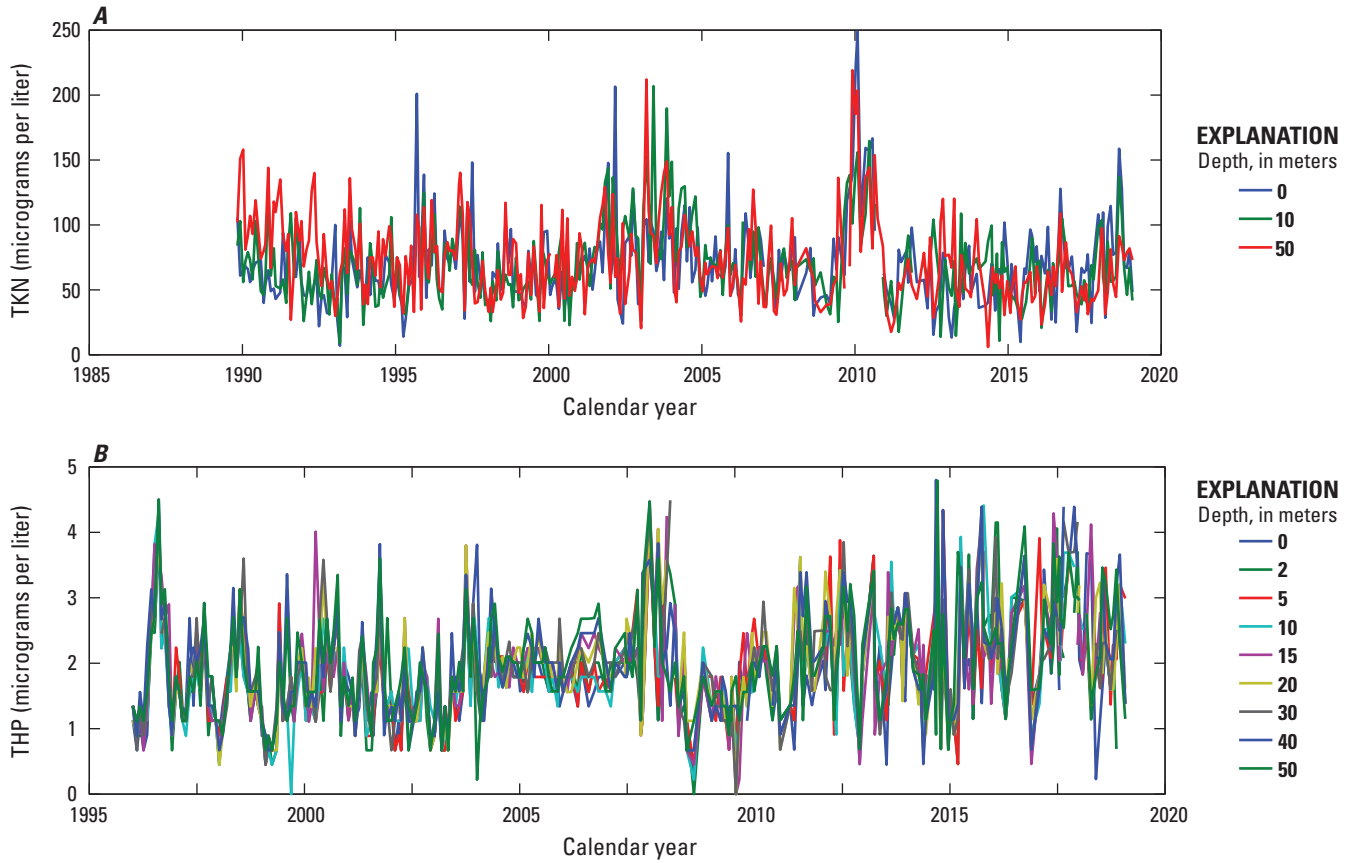
**Figure 2.5.** Time series of nutrients in Lake Tahoe: *A*, total Kjeldahl nitrogen (TKN) at the mid-Lake Tahoe profiling station (MLTP), 1990–2018; and *B*, total hydrolyzable phosphorus (THP) at the Lake Tahoe profiling station (LTP), 1996–2018. See table A1 of this report for period of record and frequency.
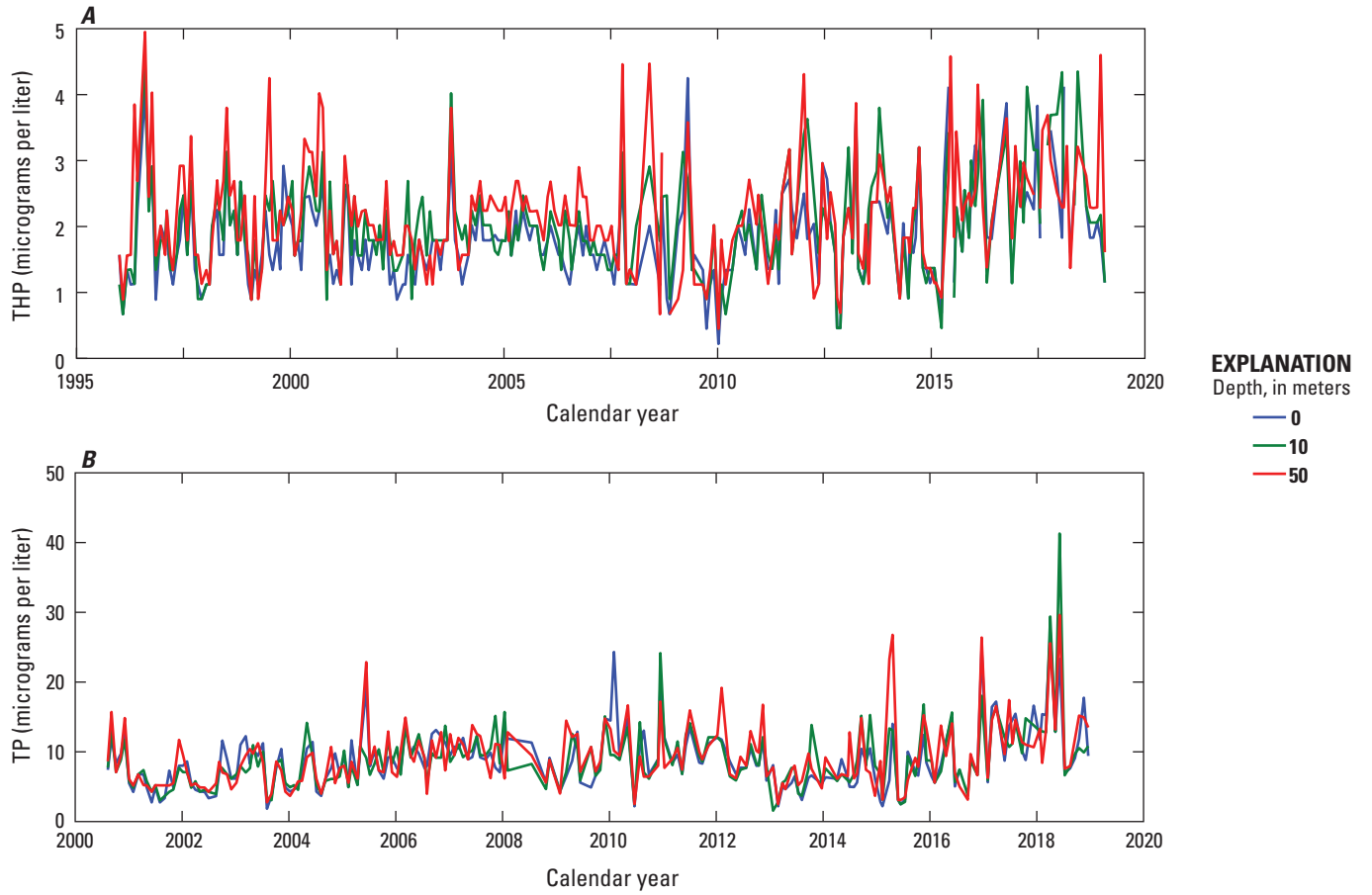
**Figure 2.6.**    Time series of phosphorus concentrations at three depths below the water surface in Lake Tahoe at the mid-Lake Tahoe profiling station: *A*, total hydrolyzable phosphorus (THP), 1996–2018; and *B*, total phosphorus (TP), 2000–18. See table A1 of this report for period of record and frequency.
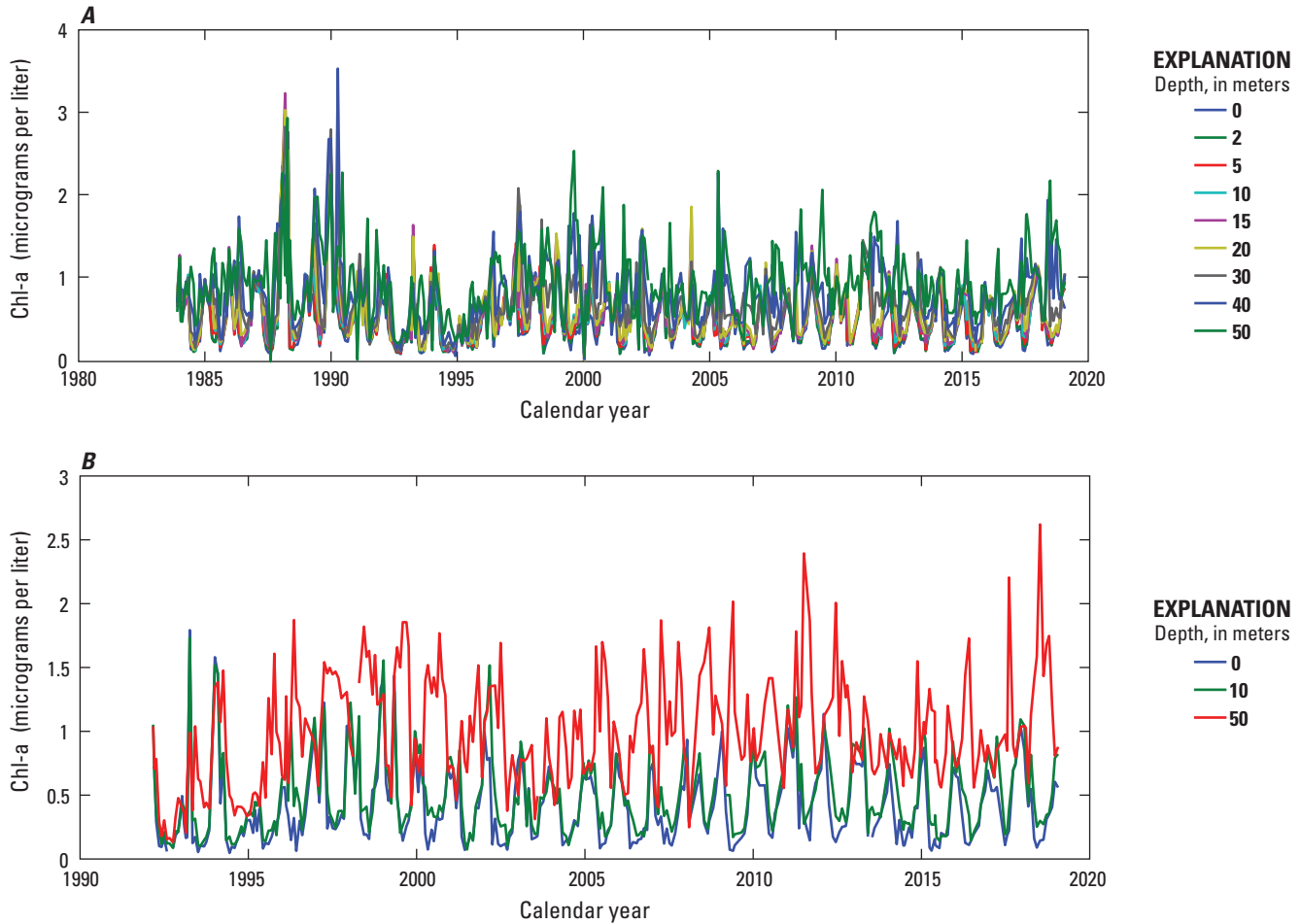
**Figure 2.7.**   Time series of chlorophyll-a (chl-a) at nine depths for two sites at Lake Tahoe: *A*, the Lake Tahoe profiling station (LTP), 1984–2019; and *B*, the mid-Lake Tahoe profiling station (MLTP), 1992–2008. See table A1 of this report for period of record and frequency.

# References Cited

Watanabe, S., and Schladow, G., 2021, Limnological data for Lake Tahoe seasonal and long-term clarity trend analysis report: Dryad, Dataset, accessed July 27, 2021, at https://doi.org/10.25338/B83P8B.

# Appendix 3.    Description of Variables Used in the Correlation Analysis

**Table 3.1.**    Description of variables measured at Lake Tahoe and used in the correlation analysis (U.S. Geological Survey, 2021; Watanabe and Schladow, 2021).

[LTP, Lake Tahoe profiling station; MLTP, mid Lake Tahoe profiling station; m, meter; SNOTEL, snow telemetry; ft$^3$/s, cubic foot per second; LTIMP, Lake Tahoe Interagency Monitoring Program]

| Variable | Description |
|---|---|
| | Summer |
| Summer_Clarity | Summer median monthly clarity values |
| Summer_T | Summer lake temperature observed at 10 m LTP |
| Strat_days | Number of stratification days |
| Peak_Strat_Day | Day of peak stratification |
| Begin_Strat_day | Day stratification started |
| End_Strat_day | Day stratification ended |
| Summer_PeakBF | Summer peak buoyancy frequency (maximum value in vertical profile) |
| Summer_MaxBF | Summer maximum buoyancy frequency (top and bottom of profile) |
| Summer_GSI | Summer Stability Index |
| Summer_NO3N | Summer median nitrate-nitrogen concentrations at 10 m LTP |
| Summer_TPH | Summer median total hydrolyzable phosphorus at 10 m LTP |
| Summer_TP | Summer median total phosphorous at 10 m LTP |
| Summer_Chla | Summer chlorophyll-a at 10 m LTP |
| Summer_Particles | Summer lake particles observed at 10 m LTP |
| SWE_max | Maximum snow–water equivalent observed at SNOTEL ward #3 site |
| Summer_Precip | Precipitation observed in Summer at SNOTEL ward #3 |
| UTR_Peakdischarge | Upper Truckee River peak discharge in ft$^3$/s |
| UTR_CM | Upper Truckee River discharge center of mass date |
| UTR_Vol | Upper Truckee River streamflow volume in acre-feet |
| BW_Peakdischarge | Blackwood Creek peak discharge |
| BW_CM | Blackwood Creek center of mass day of year |
| BW_Vol | Blackwood Creek volume of streamflow |
| Summer_Cylcotella | Summer median *Cyclotella* observed at 10 m LTP |
| Summer_BC_TN | Summer Blackwood Creek total phosphorous measured at LTIMP gage |
| Summer_UTR_TN | Summer Upper Truckee River total nitrogen measured at LTIMP gage |
| Summer_BC_TP | Summer Blackwood Creek total phosphorous measured at LTIMP gage |
| Summer_UTR_TP | Summer Upper Truckee River total phosphorous measured at LTIMP gage |

**Table 3.1.** Description of variables measured at Lake Tahoe and used in the correlation analysis (U.S. Geological Survey, 2021; Watanabe and Schladow, 2021).—Continued

[LTP, Lake Tahoe profiling station; MLTP, mid Lake Tahoe profiling station; m, meter; SNOTEL, snow telemetry; ft³/s, cubic foot per second; LTIMP, Lake Tahoe Interagency Monitoring Program]

| Variable | Description |
|---|---|
| | Winter |
| Winter_Clarity | Median monthly winter clarity values |
| Winter_T | Winter lake temperature observed at 10 m LTP |
| Mixing_Depth | Depth of maximum mixing at MLTP |
| Strat_days | Days of stratification |
| Peak_Strat_Day | Day of peak stratification |
| Begin_Strat_day | Day stratification started |
| End_Strat_day | Day stratification ended |
| Summer_PeakBF | Summer peak buoyancy frequency |
| Summer_MaxBF | Summer maximum buoyancy frequency |
| Winter_PeakBF | Winter peak buoyancy frequency (maximum value in vertical profile) |
| Winter_MaxBF | Winter maximum buoyancy frequency (top and bottom of profile) |
| Winter_GSI | Winter stability index |
| Winter_NO3N | Winter nitrate-nitrogen concentrations observed at LTP 10 m |
| Winter_TPH | Winter total hydrolyzable phosphorus observed at LTP 10 m |
| Winter_TP | Winter total phosphorus observed at LTP 10 m |
| Winter_Chla | Winter chlorophyll-a observed at LTP 10 m |
| Winter_Particles | Winter particles observed at LTP 10 m |
| Winter_Cyclotella | Winter *Cyclotella* observed at LTP 10 m |
| Winter_BC_TN | Winter Blackwood Creek total nitrogen measured at LTIMP gage |
| Winter_UTR_TN | Winter Upper Truckee River total nitrogen measured at LTIMP gage |
| Winter_BC_TP | Winter Blackwood Creek total phosphorus measured at LTIMP gage |
| Winter_UTR_TP | Winter Upper Truckee River total phosphorus observed at LTIMP gage |
| SWE_max | Maximum snow–water equivalent observed at SNOTEL ward #3 site |
| Winter_Precip | Precipitation observed in Summer at SNOTEL ward #3 |
| UTR_Peakdischarge | Upper Truckee River peak discharge in ft³/s |
| UTR_CM | Upper Truckee River discharge center of mass day of year |
| UTR_Vol_acreft | Upper Truckee River streamflow volume in acre-feet |
| BW_Peakdischarge | Blackwood Creek peak discharge |
| BW_CM | Blackwood Creek center of mass date |
| BW_Vol | Blackwood Creek volume of streamflow |
| Summer_BC_TN | Summer Blackwood Creek total phosphorous measured at LTIMP gage |
| Summer_UTR_TN | Summer Upper Truckee River total nitrogen measured at LTIMP gage |
| Summer_BC_TP | Summer Blackwood Creek total phosphorous measured at LTIMP gage |
| Summer_UTR_TP | Summer Upper Truckee River total phosphorus measured at LTIMP gage |

# References Cited

U.S. Geological Survey, 2021, USGS water data for the Nation: U.S. Geological Survey National Water Information System database, accessed August 19, 2021, at https://doi.org/10.5066/F7P55KJN.

Watanabe, S., and Schladow, G., 2021, Limnological data for Lake Tahoe seasonal and long-term clarity trend analysis report: Dryad, Dataset, accessed July 27, 2021, at https://doi.org/10.25338/B83P8B.

USGS